Corrigenda

Page x. ΔB = "external pressure" should be replaced by "internal pressure".

Page xi.
$[R_Z(NC)]$ = ratio of stress increment corresponding to normally consolidated range.
$[R_Z(OC)]$ = ratio of stress increment corresponding to overconsolidated range.

Page 3, Line 1. Replace "Barantsen" with "Barentsen".

Section 2.2, Page 7, 3rd dot. calibration factors are ΔA and ΔB, not A and B.

Page 8, Para 5, Line 4. should read as, "should stop unambiguously at 0.05 mm expansion and resume at 1.1 mm expansion."

Page 10, Para 1. Reyna et al. (1991) conducted the dilatometer tests on fills to observe their settlement.

Page 10, Para 3, Line 3. "it's" should be replaced by "its".

Page 12, Equation 2.5(a). The insitu pore water pressure, U_0, is directly calculated from the depth of the ground water table (0.9m below ground level).

Section 2.2.3, Page 13, Last dot. As the test sites at Torre Oglio and Damman consist of similar sand deposits, there is close similarity in their various profiles.

Page 14, Para 4, Line 1. Prediction of soil unit weights from DMT is based on I_D, E_D Chart (Schmertmann, 1986)

Page 15, Last Para. Evaluation of constrained modulus, M, from DMT - Laboratory tests by Mokkelbost et al. (1991) indicate that Marchetti (1980) correlations slightly overpredict the M values for OCR = 1, and considerably overpredict the M values for OCR between 1.4 and 5.5.

Page 29, Last Line. "crushers" should be replaced by "crushing".

Chapter 3. In order to correctly measure the depth of the dilatometer blade during the tests a device referred to as the depth box (see Jaksa and Kaggwa, 1994) was used.

The depth box consists of a metallic wire which is wound round a drum. Prior to test commencement the wire is stretched and attached to the hydraulic ram. During the penetration of the dilatometer blade the hydraulic ram goes down and the wire is wound around the drum and for every 1/500th revolution of the drum a pulse is generated. By counting the number of pulses it is possible to correctly determine the depth of the dilatometer blade.

Section 3.7.4, Page 62. According to the Fugro (1979) classification system the test site consists of very weakly cemented and endurated to firmly cemented and endurated carbonate sand and gravel.

Page 62, Table 3.2. Determination of bulk density in laboratory - Based on four laboratory tests on recovered soil, the average bulk density, γ_b = 1.7 t/m^3 for depths ranging between 0 and 0.9m.

Page 62, Table 3.2. The organic content of the soil was determined by heating a small portion of dried soil mass in a crucible up to 800°C and then determining the percentage loss in weight. In addition, the E_D profiles shown in Fig 5.8 show decrease in the E_D values at 1m below ground level due to the presence of organic substance.

Section 4.2, Page 78, Last para. The stiffer soil layers impose more horizontal pressure on the dilatometer membrane during penetration compared to loose layers.

Section 4.4, Page 81, Para 4, Line 2. "pore pressure is not consistent with depth" should read "pore pressure does not increase consistently with increase in depth".

Figure 4.5, Page 88. The three different curves shown in Figure 4.5 are to compare the Young's modulus evaluated from two pressure readings (formulating E_D) with that evaluated from the continuous pressure-deflection readings (formulating $E_{D(new)}$), evaluated during the same test.

Figure 4.6, Page 89. Figure 4.6 compares a number of standard dilatometer tests within a small area with a number of modified dilatometer tests.

Table 5.1, Page 96. "*" should be replaced by "Leonards and Frost (1988)".

Page 98, Para 3, Line 4. Compressible layers are common in calcareous sediments and are known as calcareous muds or oozes. In some of these layers the particle sizes can be as small as that of clay particles (Randolph et al., 1993).

Page 105, Last Para. Evaluation of Young's modulus, E_{25}, from dilatometer modulus, E_D - A number of researchers (see Section 2.3.3) have established that in normally consolidated sand the dilatometer modulus, E_D, directly gives the Young's modulus corresponding to 25% of the failure deviator stress level. This correlation has been used to evaluate E_{25} in the present research work.

Section 5.5, Page 107, Para 2, Line 4. "4" should be replaced by "40°".

Section 6.3.1, Page 136, Third dot, Line 6. "5.44MPa" should be replaced with "0.54MPa".

Page 153. Berardi, R., Jamiolkowski, M. and Lancellotta, R. (1991). *"Settlement of shallow foundations on sands, selection of stiffness on the basis of penetration resistance,"* Geotechnical Special Publication, Boulder, Colorado, June 10-12, Vol I, pp. 185-200.

Page 161, Last reference. "Geotecgnical" should be replaced by "Geotechnical".

FIELD AND LABORATORY TESTING OF CALCAREOUS SAND

by

Ranjani Kumar Jha
B.E. (Bangalore University, India)

A thesis submitted for the Degree of
Master of Engineering Science

University of Adelaide
Department of Civil and Environmental Engineering
Australia

December 1994

To my late grandparents

Mohit Lal Jha

Gandhari Devi

ABSTRACT

The present research work concentrates on the evaluation of design parameters of slightly calcareous offshore sand, using field and laboratory tests. The Marchetti flat dilatometer was used as a primary field testing device together with the electrical cone penetrometer, both of these in situ devices being supplemented by standard laboratory tests for classification, shear strength and compressibility.

Modifications of the existing dilatometer device were undertaken in order to obtain continuous readings of pressure versus deflection during membrane inflation and to provide the dilatometer blade resistance during penetration. A data acquisition system was also developed for the automatic recording of data from the modified dilatometer, linked through a microcomputer. A standard procedure is suggested for conducting the modified dilatometer tests in the field. The pressure versus deflection readings have been used to check the linearity between the dilatometer membrane pressure and deflection readings and an alternative method for the evaluation of Young's modulus of soil, from the modified dilatometer data, is proposed.

Results of the standard dilatometer (DMT), modified dilatometer (MDMT) and electrical cone penetration tests (CPT), conducted in close proximity on a marine sand, which contained 20% carbonate, are also presented and compared.

The applicability and suitability of the various DMT and CPT correlations, which are based on pure silica sand, are examined for the evaluation of design parameters of slightly calcareous sand, with the help of laboratory tests. The in situ values of design parameters, obtained from the weakly cemented layers are found to be more reliable compared to the highly cemented layers and recommended for design purposes.

The results so evaluated, are finally used for the bearing capacity and settlement calculations of foundations of different sizes and shapes and recommendations are given for appropriate sizes of square, rectangular and strip footings founded on calcareous sand at the test site.

STATEMENT OF ORIGINALITY

This work contains no material which has been accepted for the award of any other degree or diploma in any university or other tertiary institution and to the best of my knowledge and belief, contains no material previously published or written by another person, except where due reference has been made in the text.

I give consent to this copy of my thesis, when deposited in the University Library, being available for loan and photocopying.

Signed **Date:** 16/12/94

Ranjani Kumar Jha

ACKNOWLEDGMENTS

I shall remain indebted to my supervisor, Dr. G. W. S. Kaggwa, whose continuous supervision, encouragement and support helped a long way in the completion of this research work. My heartiest thanks to Mr. Mark Jaksa, for helping me with the intricacies of computer programming and Dr J. Neil Kay, whose initial research and recommendations gave the present research a proper direction.

I thank Mr. Bruce Lukas for the modifications of the field test device, the dilatometer, and Mr. Tad Sowosko, for his technical assistance during field and laboratory testing. I appreciate the friendliness and cooperative nature of all the staff members and fellow post graduates of the department and shall always remember with fondness the marvellous time I had with them. In particular, I wish to thank Mr. Paul Morgan for the review of the entire thesis prior to submission, and Mr. Abir Ghosh for help in times of need. I extend my thanks to the computer officers, especially Byron Riessen, for maintaining an excellent computing facility in the department.

I am also thankful to the MFP (Multi Function Polis) officials and particularly Mr. Bob Roach, Dean Rifle Range for allowing us to conduct the field tests within the MFP site. The geotechnical survey reports of the MFP, Adelaide, by Coffey International Pty. Ltd. and PPK consultants were of special help in locating an appropriate field test site, for which I am thankful.

I express my deepest gratitude towards my parents, Dr. Bal Krishna Jha and Mrs. Sushila Jha, whose good advice and moral support have been a source of constant inspiration to me. Finally, I wish to thank two very special people, my wife, Anima, and daughter, Surabhi, who always received me warmly back home and gave me much needed love and affection.

CONTENTS

ABBREVIATIONS

ASCE	American society of Civil Engineers
CC	calibration chamber
CPT	cone penetration test
D & M	Durgunoglu and Mitchell
DMT	dilatometer modulus test
ESOPT	European symposium on penetration testing
ICSMFE	International Conference on Soil Mechanics and Foundation Engineering
ISOPT	International symposium on penetration testing
MDMT	modified dilatometer modulus test
SPT	standard penetration test

KEY WORDS

Calcareous sand
Cohesionless soil
Correlations
Design parameters
Indirect approach, semidirect approach, direct approach
In situ testing
Sediments

KEY NOTATIONS

Δ A	external pressure applied to the membrane in free air to keep it in contact with its seating (in DMT test).
Δ B	external pressure applied to the membrane in free air to lift its centre by 1.1 mm from its seating (in DMT test).
C_1, C_2, C_3	Coefficients in Baldi et al. (1986) correlation for the determination of coefficient of earth pressure at rest.
c_1	embedment correction (in settlement calculations).
D_r	relative density of soil.
E_D	dilatometer modulus.
$E_{D(new)}$	modified dilatometer modulus corresponding to low strain.
E_{25}	Young's modulus corresponding to 25% deviator stress level.
F_R	friction ratio (in CPT test).
f_s	sleeve friction (in CPT test).
H	thickness of soil layer.
Δ_h	thickness of soil sublayer.
I_D	dilatometer material index.
I_Z	strain influence factor (in foundation settlement analysis).
K_D	dilatometer horizontal stress index.
K_o	coefficient of earth pressure at rest.
$K_{o(oc)}$, K_{oc}	coefficient of earth pressure at rest for overconsolidated soil.
$K_{o(nc)}$	coefficient of earth pressure at rest for normally consolidated soil.
K_{ou}	K_o during primary loading.
M	constrained modulus (in DMT test).
m_v	coefficient of volume change of soil.
N	number of blow counts (in SPT test).
OCR	overconsolidation ratio.
P_A	contact membrane pressure (in DMT test).
P_B	expansion membrane pressure (in DMT test).
P_C	pressure at which membrane comes back to its resting position upon depressurisation (in DMT test).
P_0	contact membrane pressure corrected for membrane stiffness (in DMT test).
P_1	expansion membrane pressure corrected for membrane stiffness (in DMT test).
ΔP	$= P_1 - P_0$ (in DMT test).

p_c'	preconsolidation pressure of soil.
q_c	cone tip resistance (in CPT test).
q_d	dilatometer blade tip resistance (in DMT test).
q_{net}	surface load excluding excavated earth.
$[R_Z(NC)]$	ratio of stress increment corresponding to overconsolidated portion of the total stress increment (in settlement analysis).
$[R_Z(OC)]$	ratio of stress increment corresponding to normally consolidated portion of total stress increment (in settlement analysis).
S	total settlement.
S_i	settlement of layer i.
S_o	membrane deflection into soil in the horizontal direction (in DMT test).
U_0	pore water pressure (from DMT test).
ϕ	angle of friction of soil.
ϕ'	effective angle of friction of soil.
ϕ'_{ax}	effective angle of friction of soil for axial strain conditions.
ϕ'_{ps}	effective angle of friction of soil for plane strain conditions.
γ_b	bulk density of soil.
γ_d	dry density of soil.
μ	Poisson's ratio of soil.
σ_d'	vertical effective overburden stress at the mid-hight of each layer/sublayer.
σ_f'	final effective vertical stress at the centre of each layer/sublayer
σ_v	vertical overburden stress.
σ_v'	vertical effective overburden stress.
$\Delta\sigma_v'$	increase in the vertical effective stress in each layer/sublayer.
σ_o'	effective initial overburden stress at the mid height of each layer/sublayer.

Chapter 1

INTRODUCTION

1.1 Introduction

This research work is aimed at evaluating the design properties of calcareous sand with the help of field and laboratory tests. Calcareous sand is becoming an important area of study as it is found in most of the offshore areas, as a result of deposition of sea sediments. In Australia most of the coast-line is calcareous in nature (Poulos, 1980; Jewell, 1993). Due to increases in the world population, lack of space and diminishing resources globally, there is a trend for growth towards the coastal regions. The rate of construction in the offshore regions has increased considerably and the design parameters of calcareous sand need to be thoroughly examined in order to make the construction safe and durable.

Even though calcareous sand may consist of a high percentage of silica particles, its behaviour differs from that of normal silica sand owing to the presence of different types of carbonates (Poulos, 1980). These carbonates are usually present in the form of calcium and magnesium carbonates, causing cementation.

As a result of natural cementation, calcareous sand deposits behave differently to the ordinary sands and the design parameters need to be evaluated independently. However, due to varying degrees of cementation, differences in origin, age and types of binding materials, as well as sampling disturbances, it is not possible to establish simple procedures or correlations for the evaluation of design parameters of

calcareous sand. Therefore, the best option is to use the existing laboratory and in situ tests for the purpose, based on local site experience.

Geotechnical tests may be divided into two categories; in situ tests and laboratory tests. The in situ tests aim at evaluating the design properties of soil under natural conditions in the field, without causing much disturbance to them, and are getting increasingly popular with time. On the other hand, the laboratory tests are conducted on samples obtained from the field, thereby causing disturbance to their original ground conditions. Many types of samplers have been developed for the purpose of obtaining good quality samples, so that the original soil properties can be determined from the laboratory tests. However, assessing the properties of cohesionless soils using laboratory tests is not easy because collecting undisturbed soil samples of such soils from depth is extremely difficult. Even with the utmost care and using the most sophisticated of samplers, some soil disturbance is bound to occur. Accordingly, there is more reliance on in situ tests.

Various in-situ devices have been developed for this purpose. The cone penetration test (CPT), standard penetration test (SPT), dilatometer modulus test (DMT), plate load test and screw plate test are all used. Amongst these, Marchetti's flat dilatometer is a relatively recent development. Marchetti (1980) and Schmertmann (1986) described the flat dilatometer and suggested different correlations for the assessment of soil parameters. It has been found that compared to other tests, the DMT is a cost-effective and time efficient in-situ testing device.

The DMT and CPT are based on the principle of a penetrating wedge, or cone, of known dimensions, into the soil and interpreting soil parameters by correlating penetration data to laboratory measurements. The CPT and DMT correlations for clay soils have been based directly on the laboratory findings (Marchetti, 1980; Campanella and Robertson, 1983; Jamiolkowski et al., 1985; Powell and Uglow, 1988 etc), as it is possible to obtain relatively undisturbed samples of clay soils. However, in the case of cohesionless soils, these correlations have been based on numerous field tests and calibration chamber test results, conducted on artificially deposited sand under known boundary conditions (Bellotti et al., 1979, 1986; Baldi et al., 1981, 1982, 1985, 1986; Marchetti, 1979, 1980, 1985; Villet and Mitchell, 1981; Lacasse and Lunne, 1986, 1988; Jamiolkowski et al., 1986, 1988 etc.).

The CPT has been in use for more than half a century and is very popular for site investigation and geotechnical design. The introduction of CPT in a recognisable

form was as early as 1934 (Barantsen, 1936). The CPT correlations make use of effective overburden pressure together with cone tip resistance and sleeve friction for the determination of soil parameters such as relative density, friction angle and constrained, tangent and secant moduli. However with CPT, the direct measurement of horizontal stress in the field is not possible.

It has been found that many soil parameters can be better correlated to the horizontal stress acting in the soil mass rather than the vertical stress (Baldi et al., 1981; also supported by Schmertmann, 1978; Holden, 1976; Veismanis, 1974 and others). By doing so, the correlations can be applied to both normal as well as overconsolidated soils, taking into account the stress history. As the CPT does not give a direct measurement of the horizontal stress within the soil, the DMT proves to be of immense value, as it has the capability of sensing the horizontal stress of the soil at the point of testing. Due to this ability, the DMT proves particularly useful in the evaluation of the coefficient of earth pressure at rest, K_o.

It was also realised that simultaneous use of DMT and CPT would be more beneficial (Marchetti, 1985; Baldi et al., 1986) because the dilatometer directly measures the horizontal stress in the soil which the CPT does not measure. On the other hand, the electric cone penetrometer test gives the values of cone tip resistance swiftly and accurately, which the DMT is not capable of. The two values recorded adjacently on site, respectively from DMT and CPT are used to evaluate the strength and deformation parameters of normally, as well as overconsolidated, sand deposits and assist in the evaluation of overconsolidation ratio and preconsolidation pressure, required for the analysis of foundation settlement on cohesionless soils (Schmertmann, 1986a; Leonards and Frost, 1988; Berardi et al., 1991), making the DMT one of the best available tools when used together with the CPT.

1.2 Objectives and scope

One of the areas that is being explored is to find out the applicability of the DMT and the CPT in the evaluation of the design parameters of soils of different mineralogical composition, such as calcareous sand and chalk (Power, 1982; Fahey, 1993) and study the behaviour of foundations resting on these sands (Randolph et al., 1993). In fact, attempts have already been made to apply CPT to evaluate the parameters of calcareous sediments (Joustra and Gjit, 1982; Ortigo et al., 1986). It is still a subject of ongoing research and results so far indicate that the CPT is capable of giving reasonably good results even in these types of sediments.

The suitability and adaptability of the DMT and CPT and their standard correlations for the identification and evaluation of parameters of calcareous sands, have not been fully investigated. A literature review is done and a number of laboratory and field tests have been conducted as a part of the present research to evaluate the design parameters of calcareous sand. Emphasis is mainly given to evaluate two of the commonly used design parameters, namely, the angle of friction, ϕ, and Young's modulus, E. The use of these parameters is illustrated in bearing capacity and settlement calculations for several types of shallow foundations.

Another important aspect of this research has been to upgrade the existing DMT device from manual to automatic data acquisition. The CPT test has undergone tremendous changes since it was first invented (Searle, 1979; Meigh, 1987) and data acquisition systems have been developed for the automatic recording of the CPT data through the microcomputer (De Ruiter, 1971, 1981; De Beer et al., 1988; Meigh, 1987 etc.). On the other hand the DMT device has not undergone much changes or upgrading, in spite of its increasing popularity.

The existing DMT instrument suffers from two major limitations, namely, (a) it is manually operated, causing human error in the data recording, and, (b) it relies on only two readings of pressure and deflection for the interpretation of soil properties. During the current research work, steps have been taken towards the upgrading and modifying of the existing DMT device, in order to make it more efficient. A data acquisition system has been developed for the DMT test, which is a modified version of the CPT data acquisition system currently in use at the University of Adelaide.

The continuous pressure versus deflection data, recorded from the modified DMT test, is used for the direct evaluation of the Young's modulus of calcareous sand, using a different approach. Evaluations of the modulus of elasticity, using both the modified dilatometer and the standard dilatometer, have been undertaken, enabling a comparison between the results, and advantages of using the modified dilatometer are discussed. Other potential advantages of the modified dilatometer data are also highlighted.

1.3 Thesis layout

This thesis focuses on the usefulness of the DMT and CPT tests, for the evaluation of some of the commonly used design parameters of moderately calcareous offshore

sands, such as, the angle of friction (used for the assessment of the bearing capacity of a foundation) and Young's modulus (used for the prediction of settlement of a foundation). Detailed description of the development of an automated dilatometer device, and its advantages for a more realistic evaluation of soil parameters, are also important parts of this thesis. A layout of the thesis is as given below.

A literature review of the dilatometer and cone penetration tests in cohesionless and calcareous sand is presented in Chapter 2, along with the characteristic properties and classification systems for calcareous sands. At the end of Chapter 2, the methods suggested for settlement calculations of footings resting on cohesionless soils, utilising DMT and CPT data, are described.

Chapter 3 describes the developments for automation of the dilatometer, its modifications and the setting up of a standard procedure for performing the modified dilatometer tests in the field. Selection of a suitable test site for conducting the field tests, based on the geotechnical survey reports of the Adelaide metropolitan area, as well as field and laboratory testing programs, are also covered.

The interpretation of results from the modified dilatometer tests are presented in Chapter 4. A method is proposed for the direct evaluation of Young's modulus of elasticity from the modified dilatometer data and the results are compared to those obtained from the standard dilatometer. Subsequently, the other possible applications of the modified dilatometer data are described.

In Chapter 5 the various DMT and CPT correlations established on pure silica sand are used for the evaluation of the parameters of slightly calcareous sand, using laboratory tests as the basis. Different ways for detecting the layers of relatively low and high cementation are suggested, based on DMT and CPT data.

In Chapter 6 the field and laboratory determined design parameters are used for the evaluation of the bearing capacity and settlement of typical shallow foundations, located at the test site.

Finally, a summary of the research undertaken, the conclusions drawn from it, and recommendations for future research, are described in Chapter 7 of the thesis.

Chapter 2

DILATOMETER AND CONE PENETRATION TESTS ON COHESIONLESS AND CALCAREOUS SANDS

2.1 Introduction

The flat dilatometer is an instrument originally devised by Silvano Marchetti (1980). Since its invention, it has gained popularity as a handy probing instrument, capable of giving a reasonable idea of soil properties. The dilatometer consists of a flat steel plate, 94 mm wide and 14 mm thick. Its cutting edge makes an angle of 16° into the soil. There is a thin expandable metal membrane on one side of the plate.

In-situ testing of soil using the flat dilatometer involves jacking the dilatometer blade into the ground with the help of a penetrometer rig and expanding the membrane in the horizontal direction against the soil with the help of gas pressure. The pressure readings required for prescribed movements of membrane are recorded and used in evaluating dilatometer indices, which are subsequently related to the soil properties.

The degree of disturbances caused to the soil due to various in-situ devices was studied by Baligh (1975). It was found that the disturbance caused during the penetration and expansion stage of the DMT is relatively minor. This is due to the fact that the shear stress concentration is more towards the cutting edge compared to the side. Since the dilatometer membrane is laterally placed, it is less affected by the shear stress concentration zone.

The other advantage of the DMT is that the apex angle of the blade is 16°, which is significantly less than the 60° apex angle of most conical tips. In addition, the dilatometer is capable of sensing horizontal stress of the soil directly because the membrane expands horizontally into the soil. These positive aspects make the dilatometer superior to other conical tip devices.

2.2 The DMT in situ testing device

The dilatometer assembly shown in Figure 2.1a comprises of the following parts:

- Steel blade (235 mm long, 95 mm wide and 14 mm thick) and expandable metallic membrane (circular in shape with 60 mm diameter). Figure 2.1b shows details of the dilatometer blade.
- Control unit with pressure read out system with pneumatic electrical connections and valves.
- Calibration unit with pressure gauge, vacuum and pressure source for determining A and B membrane calibration.
- Pneumatic electrical cable to transmit gas pressure and electrical continuity from the control unit to the blade.
- Ground cable to provide electrical continuity between the push rod system and the calibration unit.
- Equipment to push the dilatometer blade into the soil. This can be accomplished with a truck similar to the one used for the cone penetration testing, shown in Figure 2.1c.
- Push rods and adaptors to transfer the thrust from the surface insertion equipment and to carry the pneumatic electrical cable from the surface control unit to the dilatometer blade, shown in Figure 2.1c.
- A gas pressure tank with suitable regulator and tubing, connected to the control unit. Usually dry nitrogen gas is used for this purpose, which is cheap, readily available and maintenance free.

2.2.1 Method of testing

In situ testing with the Marchetti dilatometer consists of three stages. The first stage is preparation for testing; the second stage is testing; and the third stage is after checks. Details of the standard testing procedure are given by Schmertmann (1986). The main features are as summarised below.

Stage 1: Preparation for testing

The dilatometer blade is checked to conform with the manufacturer's internal tolerance adjustments. The blade should be free of any bends and its penetrating edge should not deviate more than 2 mm from the axis of the rods to which the blade attaches. The penetrating edge should be sharp and straight. The membrane should be free of deep scratches and should expand without any popping or snapping sounds upon pressurisation.

The pressure source and electrical cable are attached to the control box. The control unit and cable are checked for gas leakage. For this purpose the blade end of the cable is plugged with an appropriate fitting and pressure is applied to the cable through the control unit. Then the flow control valve is closed and the pressure monitored to detect any pressure drop that would indicate a leakage in the system. Leakages in excess of 100 kPa per minute are unacceptable and require repair. Smaller leaks may not cause problems.

The electrical cable is attached to the dilatometer and the two ends of the electrical ground cables are connected to the control unit and blade, respectively. The centre of the blade is pressed down until it makes contact with the support pedestal. At this contact the electrical or audio signal should sound. If not, appropriate repairs should be undertaken.

The correction values ΔA and ΔB, which account for the membrane stiffness, are determined using the calibration equipment, where ΔA is gas pressure inside the membrane required to overcome the stiffness of the membrane and move it inward to a centre expansion of 0.05 mm. Actually this is a negative gas or suction pressure, but recorded as positive. ΔB is the gauge pressure inside the membrane required to overcome the stiffness of the membrane and move it outward to a centre expansion of 1.10 mm in free air.

ΔA and ΔB, known as membrane stiffness calibration pressures, should fall within the tolerance given by the manufacturer for the type of membrane used and are recorded as positive values. During the calibration test the electrical or audio signal should stop unambiguously at 0.5 mm expansion and again at 1.0 mm expansion. Any membrane that fails these checks, should be replaced.

New membranes require nearly 20 cycles of preconditioning, expansion and deflation to reach an approximately stable value of ΔB. Also the ends of all the cables should be capped immediately after releasing from any connections. This prevents any contamination of cables and corrosion of the terminals.

Stage 2: Field testing

A step by step procedure for testing is as given below.

Step 1: The vent valve is opened and the dilatometer blade is jacked to its first depth. The push rod is kept vertical while the dilatometer is advanced into the soil. For determining the quasi static bearing capacity of the soil, an extra reading is needed. For this purpose, the total push or total thrust force, P, required to advance the dilatometer blade to a new test depth is recorded. So the value of thrust required during the last 10 mm penetration or the number of blows for each 150 mm of penetration is noted down. If using the blow counts, to estimate the static force, an average of the blow counts is taken for 150 mm above and below the test depth. The rate of penetration is of secondary importance in case of sands and could vary between 10 to 100 mm per second. In silts penetration rates are maintained between 10 and 30 mm per second.

While advancing the blade as per Step 1 above, an electrical or audio signal should be produced by the dilatometer to ensure that the membrane is flush with the plane of the blade.

Step 2: Once the test depth is reached, the static force should be removed from the rods and the vent valve closed within 15 seconds of reaching the test depth. The gas flow valve on the control unit is used to pressurise the membrane. The pressure gauge reading at the instant the signal stops is pressure, P_A, which indicates the pressure at which the membrane just lifts off its resting position. This is recorded within 15 to 30 seconds of membrane pressurisation. Then, within the next 15 to 30 seconds the gas pressure is increased until the signal returns. At this instant the pressure reading, P_B, is recorded, indicating the pressure which causes 1.1 mm horizontal deflection of the membrane into the soil. Without delay the vent valve is opened in order to depressurise the membrane and the gas flow is also stopped by closing the gas flow control valve. The procedure prevents further expansion of the membrane which could permanently deform it, thereby changing its calibration.

Research by Reyna et al. (1991) shows that the P_A and P_B readings are influenced by the rate of membrane pressurisation. A slow rate of membrane pressurisation decreases the P_A and P_B values. However, Schmertmann (1986) recommends a time of 15 to 30 seconds for the complete membrane pressurisation from P_A to P_B.

Step 3: Research work and testing (Schmertmann, 1986) has indicated that another pressure reading, denoted by P_C, corresponding to the pressure against the membrane when it deflates and returns to original lift off position, provides an approximate measure of the initial in situ water pressure, U_0, in sands or sandy layers. For measuring P_C, a controlled de-pressurisation from P_B to P_C is allowed within a period of 15 to 30 seconds. A profile of in situ water pressure, U_0, so obtained is of value for the geotechnical evaluation of the site.

At shallow depths in very weak soils, sometimes it is difficult to receive a signal for recording pressure reading, P_A. This is because the horizontal pressure acting on the membrane in weaker soils is too low to keep the membrane seated in it's resting position. Thus another membrane with low and consistent calibration should be chosen. Alternatively, an initial suction pressure can be applied behind the membrane and then the flow control valve closed before advancing to the test depth. This is accomplished with the calibration unit. Firstly the ΔA pressure reading (vacuum) is recorded as a negative value and then P_B upon pressurisation. If pressure P_B is out of the gauge range, this method is not used and no test is performed until a depth is reached where the initial signal is obtained.

Step 4: The steps 1 to 3 above are repeated for every new test depth and pressure readings P_A, P_B and P_C are recorded up to the maximum depth of sounding.

Stage 3: After test checks

After completing the final sounding, the blade is withdrawn and checked to ensure whether any significant damage has been caused to the membrane or cutting edge. The calibration should be rechecked and if any deviation is found from the initial calibrations, or any defects with the signals is detected, the defect should be rectified and the test repeated to obtain proper pressure readings.

2.2.2 Mechanism of DMT penetration

In order to analyse DMT results, the test mechanism needs to be understood. The test mechanism of a dilatometer, as proposed by Marchetti (1980) is outlined below.

Penetration mechanism of dilatometer

The penetration mechanism of a dilatometer was considered by Marchetti (1980) to be similar to a complex loading test on the soil. He compared the penetration process to that of the expansion of a flat cavity model. The analysis indicated that the measured horizontal total pressure against the blade was susceptible to the in situ horizontal stress.

The dilatometer penetration causes a horizontal displacement of 7 mm (half the thickness of the dilatometer blade), of the soil, originally on the vertical axis, which is considerably lower than that caused by 18 mm conical tips. It was shown by Baligh (1975) that penetration of the dilatometer causes more soil disturbance near to the edge of the blade whereas the soil facing the membrane suffers less disturbance. Hence the modulus is likely to be more accurate.

Reduction of field measurements

In the field, pressure readings P_A and P_B, corresponding respectively to 0.05 and 1.1 mm membrane deflections, are recorded and corrected for membrane stiffness, using the following equations:

$$P_0 = P_A + \Delta A \qquad (2.1\ a)$$

$$P_1 = P_B - \Delta B \qquad (2.1\ b)$$

The difference ΔP is computed as follows:

$$\Delta P = P_1 - P_0 \qquad (2.2)$$

The value of ΔP is then used to determine the modulus of elasticity of the soil using the theory of elasticity. The dilatometer was considered by Marchetti (1980) to be formed of two elastic half spaces, having Young's modulus E and Poisson's ratio, μ, subjected to conditions of zero deflection external to the loaded area. The equation

used for these conditions was originally formulated by Gravesen (quoted by Marchetti, 1980) and is of the following form:

$$S_o = \frac{2D.\Delta P}{\pi} \cdot \frac{1-\mu^2}{E} \qquad (2.3)$$

where,

$\frac{E}{(1 - \mu^2)}$ = E_D = dilatometer modulus,

E = Young's modulus of elasticity,

μ = Poisson's ratio,

S_0 = net membrane deflection = 1.1 mm,

ΔP = change of membrane pressure causing 1.1 mm deflection,

D = membrane diameter.

For a membrane with diameter, D = 60 mm and horizontal central deflection into the soil, S_O = 1.1 mm, Equation 2.3 becomes:

$$\frac{E}{1-\mu^2} = 38.2\Delta P \qquad (2.4)$$

Marchetti (1980) termed the ratio $\frac{E}{1-\mu^2}$, the dilatometer modulus, E_D.

Further, Marchetti (1980) formulated three dilatometer indices, namely, the dilatometer modulus (E_D), material index (I_D) and the horizontal stress index (K_D), derived from the three pressure readings, P_A, P_B and P_C, obtained during the test. The indices I_D, K_D and E_D are formulated as follows:

Material index, $I_D = \Delta P / (P_0 - U_0)$ (2.5 a)

Horizontal stress index, $K_D = (P_0 - U_0) / \sigma_v'$ (2.5 b)

Dilatometer modulus, $E_D = 38.2\ \Delta P$ (2.5 c)

Where, $U_0 = \gamma_w . Z_w$ = pore water pressure prior to penetration,

σ_v' = in situ vertical effective stress at point of testing,

γ_w = unit weight of pore water,

Z_w = depth of point of testing below the water table.

Using the indices I_D, K_D and E_D at various depths from dilatometer soundings and an independent knowledge of soil profiles, Marchetti (1980) developed correlations

relating the three indices to the important soil properties. Some of the typical DMT results are discussed below.

2.2.3 Typical DMT results on cohesionless soils

Typical results of dilatometer tests at Torre Oglio, Italy, and Damman, Saudi Arabia, where the soil was mainly sand, are shown in Figures 2.2 and 2.3 (taken from Marchetti 1980). The important features of these tests are discussed below:

- At both the sites, the P_0 profiles vary between 100 to 400 kPa and P_1 profiles vary between 250 to 2500 kPa. This shows that the P_0 and P_1 profiles are consistent for same type of soil.

- The material index (I_D) profiles, indicative of the material type, are similar and vary between 2 and 10. Compaction does not appear to have any significant influence on the I_D profiles and this shows that I_D is a good material index which only changes when there is a change in the type of soil rather than a change in vertical or horizontal stresses.

- The profiles of dilatometer modulus, E_D, are also consistent at both sites and vary between 5 and 60 MPa. Compaction significantly increases E_D values at Damman, with E_D values lying between 10 and 70 MPa after compaction. This is quite logical as the stiffness of a soil increases with compaction.

- In both the sites K_D profiles, indicative of the horizontal stress index, are similar at depths greater than 4 metres. As K_D is proportional to P_0 which increases with compaction, there is a significant increase in the K_D values after compaction.

- P_0, P_1, I_D, K_D and E_D profiles at the Torre Oglio test site resembles to the respective profiles of the Damman test site. As both sites were of similar sand deposits, the similarities of the profiles is justified and shows that DMT gives consistent results.

2.3 Original DMT correlations

Once the required soil data were available, along with corresponding I_D, K_D and E_D values, Marchetti (1980) established various correlations relating the dilatometer indices to the known soil properties for the in situ evaluation of soil properties. Some

of the original DMT correlations for predicting the in situ soil properties are described below.

2.3.1 Determination of soil type (I_D)

The data indicated that the material index I_D was closely related to the grain size or soil type and as the soil fines decreased, the value of I_D increased. Marchetti (1980) recommended in Table 2.1 for the assessment of soil type based on grain size.

Table 2.1 Soil classification based on dilatometer material index, I_D (after Marchetti, 1980)

I_D values	$I_D > 1.8$	$0.6 < I_D < 1.8$	$I_D < 0.6$
Type of soil	Sand	Silt	Clay

The chart suggested by Schmertmann (1986) for identifying the type of soil and density is shown in Figure 2.4. According to this figure, soils could be classified in terms of type, unit weight and consistency, based on their position in the E_D versus I_D chart. A number of researchers (Schmertmann, 1982; Lacasse and Lunne, 1986; Lutenegger and Kabir, 1988; Bogossian et al., 1989) have found that I_D is a reliable material index which changes only with the material type and is not affected due to compaction or saturation of soil.

Powell and Uglow (1988) had mixed success in identifying certain soil types and predicting their densities. It was thought that the high degree of overconsolidation and age of the soil deposits might have affected the I_D values. Moreover, it was found that the unit weights determined from the DMT under estimated the true values, and large increases in the assessed unit weights were recorded for small increases in actual unit weights. It was concluded that the DMT indicated the variations in the unit weight but overestimated the variations.

2.3.2 Correlation between constrained tangent modulus (M) and dilatometer modulus(E_D)

Marchetti (1980) investigated whether a correlation existed between the constrained modulus, M, and E_D. Reference values of M were evaluated from CPT using the correlation $M = 2.5\ q_c$ (based on Mitchell and Gardner, 1975) and also from standard

penetration test (D'Appolonia et.al., 1970), for uniform and normally consolidated soils.

Comparisons of the DMT based E_D profiles, CPT based M profiles and SPT evaluated $\frac{E}{1-\mu^2}$ profiles showed similar trends.

Marchetti (1980) introduced another ratio R_M (M/E_D) and proposed the following correlations for the evaluation of R_M in sand. Once R_M is known, M can be easily evaluated, as $M = R_M \cdot E_D$.

For $0.6 < I_D < 3$

$$R_M = R_{M,O} + (2.5 - R_{M,O}) \log_{10} K_D \qquad (2.6\ a)$$

where $R_{M,O} = 0.14 + 0.15(I_D - 0.6)$

For $I_D \geq 3.0$

$$R_M = 0.5 + 2 \log_{10} K_D \qquad (2.6\ b)$$

For $K_D > 10$

$$R_M = 0.32 + 2.18 \log_{10} K_D \qquad (2.6\ c)$$

The computed value of R_M should always be equal to or greater than 0.85.

Figure 2.5 shows the following facts:

- $R_M = M / E_D$ is not a constant and an additional parameter, K_D, is necessary for establishing a relation between M and E_D.
- I_D has no influence on the correlation, except at low K_D values.
- Calibration chamber tests by Bellotti et al. (1979) revealed that Equations 2.6 (a-c) gives good results in the case of sand possessing intermolecular attraction, (mainly due to cementation).

Lacasse (1985) and Lacasse and Lunne (1986, 1988) compared the values of M evaluated from the Marchetti (1980) correlation to that predicted from the cone penetration tests, screw plate tests and the actual settlement of silos and came to the conclusion that Marchetti (1980) correlations give genuine M values in case of loose sand deposits. However, large scale laboratory test results by Mokkelbost et al. (1991), conducted on three different types of silica sands revealed that Marchetti (1980) correlation does not correctly predict the M values in case of overconsolidated sand deposits.

2.3.3 Correlation between dilatometer modulus (E_D) and Young's modulus (E)

Attempts have been made to relate the dilatometer modulus, E_D, directly to the Young's modulus, E_{25} (corresponding to 25 % of the failure deviator stress), based on laboratory and calibration chamber test data (Bellotti et al., 1985; 1986; Baldi et al., 1986; Campanella and Robertson, 1983; Robertson and Campanella, 1984; Jamiolkowski et al., 1988; Leonards and Frost, 1988; Berardi et al., 1991).

Their results indicate that the ratio, $E_{25}/E_D = R_E$, is close to 1 in normally consolidated sands and varies up to 4 in overconsolidated sands. A summary of E_{25}/E_D values determined for different types of sands is presented in Equations 2.7 (a-c).

NC Ticino sand	$R_E = E_{25}/E_D = 0.88 \pm 0.27$	(2.7 a)
OC Ticino sand	$R_E = E_{25}/E_D = 4.29 \pm 0.62$	(2.7 b)
OC Hokksund sand	$R_E = E_{25}/E_D = 2.49 \pm 0.74$	(2.7 c)

Leonards and Frost (1988) proposed values of E_{25}/E_D = 0.7 and 3.5 for normally consolidated and overconsolidated sands respectively and considered these values suitable for the settlement calculations of shallow foundations on granular soils.

2.3.4 Correlation between horizontal stress index (K_D) and overconsolidation ratio (OCR)

For the purpose of correlating overconsolidation ratio to K_D, Marchetti used the following equation:

$$OCR = \sigma'_{v\,max}/\sigma'_v \qquad (2.8)$$

where,

$\sigma'_{v\,max}$ = the maximum past effective overburden pressure experienced by the soil, determined from the oedometer tests and found to be in reasonable agreement with the estimate based on geological history,

σ'_v = the current effective overburden pressure.

Only three experimental data were available at that time for cohesionless soils, where $I_D > 1.8$, and a tentative relation between OCR and K_D was proposed, as shown in

Figure 2.6. Further data was necessary at that stage for the establishment of a better correlation between K_D and OCR on cohesionless soils.

2.3.5 Correlation between coefficient of earth pressure at rest (K_o) and dilatometer horizontal stress index (K_D)

For the purpose of correlating K_o and K_D, Marchetti (1980) referred to K_o values evaluated by Ladd. et al. (1977) who estimated the in situ K_o in the range of 0.40 $\pm$0.05 for the test site at Torre Oglio. Not many tests were conducted on sandy soils at that time and on the basis of data from all types of soils, Marchetti (1980) gave a tentative correlation between K_o and K_D, shown in Figure 2.7.

Marchetti (1980) found that a single curve fitted all the experimental data. When the scatter of the correlation K_o versus K_D was investigated, making use of the parameter I_D, it was also found that material type, or I_D, had no significant effect on K_o versus K_D correlation. It was therefore concluded that the correlation is valid for all soils, irrespective of their type. The correlation proposed by Marchetti is:

$$K_o = (K_D / 1.5)^{0.47} - 0.6 \qquad (2.9)$$

Calibration chamber tests on cemented sands (Bellotti et al., 1979; Senneset and Janbu, 1982) showed that the continuous line in Figure 2.7 significantly overpredicted K_o, indicating that K_D values were affected by additional strength contributed by cementation, besides the horizontal stress σ_h.

From Marchetti's 1980 work it appears that more emphasis was given to clayey soils, with little data on cohesionless soils. Not much was done on the measurement of ϕ and K_o in cohesionless soils up to that stage.

2.3.6 Problems and amendments

Assessment of K_o in sand is a very difficult task, whether it be in situ determination or laboratory testing. The in situ determination of K_o relies on penetrating some device into the soil, causing disturbance. At the same time laboratory evaluated K_o valucs cannot be relied upon as undisturbed samples of sand are difficult to obtain even with the most sophisticated samplers.

Different methods have been adopted for the measurement of K_o and these can be categorised as direct, semi-direct and indirect methods. Direct methods aim at measuring K_o by direct application of instruments. Hydraulic fracturing, Menard pressuremeter, Gloetzl total stress cell and self boring pressuremeter (SBP) are some of the instruments used for this purpose. But apart from SBP, others are not really applicable for sand. The functioning of SBP has also been questioned as, according to Fahey and Randolph (1985), penetration of even an infinitely thin cylinder changes the original K_o values due to stress variation. Semidirect methods are based on the principle of inserting a pressure measuring instrument in to the soil and then back extrapolating the results to assess the lateral stress for zero thickness. The stepped blade (Handy et al., 1982) is one such instrument but it can not penetrate through dense sand easily. Semidirect methods have also been criticised as the lateral stress varies with factors other than blade thickness.

Because of the shortcomings with direct and semidirect methods, attention has been focussed on indirect methods. In the indirect methods, some independent readings are taken in the field which do not give the soil properties directly but can be related to the soil properties, eg. pressure readings P_A, P_B, P_C in case of DMT; q_c and F_R in case of CPT; blow counts (N) in case of SPT (Standard penetration test), etc. Soil properties, eg angle of friction, modulus of elasticity, grain size etc. are determined by laboratory testings and then these properties are related to the independent field readings to give correlations.

However, as pointed out, laboratory determination of design parameters of sand is difficult due to sampling disturbances and may give rise to misleading correlations when taken as reference values in the indirect correlations. Still, the indirect methods have been relied upon by many researchers, such as Marchetti (1979, 1980, 1985); Bellotti et al. (1979); Schmertmann (1982, 1983); Baldi et al. (1986); Lacasse and Lunne (1986, 1988) etc. for the determination of K_o and ϕ using DMT. A progressive history for the evaluation of K_o and ϕ is presented below.

2.4 Available correlations for friction angle and coefficient of earth pressure at rest

In order to check the validity of K_o - K_D (Marchetti, 1980) correlation, many dilatometer and calibration chamber (CC) tests were conducted on sand. CC tests by Schmertmann (1983) proved that the K_o - K_D correlation changes with variations in ϕ

or D_r (relative density) and attempts were made to formulate K_o - K_D - ϕ correlations rather than K_o - K_D correlation.

Various approaches were made towards the simultaneous evaluation of K_o and ϕ. A common feature is that all of them used the bearing capacity theory of cone and wedges, proposed by Mitchell and Durgunoglu (1973) and Durgunoglu and Mitchell (1975). The important feature of this theory is that it takes into account the important K_o and ϕ variables. In simple terms, the D & M equation for cohesionless soils is as follows.

$$q_f = c\, N_c \in_c + B\, \gamma_s\, N_{\gamma q} \in_{\gamma q} \qquad (2.10)$$

where, q_f = ultimate bearing capacity, c = cohesion, B = penetrometer width, γ_s = unit weight of soil, N_c, $N_{\gamma q}$ = bearing capacity factors and $\in_c$,$\in_{\gamma q}$ = shape factors, determined from Durgunoglu and Mitchell (1975) and Brinch Hansen (1961, 1966) equations, respectively. For simplicity, Durgunoglu and Mitchell (1975) produced a chart giving values of shape and bearing capacity factors as a function of angle of friction, relative depth and penetrometer to soil friction angle.

Lunne and Mitchell (1977) worked out the product $N_{\gamma q} \cdot \in_{\gamma q}$ for a cone with 60° apex angle, 10 sq cm tip cross section and plotted it as a function of relative depth and K_o. These standard charts can be directly used if penetrometers of exact dimensions are used under similar conditions.

Given below is a description of various methods which have been proposed for the evaluation of ϕ and K_o. All these methods require the application of either DMT or both DMT and CPT.

2.4.1 Schmertmann (1982) method for the determination of ϕ

Schmertmann (1982) realised that penetration of dilatometer blade into the soil involves a bearing capacity failure. He determined the dilatometer blade bearing capacity from DMT thrust data by accounting for the various frictional forces and equated it to the D & M equation. The approximate value of K_o required in this equation was calculated from the Marchetti (1980) correlation and the penetrometer to soil friction value was assumed to be 0.5. All the other unknowns were known and the only unknown ϕ was evaluated. As the dilatometer blade penetration

approximates plane strain conditions, (length/breadth = 7), the ϕ yielded by this method can be used for plane strain conditions.

Schmertmann (1982) also did a parametric study of Durgunoglu and Mitchell equation (1975). The theoretically derived cone bearing capacity, q_c, and dilatometer blade bearing capacity, q_d, were compared for different key variables, namely, the angle of friction, K_o and relative depth. It was found that the theoretically derived q_d/q_c ratios do not vary significantly with K_o or relative depth and varied primarily with ϕ'. Such a variation of q_d/q_c with ϕ' led to a relation, analytically represented in the following form.

$$q_d/q_c = 2.3 - 0.04\ \phi_{ps}' \qquad (2.11)$$

where,

q_c = cone tip resistance,

q_d = dilatometer blade tip resistance,

ϕ_{ps}' = effective angle of friction for plain strain conditions.

According to this finding, if values of q_d and q_c are available from adjacent locations, ϕ_{ps}' can be evaluated. Schmertmann's (1982) method could be in error, because it assumes the dilatometer rod to soil friction as zero. Such an assumption was necessary in order to abstract q_d from DMT thrust data, as the standard dilatometer blade is not fitted with a load cell. In practice, some friction definitely exists between soil and push rods and neglecting it totally does not appear logical.

Schmertmann (1982) commented that the use of Durgunoglu and Mitchell (1975) theory results in conservative values of ϕ' and this conservatism was counterbalanced when assuming dilatometer blade to soil friction angle as zero. This method was recommended for further trials.

2.4.2 Schmertmann K_o - K_D - ϕ Correlation (1983)

Based on the available calibration chamber data, Schmertmann (1983) drew a tentative correlation between K_o and K_D with ϕ as a parameter. The results of ϕ predicted from this correlation are shown in Figure 2.8, superimposed over Marchetti's (1980) correlation results It can be seen that K_o, K_D correlation is different for different values of ϕ. The correlation between K_o, K_D and ϕ was expressed by Schmertmann (1983) as:

$$K_o = \frac{40 + 23\,K_D - 86K_D(1 - \sin\phi_{ax}') + 152\,(1 - \sin\phi_{ax}') - 717(1 - \sin\phi_{ax}')^2}{192 - 717\,(1 - \sin\phi_{ax}')} \quad (2.12)$$

Where, ϕ_{ax}' = effective angle of friction for axial strain conditions and is same as ϕ', as determined from standard triaxial compression tests.

2.4.3 Schmertmann, Durgunoglu and Mitchell method (1983)

Use of Equation, (2.12), requires the knowledge of one of the two unknowns, K_o or ϕ_{ax}'. So Schmertmann (1983) proposed a method of simultaneous evaluation of K_o and ϕ_{ax}', using DMT and CPT data, aiming at evaluating K_D from DMT and q_c from the CPT

This method consists of the following steps.

1. K_D is measured from DMT and cone tip resistance, q_c, from CPT, at the same depth.
2. A trial value of K_o is assumed.
3. A trial value of ϕ_{ax}' or ϕ_{ps}' is obtained from $\phi_{ax}' = f(q_c)$, or $\phi_{ps}' = f(q_d)$, using D & M equations (Durgunoglu and Mitchell, 1975).
4. If ϕ_{ax}' is obtained from q_c, then K_o is calculated in Step 5. On the other hand, if ϕ_{ps}' is estimated from q_d, ϕ_{ax}' is obtained by using either Equation 2.13a or 2.13b, relating the plane to axial strain friction angles, as proposed by Schmertmann (1983).

$$\phi_{ax}' = \phi_{ps}' - (\phi_{ps}' - 32) / 3 \text{ for } \phi_{ps}' > 32^\circ \quad (2.13\,a)$$

$$\phi_{ax}' = \phi_{ps}' \text{ for } \phi_{ps}' \leq 32^\circ \quad (2.13\,b)$$

5. Using ϕ_{ax}', as calculated in Step 4, K_o is computed from Equation 2.12.
6. The value of K_o, calculated in Step 5, is compared with the trial value assumed in Step 2.
7. Steps 2 to 6 are repeated until the value of K_o agrees to within 10 %.

In order to check the reliability of this procedure, six of the earlier calibration chamber test data (Jamiolkowski et al., 1979; Baldi et al., 1981, 1982, 1986 ; and Bellotti et al., 1982), on pluvially deposited medium fine quartz sand from the Ticino

river, were analysed by Schmertmann (1983). Considering ideal laboratory conditions and artificially deposited sands, this method yielded reasonable values of K_o. On the whole there is a tendency for K_o to be overestimated and the ratio of Schmertmann K_o to the actual was 1.22 ± 0.18.

2.4.4 Marchetti compact graphical form of D & M equation

Schmertmann's method of applying the D & M equation (1983) was further summarised by Marchetti (1985), as shown in Figure 2.9. The chart can predict friction angle from q_c if an estimate of K_o is available.

An analysis of the chart by Marchetti showed that (a) the maximum difference between $\phi_{D\&M}$ (Schmertmann, 1983) and ϕ predicted from Figure 2.9 was 0.2°, at a depth of 2 metres, and (b) the maximum error was 0.8°, at a depth of 1 metre. These errors were found in the most unfavourable zone of this chart, where $\phi > 46°$.

2.4.5 The compact K_o chart (Marchetti, 1985)

The Schmertmann method of applying the D & M equations involved complex computations, and the earlier chart, Figure 2.9, had two unknowns. So, Marchetti (1985) suggested another chart in which one of the unknowns was eliminated, shown in Figure 2.10.

This chart was also obtained from the Schmertmann D & M method. In this chart, one of the two unknowns, ϕ, is eliminated, leaving only one unknown K_o. Hence this chart is a simplified version of Figure 2.9. From this chart K_o can be estimated if K_D and q_c are known. Having obtained the value of K_o from this chart, Figure 2.9 can be used to estimate the friction angle, ϕ. The curves in Figure 2.10 can be expressed by the following analytical form for predicting the values of K_o, given in Equation 2.14.

$$K_o = C_1 + C_2 K_D + C_3 \left\{ \frac{q_c}{\sigma_v'} \right\} \qquad (2.14)$$

where, C_1, C_2, C_3 are coefficients experimentally determined from calibration chamber tests, conducted on Po river sand. Marchetti (1985) prescribed values of 0.376, 0.095 and -0.0017 respectively, for these constants.

Baldi et al. (1986) also conducted calibration chamber tests on the Po river sand for different boundary conditions and modified the coefficients slightly. The new values of C_1, C_2, C_3, as suggested by Baldi et al. (1986) were respectively (0.376), (0.095) and (-0.0046).

In natural sands, some modifications in the values of C_1, C_2, C_3, would be necessary to take account of local conditions and experience. The value of K_o, calculated by Equation 2.14 can be used together with the graphical form of Marchetti (1985), Figure 2.9, for estimating the value of ϕ.

2.4.6 The dual scale K_o chart (Baldi et al, 1986)

For the purpose of re-evaluating the accuracy of his compact K_o chart, Marchetti (1985) referred to the Po river valley sand data of Jamiolkowski et al. (1985). This was slightly overconsolidated sand with known overconsolidation ratio ranging from 1.3 to 1.7, and K_o ranging from 0.5 to 0.6. Some 90 pairs of adjacent DMT and CPT soundings were available. Out of these 90 pairs, 25 pairs of values of q_c and K_D were selected for the purpose of re-analysis resulting in Figure 2.10.

After comparing the two values of K_o (the first one obtained from Figure 2.10 and the second one obtained from the original test report of Jamiolkowski et al., 1985), it was noted that the average K_o predicted from Figure 2.10 was 0.92, considerably higher than the expected value of 0.55. The cause of the high values of K_o, obtained from Figure 2.10 was attributed to either (a) actual variation of K_o in the ground (b) local prestressing in the loose layers which increased K_D and (c) local cementation.

In brief, the Po river data on plotting along with the compact K_o chart indicated a shift of the curves to the right, especially for the higher values of K_D, (see Figure 2.11, referred to as the dual scale chart).

Figures 2.9, 2.10 and 2.11 appear to be the latest references available for determining the values of K_o and ϕ.

2.4.7 K_o - OCR relationship in soil

Once the values of K_o and ϕ' are known from one of the methods discussed earlier, established relationships between K_o and OCR can be used to predict the OCR values. Mayne and Kulhawy (1982) reviewed laboratory data from over 170 different soils

and simple empirical results relating K_o to OCR and ϕ' for normally consolidated and overconsolidated soils were presented.

The simplest relationship adopted was that of Schmidt (1966), which can be written as:

$$K_{ou} / K_{onc} = (OCR)^{\alpha} \qquad (2.15)$$

where,

K_{ou} = K_o during primary loading,
K_{onc} = K_o for normally consolidated soil, and
α = an exponent termed as the at rest rebound parameter of soil.

Schmidt (1966) proposed that the parameter "α" was uniquely related to effective friction angle, ϕ', of the soil. This approach appeared to be reasonable, based on the general trend between α and $\sin\phi'$. The hypothesis stated that:

$$\alpha = \sin\phi' \qquad (2.16)$$

Also, for the value of K_{onc}, several theoretical and empirical relationships have been postulated. Amongst these, the simplest and the most widely used is the formula of Jaky (1944).

$$K_{onc} = 1 - \sin\phi' \qquad (2.17)$$

A statistical analysis conducted by Sherif et al. (1974) on K_{onc} for cohesionless soils yielded the following relationship:

$$K_{onc} = 1 - 0.998 \sin\phi' \qquad (2.18)$$

Substituting the value of α from Equation 2.16 and K_{onc} from Equation 2.17, into Equation 2.15, the following relationship is obtained.

$$OCR = \left(\frac{K_{ou}}{1 - \sin\phi'}\right)^{\frac{1}{\sin\phi'}} \qquad (2.19)$$

Regardless of the methods used to calculate K_{ou} and ϕ', OCR can be determined from the Mayne and Kulhawy (1982) correlation, Equation 2.19.

Schmertmann (1983), modified Equation 2.19 to the following form:

$$OCR = \left(\frac{K_{ou}}{1 - \sin\phi'} \right)^{\frac{1}{0.8 \sin\phi'}} \qquad (2.20)$$

Equation 2.20 showed good agreement with the results of Hendron (1963) and was adopted for settlement predictions, together with DMT data (Leonards and Frost, 1988).

2.5 DMT and CPT data for settlement calculation

The dilatometer test gives soil compressibility data for the computation of foundation settlement. Schmertmann (1986a) proposed two methods for predicting settlement from DMT data; an ordinary method and a special method. The settlement of a flexible foundation of a given shape, size, loading magnitude and embedment depth is calculated via a step by step procedure. The details of the two methods are given below.

2.5.1 Ordinary method, Schmertmann (1986a)

1. A DMT sounding is performed at the site where settlement analysis is required. Profiles of the constrained tangent modulus, M, are obtained for the soil layers of interest.
2. The compressible soil layers of similar soils are divided into layers and sublayers.
3. For each layer and sublayer, the average value of M is obtained.
4. The vertical stress increase, at the mid height of each layer and sublayer is calculated by any suitable method.
5. The one dimensional settlement, S_i of each layer or sublayer is calculated using the following equation:

$$S_i = \frac{\Delta\sigma_v' \cdot H}{M} \qquad (2.21)$$

   where H = thickness of the layer or sublayer.
6. By adding all the contributions from the layers and sublayers in Step 5, the total one dimensional settlement is obtained.

2.5.2 Special method, Schmertmann (1986a)

The Schmertmann special method differs from the ordinary method in the sense that here all the layers and sublayers are taken into account in calculating the settlement. Also, some additional calculations are made to adjust M to average vertical effective

stress during the loading. The step by step procedure of the special method is as follows.

1. A DMT sounding at each settlement analysis location is done and the variation of M with depth is obtained through the soil layers .
2. The compressible soil is divided into layers and/or sublayers of similar soil type and stiffness.
3. The average value of M is obtained for each layer/sublayer.
4. The vertical stress increase, $\Delta\sigma_v'$, at the mid height of each layer/sublayer is calculated.
5. The initial effective overburden stress, σ_0', at the mid height of each layer/sublayer in Step 2 is calculated, before the settlement commences.
6. The value of effective stress at the time of performing DMT, σ_d', is also calculated at the mid point of every layer/sublayer. Generally, $\sigma_d' = \sigma_0'$ but the two may differ because of excavation, surcharge, dewatering etc.
7. If σ_0' differs from σ_d', then σ_0' is used for further calculations.
8. The preconsolidation pressure, p_c', is determined based on the overconsolidation ratio.
9. p_c' obtained in Step 8 is compared to $(\sigma_0' + \Delta\sigma_v')$ to check which compression case applies to each of the layers / sublayers. There can be three cases, namely:
   Virgin compression, where OCR = 1 ie. $(\sigma_0' + \Delta\sigma_v') > p_c'$
   Re compression, where OCR > 1 and $(\sigma_0' + \Delta\sigma_v') < p_c'$
   Re compression and virgin loading, where OCR > 1 and $\sigma_0' < p_c' < (\sigma_0' + \Delta\sigma_v')$
10. If the preconsolidation pressure $p_c' > (\sigma_0' + \Delta\sigma_v')$, then the M value for overconsolidation case is used and settlement involves recompression. On the other hand, if $(\sigma_0' + \Delta\sigma_v') > p_c'$ then the M value for normally consolidated soil is used.
11. The M value hence selected in Step 10 is incorporated in Step 3 and a realistic value of M is obtained.
12. The magnitude of settlement is obtained for each layer/sublayer using Equation 2.21.
13. The overall settlement of the foundation is calculated by summing up the settlement of the individual layer/sublayer.

Schmertmann (1986a) found that the DMT provided good estimates for the computation of settlement. The method involved the application of a simple and general stress-strain equation for one dimensional compression. Because the DMT determined M relates only to the in situ effective stress, using such M in settlement analysis required adjustments to the different effective stress levels applicable to the particular problem. Effects such as pseudo-elastic settlement, structural rigidity, three dimensional effects, creep, aging, etc, often cancel each other. Schmertmann (1986a) found an error of 10% in the results predicted by this method and therefore suggested that it could be used for most practical purposes.

2.5.3 Leonards and Frost (1988) method of predicting settlement of shallow foundations on granular soils

The Iowa stepped blade (Handy et al., 1982), Marchetti Dilatometer (Marchetti, 1980), Screw Plate and Self boring pressuremeter (Wroth and Hughes, 1973; Baguelin et al., 1974) are some of the in situ testing devices for predicting settlement of foundations. A number of researchers over the years found out that the resistances of the various penetration devices are not fully capable of sensing the effects of overconsolidation on the compressibility of soils (Lambrechts et al., 1978; Jamiolkowski et al., 1985, 1988; Bellotti et al., 1986 etc.) and there is need of an instrument which can directly sense the compressibility of soil.

Leonards (1985) argued that amongst all these tests, the most applicable one was the Marchetti dilatometer, as it is capable of sensing the soil compressibility directly, particularly in loose deposits, where compressibility could cause a major practical problem.

Leonards and Frost (1988) presented a method, based on Schmertmann (1970) method, for visualising the effects of overconsolidation in reducing the compressibility of all types of soils. They proposed a general method for the prediction of the settlement of shallow foundations, applicable both to normally consolidated and overconsolidated sands. A step by step description of this method is as follows.

1. At the location where settlement prediction is required, parallel DMT and CPT soundings are performed.
2. The soil profile is divided into layers of similar characteristics.

3. From DMT and CPT data, the average values of q_c/σ'_v and K_D are determined for each layer.
4. Making use of q_c/σ'_v and K_D and using the compact graphical form (Marchetti, 1985) or compact K_o chart (Baldi et al., 1986), $K_{(OC)}$ and ϕ_{ps}' for each layer is calculated.
5. ϕ_{ps}' is converted into ϕ_{ax}', using Equation 2.13 a, 2.13 b.
6. From ϕ_{ax}' and $K_{(OC)}$ calculated above, the OCR is calculated using Equation 2.19 or 2.20 for each layer.
7. The initial vertical effective stress, σ_v', is calculated at the centre of each layer.
8. The preconsolidation pressure, p_c', is calculated for each layer, using Equation 2.22

$$p_c' = \sigma_v' \times \text{O.C.R.} \tag{2.22}$$

9. The stress increase $\Delta\sigma_v'$ at the centre of each layer, due to the applied load, is calculated, based on the 2:1 (vertical : horizontal) load distribution assumption.
10. The final stress, σ_f', at the centre of each layer is calculated as

$$\sigma_f' = \sigma_v' + \Delta\sigma_v' \tag{2.23}$$

11. The portion of the load increment that falls in the OC range $[R_Z(OC)]$ and the NC range $[R_Z(NC)]$ are determined by the following equations.

$$[R_Z(OC)] = \left(\frac{p_c' - \sigma_v'}{\sigma_f' - \sigma_v'}\right) \tag{2.24 a}$$

$$[R_Z(NC)] = \left(\frac{\sigma_f' - p_c'}{\sigma_f' - \sigma_v'}\right) \tag{2.24 b}$$

12. The average value of E_D for each layer is calculated.
13. The value of strain influence factor I_Z is determined for each layer from Schmertmann et al.(1978) improved influence factor diagram.
14. The settlement of each layer is determined by the following equation:

$$S = c_1\, q_{net}\, I_Z\, \Delta_h \left[\frac{[R_Z(OC)]}{[E_Z(OC)]} + \frac{[R_Z(NC)]}{[E_Z(NC)]}\right] \tag{2.25}$$

where,

$$E_Z(OC) = 3.5\ E_D \quad (2.26\ a)$$

$$E_Z(NC) = 0.7\ E_D \quad (2.26\ b)$$

q_{net} = surface load excluding excavated earth
S = estimated settlement
c_1 = embedment correction
q_{net} = surface load - load of the excavated earth
Δ_h = height of the sublayer
E_D = dilatometer modulus

15. Repeat for all the layers and sum to give total settlement.

This method of settlement analysis using DMT data is the improved version of previous ones in the sense that it takes into consideration the effects of overconsolidation in reducing the soil compressibility.

2.6 Literature review of calcareous soil and CPT experience

2.6.1 Origin, location and characteristics of calcareous sediments

The sea bed comprises of approximately 30% calcium carbonate which originates from the decay of various sea organisms and its subsequent settlement on to the sea bed. Hence the sediments covering the sea beds are mainly biogenetic in nature.

Due to the on going offshore developments, it has become increasingly important to assess the properties of these sediments, as their properties differ from usual soils. Calcareous sediments, besides being present in the sea beds, are also present in locations which were once covered by the sea. The soil found in such locations consist mainly of sand and silt with varying percentages of carbonate content.

Rezak (1974) found that carbonate sediments (a) varied in size, shape and void ratio, (b) could not be compacted to the same density as non-carbonate sediments, (c) had lower shear strength than non-carbonate sediments and (d) were susceptible to dissolution, cementation, bio-erosion and bacterial activity.

Poulos (1980), after a thorough review of properties of carbonate soils, concluded that many of their properties were within comparable limits to those of conventional soils. However the high susceptibility to crushers and intermolecular cementation in

the case of carbonate soils play crucial role in strength and compressibility parameters. With the variations in carbonate content and degree of crushability, the behaviour of carbonate soils change.

Datta et al. (1979) found that soils with a carbonate content greater than 40% behaved like cohesionless soils. With a carbonate content less than 40% the soil gradually behaves like cohesive soils. It was also noticed that carbonate soils with low crushability suffered volume reduction during shear.

Joustra and Gijt (1982) performed crushing tests on many types of soils, including calcareous soils, using a Bol apparatus. The values of the coefficient of crushing, C_c, obtained for the calcareous soils of North Rankine and Bombay High were respectively 5.35 and 2.75. These values are higher than the C_c value of a typical quartz sand from Meuse river, which was 2.05. A visual study by Joustra and Gijt (1982) revealed that the crushing resulted in more disintegration of particles in calcareous soils, thereby causing a shift in the grain size distribution curve, making it appear more uniformly graded.

Kaggwa and Poulos (1990) found that carbonate sediments were less resistant to cyclic loading than the silica sands, mainly due to the greater tendency of particle crushing.

2.6.2 Classification system for carbonate sediments

Various classification systems have been proposed for carbonate sediments. These classification systems have been based on the grain size, base material, degree of induration or cementation, bedding or lamination, origin of carbonate and colour, etc.

Fookes and Higginbottom (1975) proposed a classification system based on grain size and degree of cementation. Clark and Walker (1977) took into consideration the origin of the carbonate particles, in addition to grain size and degree of induration, for classifying them.

Fugro (1979) utilised the CPT q_c for classifying the various carbonate sediments, as shown in Figure 2.12. Beringen et al. (1982), proposed a chart, based on the CPT data to demarcate carbonate sands from clays, with varying degrees of induration. Beringen et al. (1982) also found that their line fitted well the data obtained from North sea and Bombay High soils.

Joustra and Gijt (1982) examined the CPT data, obtained from offshore regions of Australia and India and observed that the cone resistance, q_c, was as high as 76 MN/m^2 whereas unit sleeve friction, f_s, remained as low as 0.50 MN/m^2 in 90% calcareous soil. In general the CPT data on calcareous soils revealed high cone resistance and low friction ratios.

2.6.3 CPT experience in calcareous sediments

Ortigo et al. (1986), used CPT to calculate the values of angle of friction, ϕ, of calcareous sediments at Campos Basin, Brazil. The carbonate content of this soil was between 25 to 30% and the submerged density was approximately 8 kN/m^3. The values of ϕ were evaluated from CPT correlations established by Senneset and Janbu (1982) and Campanella and Robertson (1983), for clean silica sands.

Samples were then recovered from the test site and shear box tests conducted on these samples to determine the angle of friction, ϕ. The calculated cohesion was small and could be neglected. The laboratory obtained ϕ values were compared with CPT interpreted values. This comparison showed that the laboratory obtained maximum and minimum values of ϕ fell within the limits of CPT interpreted values.

Ortigo et al. (1986) concluded that the CPT interpreted ϕ values in the calcareous sediments of Campos Basin were suitable for assessment of skin friction of offshore piles.

2.7 Discussion

The whole literature review of DMT and CPT on cohesionless soils can broadly be summarised under two headings, namely, (a) DMT and CPT tests in pure silica sand and (b) DMT and CPT tests in calcareous sand. A summary of both the cases is given below.

2.7.1 Summary for silica sand

Both the DMT and CPT are simple, swift and cost effective in situ testing devices and are excellent profiling tools (Ervin, 1985). The DMT has also proved to be useful in providing compaction control (Schmertmann et al., 1986; Hryciw and Dowdig, 1988). Both the DMT and CPT correlations have been formulated with the help of

calibration chamber tests because of difficulties in obtaining undisturbed samples and refer to clean silica sands.

The DMT has the advantage over the CPT of measuring the horizontal stress of the soil. It can be used with CPT for recording the extra horizontal stress readings, which is helpful in the evaluation of important soil properties, such as K_o, ϕ, OCR and p_c'. The evaluation of K_o as a function of K_D and $\left(q_c/\sigma_v'\right)$, with the combined use of DMT and CPT, is the best procedure at present for the determination of K_o in uncemented and predominantly quartz sand.

The Dilatometer is presently the most practical tool for evaluating OCR and preconsolidation pressures in sand. The DMT obtained values of OCR and p_c' are used for the calculation of foundation settlements and the results have been found to be within acceptable limits of accuracy. The ratios of calculated to measured settlements fall in the range of 1.2, adequate for most practical purposes.

There are contradictory findings regarding the evaluation of constrained modulus, M, based on the M versus E_D correlation (Marchetti, 1980). According to some of the findings, the DMT gives reliable estimates of M in loose and normally consolidated sand whereas others are of the opinion that it underestimates the values of M in overconsolidated sands.

2.7.2 Summary for calcareous sand

The DMT has not been previously used in calcareous sand for the purpose of identification or evaluation of properties. However, there is some CPT experience available in calcareous sand. The values of angle of friction, ϕ, evaluated for a soil containing 90% carbonate content and assuming uncemented behaviour, was found to be within the maximum and minimum laboratory evaluated results and was used for pile design.

The CPT obtained values of q_c and f_s in calcareous sediments are found to be respectively too high and too low compared to silica sand and therefore it can be successfully used for their identification.

Calibration chamber tests reflect that the M versus E_D correlation (Marchetti, 1980) corresponds well to data obtained from sand possessing intermolecular attraction.

However, the K_o versus K_D correlation (Marchetti, 1980) over predicts the K_o values in cemented sands because of the extra horizontal strength due to cementation.

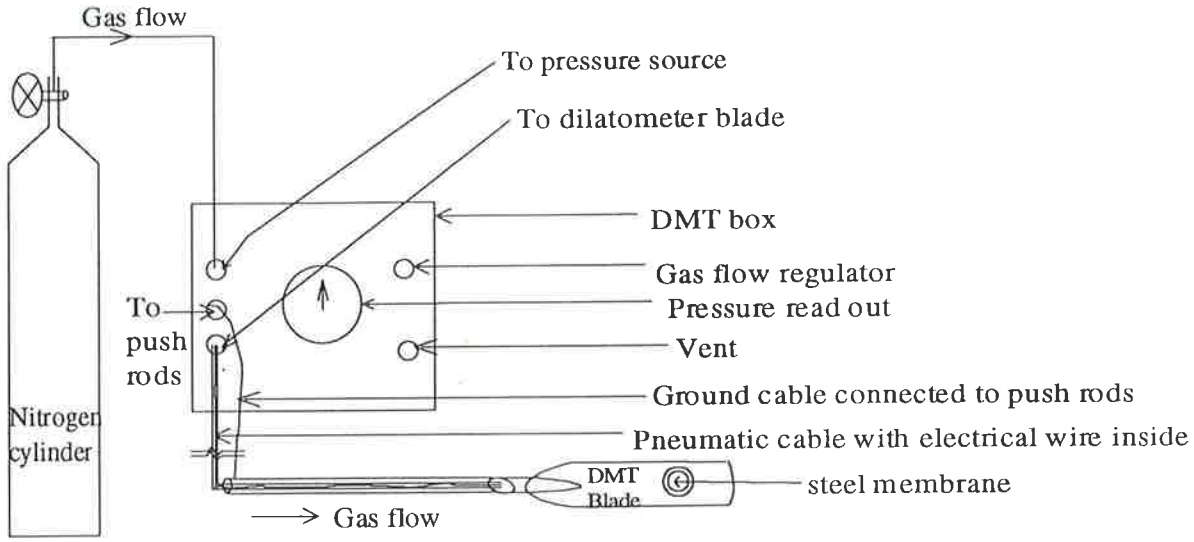

(a)

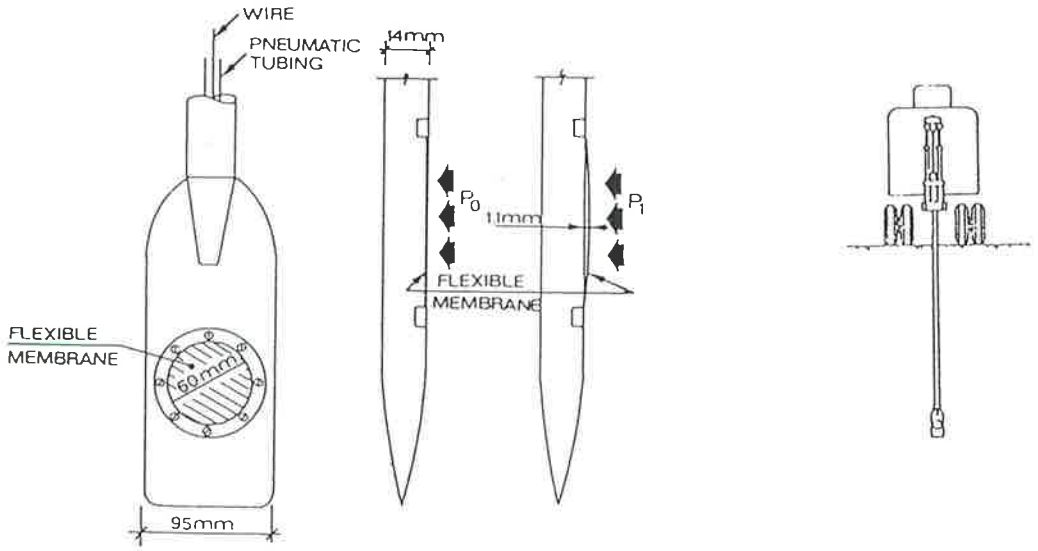

(b) (c)

Figure 2.1 Marchetti flat dilatometer (a) the assembly; (b) dilatometer blade; (c) penetrating dilatometer blade.

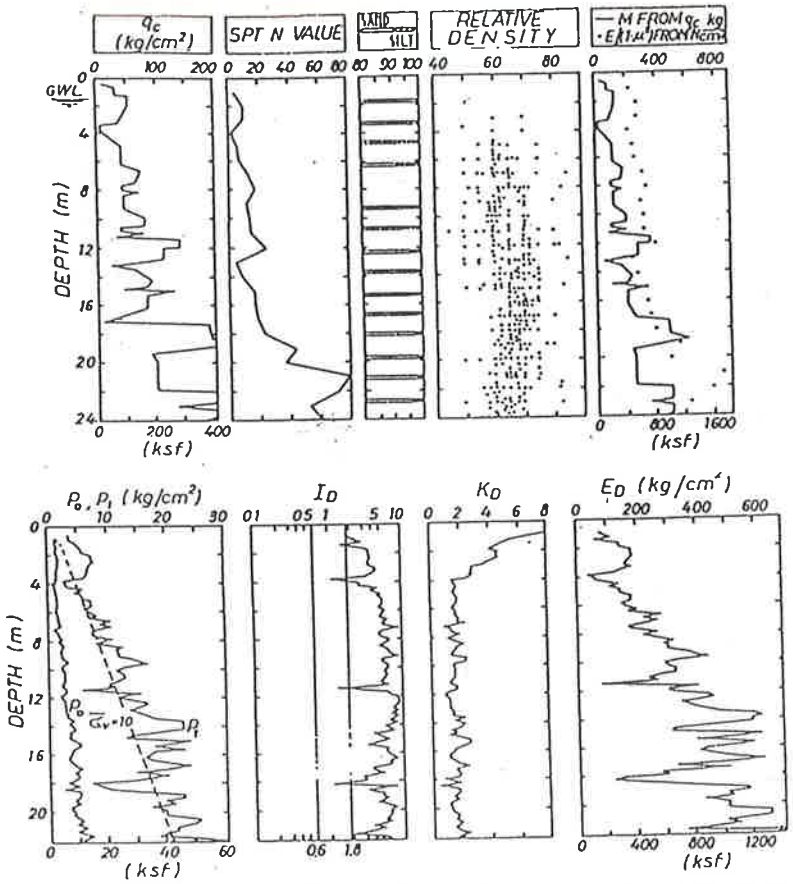

Figure 2.2 Soil data and DMT results at Torre Oglio, Italy (Marchetti, 1980)

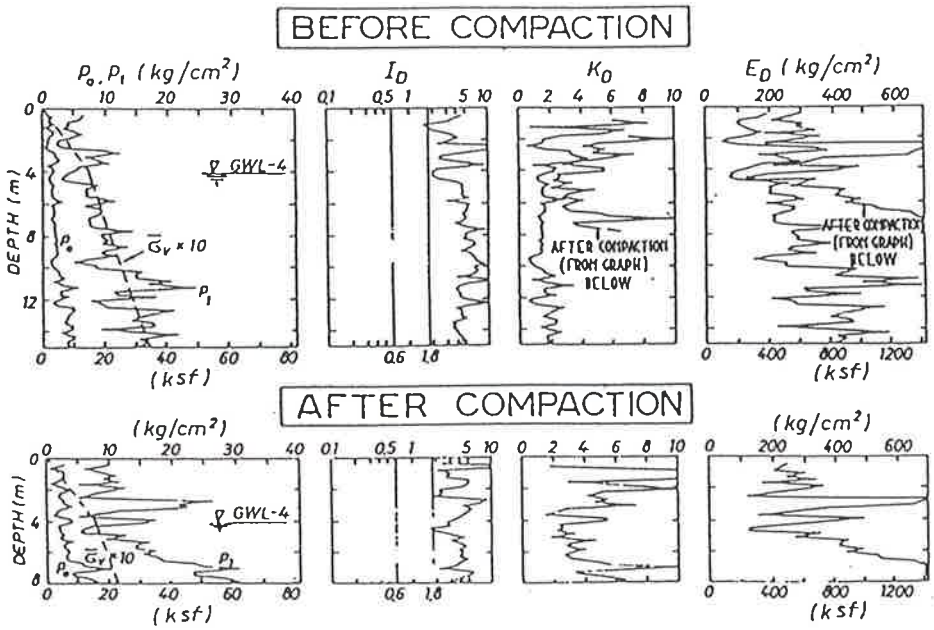

Figure 2.3 DMT results at Damman, Saudi Arabia (Marchetti, 1980)

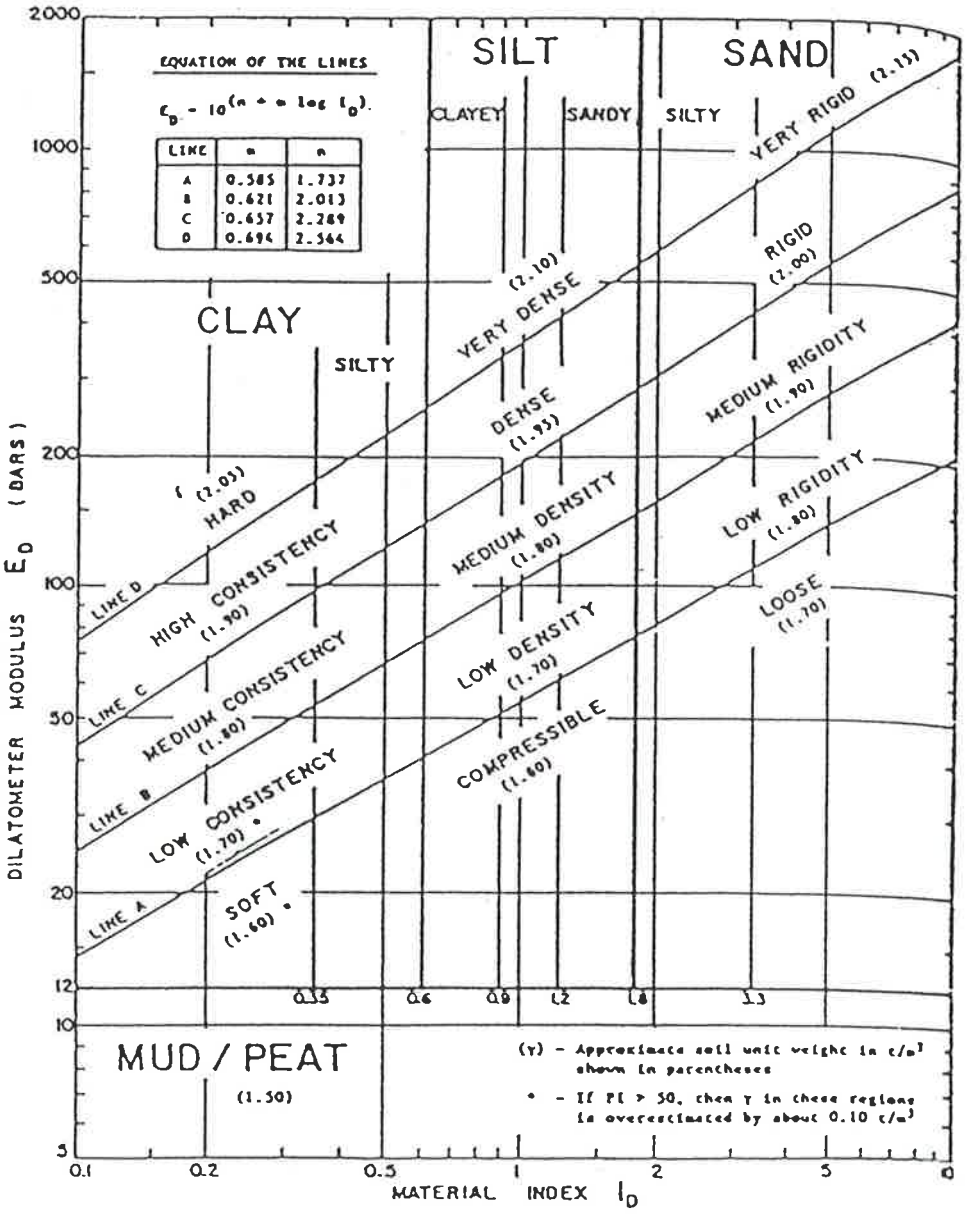

Figure 2.4 **Soil classification and approximate soil density based on E_D and I_D (Schmertmann, 1986)**

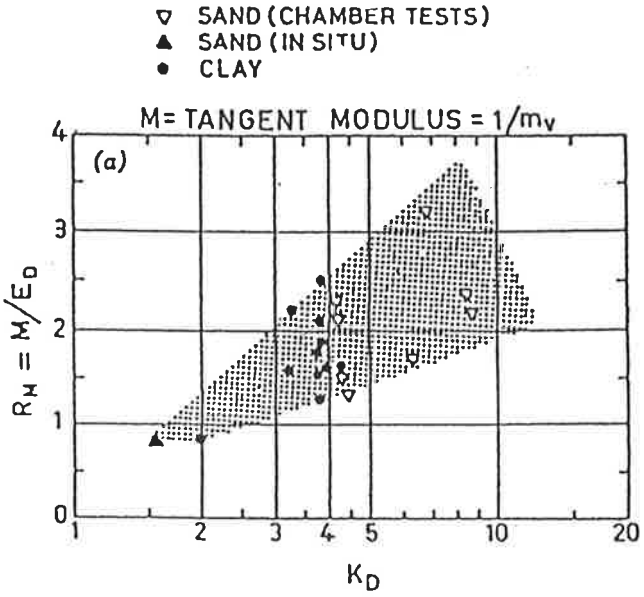

Figure 2.5 **Correlation between R_M and K_D for predicting M (Marchetti, 1980)**

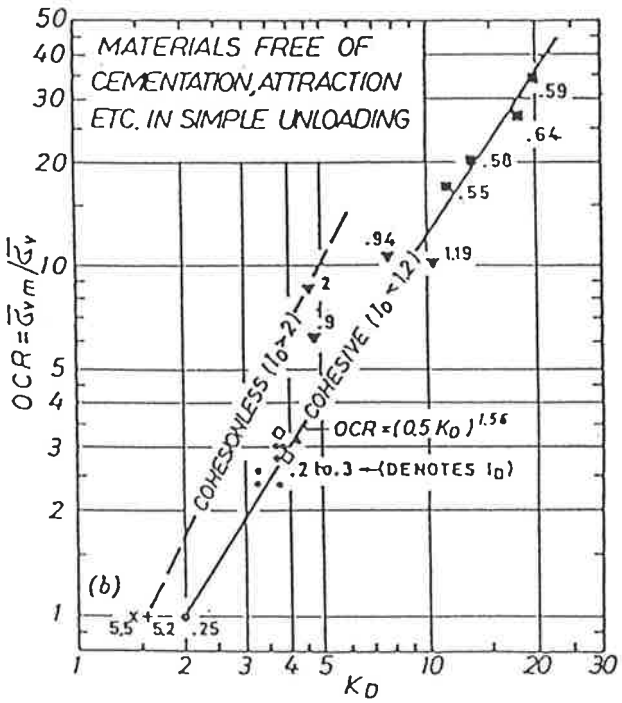

Figure 2.6 **Correlation between OCR. and K_D for predicting OCR (Marchetti, 1980)**

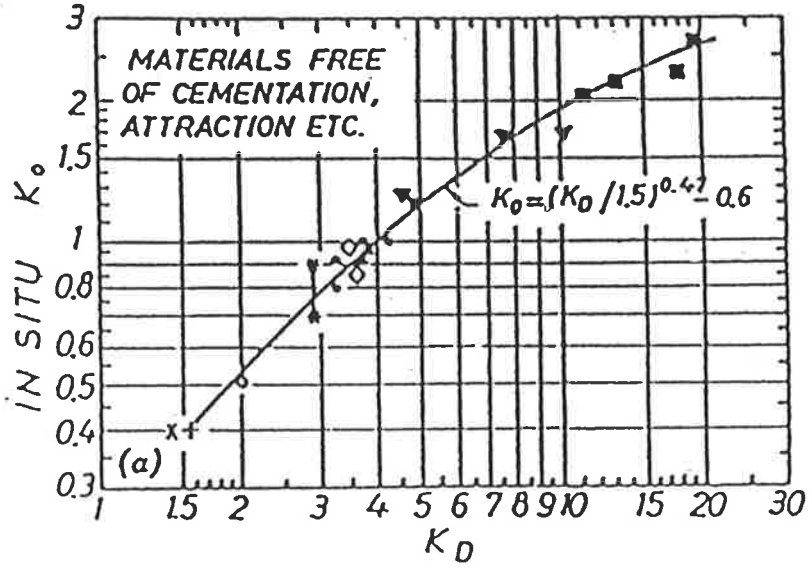

Figure 2.7 Correlation between K_o and K_D for predicting K_o (Marchetti, 1980)

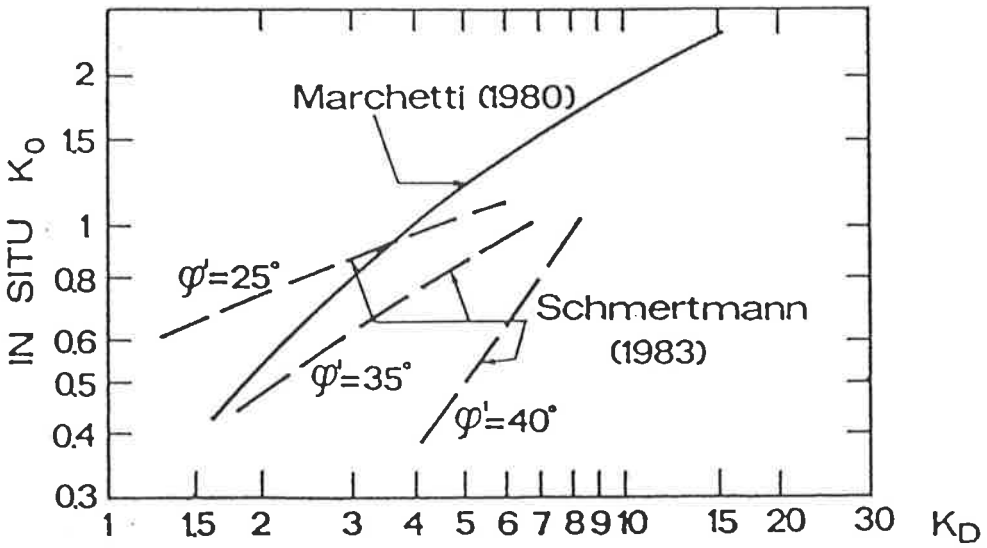

Figure 2.8 Values of ϕ predicted from Marchetti (1980) and Schmertmann (1983) correlation (Marchetti, 1985)

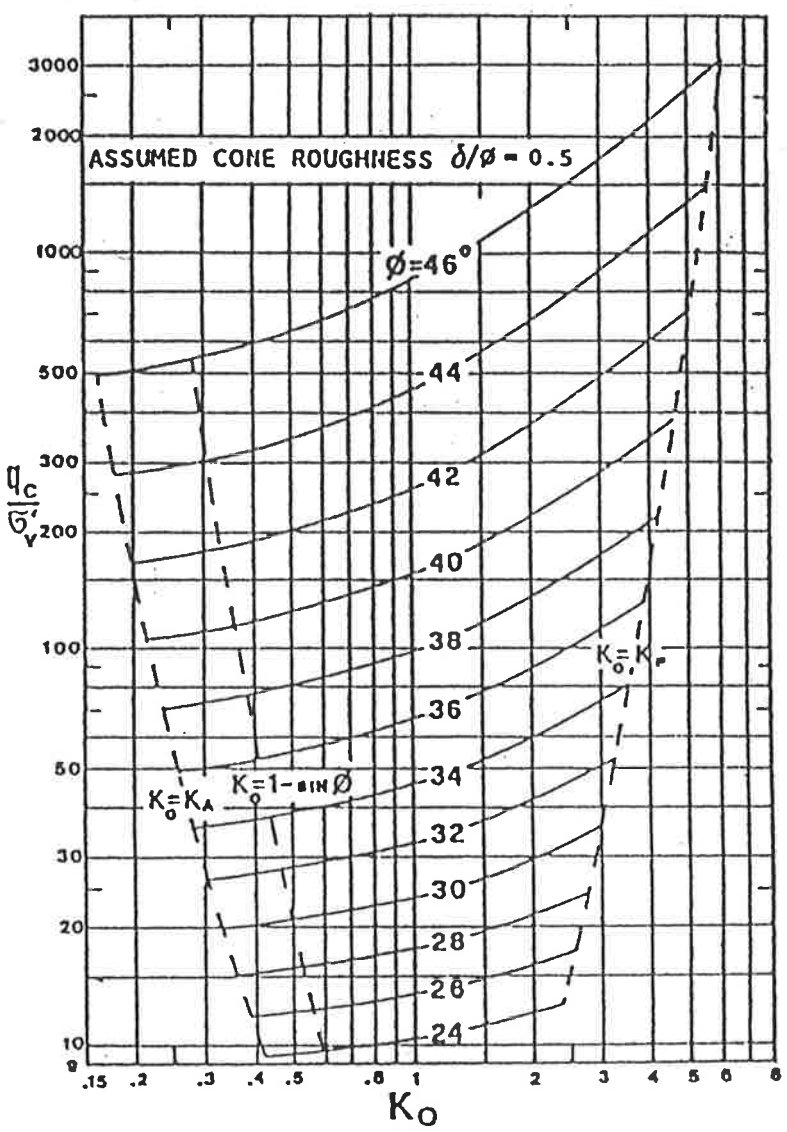

Figure 2.9 **Compact graphical form for predicting K_o and ϕ (Marchetti, 1985)**

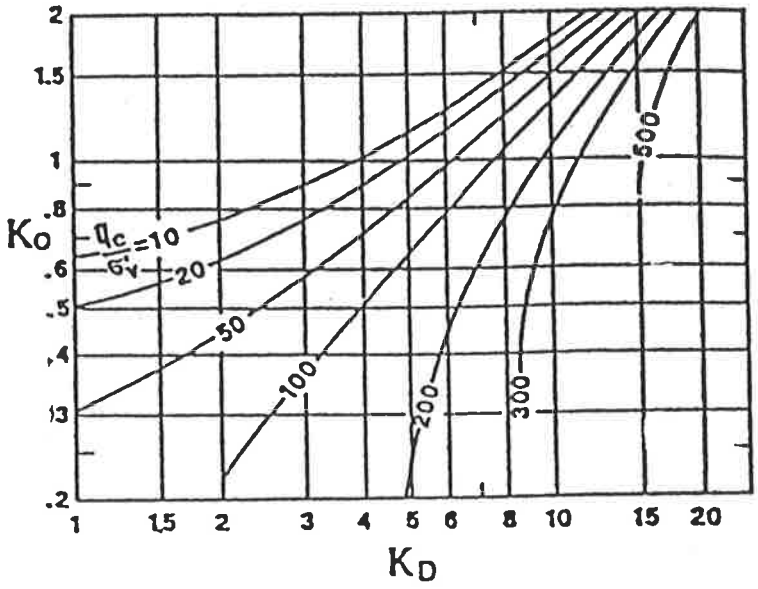

Figure 2.10 Compact K_o chart for predicting K_o from K_D and q_c (Marchetti, 1985)

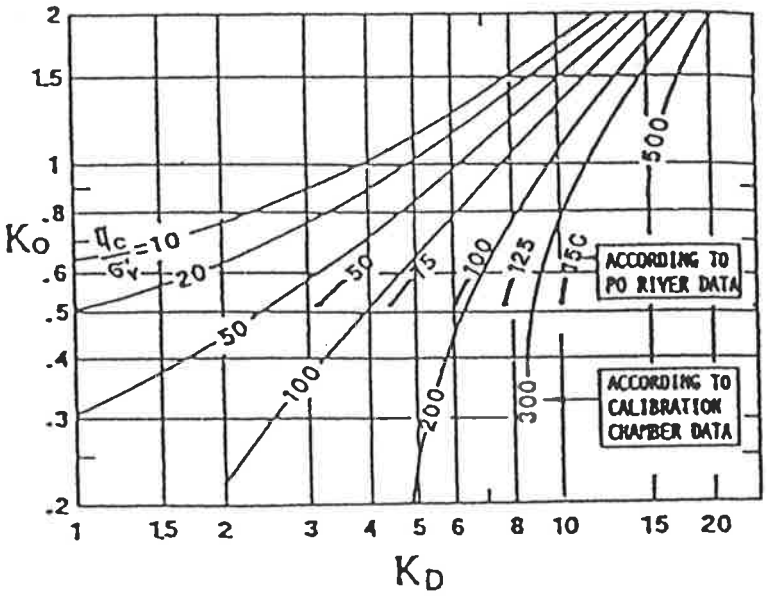

Figure 2.11 Dual scale K_o chart, showing a shift of curves when fed with Po river data (Baldi et al., 1986)

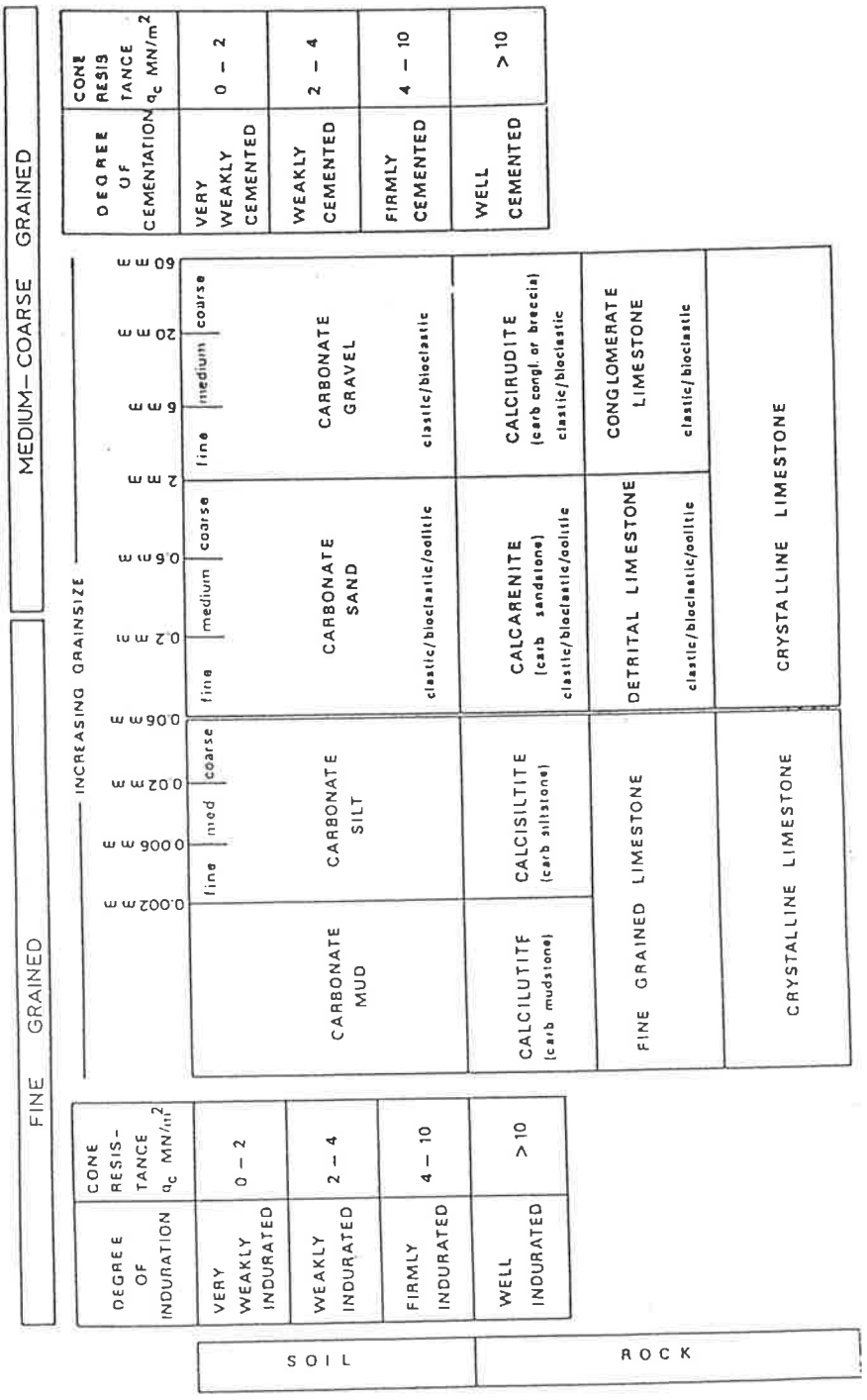

Figure 2.12 Classification of carbonate sediments based on CPT data (Fugro, 1979)

Chapter 3

MODIFICATIONS TO THE DILATOMETER AND DESCRIPTION OF TESTING PROGRAM

3.1 Introduction

After a literature review of dilatometer tests on cohesionless soils and subsequent dilatometer testing on calcareous sediments, it was realised that the standard dilatometer had certain limitations and it would be more effective if a number of changes were made to the existing equipment. The reasons for incorporating these changes, the way these changes have been done and the standard procedure for conducting the modified dilatometer tests on field are described in this chapter. In the subsequent sections the field test site selection and field and laboratory testing programs are described

3.2 Modifications to the dilatometer

Some of the major drawbacks of the standard dilatometer are as mentioned below.

(a) The greatest, and probably the most important drawback of the standard dilatometer, is that it relies on the pressure readings at three key positions only and presumes a universal linear relation between deflection and pressure. Therefore, the various soil properties and the modulus of elasticity, in particular, are susceptible to error.

(b) In gravelly and cemented soils, the membrane frequently encounters a gravel, shell or crust, blocking further membrane expansion and pressure reading P_B is not achievable, thereby making the interpretation of that particular layer impossible.

(c) In very weak and compressible soils, where settlement can cause major problems, the present dilatometer occasionally fails to give the first signal at pressure reading P_A. This is because the horizontal pressure in weak soils is not enough to keep the membrane in contact with the blade surface and the membrane protrudes outwards to a deflection more than 0.05 mm, resulting in no initial pressure reading P_A upon pressurisation. In such a condition either a more flexible membrane is used or a suction pressure is applied, to get the pressure reading P_A.

(d) There is no provision of measuring the dilatometer blade tip resistance which could be helpful in the evaluation of the angle of friction.

(e) Due to the manual recording of the DMT readings, there is possibility of operator error, and variability of actual reading with different operator.

In order to make the dilatometer more effective a number of changes were done to the existing dilatometer device. These modifications included the addition of a load cell, the alteration of the membrane assembly, as well as automatic data acquisition.

3.2.1 Addition of load cell

The original DMT equipment, developed by Marchetti (1980) and later standardised by Schmertmann (1986), has no means of measuring the dilatometer blade tip resistance, q_d. However, evaluation of the angle of friction in sand by the DMT requires, in addition to the usual pressure and deflection readings, measurement involving bearing capacity failure, which is not available from membrane deflection. Instead q_c values from a CPT, conducted adjacent to DMT, are used. This may lead to significant error if the nature of soil changes abruptly. So recording directly the DMT blade tip resistance, q_d, at the same spot was considered necessary and a load cell was installed between the top of the dilatometer blade and the push rods (see Figure 3.1).

By doing so, recording of the q_d value exclusive of the frictional forces, mobilised along the rods, is possible. Measuring q_d this way is more accurate than measuring the total thrust value because the later includes all the frictional resistance of the soil on the push rods and dilatometer blade.

3.2.2 Alteration to dilatometer membrane assembly

3.2.2.1 Reasons and benefits of alterations

In order to examine the validity of the basic assumption that there is a linear relationship between the dilatometer membrane deflection and pressure, it was decided to investigate the variation of membrane deflections with pressure. Determination of pressure versus membrane deflection relationship is useful because:

(a) The DMT causes minimal soil disturbance during penetration and the stress versus strain behaviour in situ can be determined with more reliability, rather than using laboratory tests.

(b) Where the expansion of the membrane into the soil causes any failure, the critical deflection to cause failure as well as the mode of failure, can be obtained.

(c) The deflection curve can be used to examine the behaviour of the soil, whether linear or non-linear.

(d) The deflection curve can be used to determine the Young's modulus of calcareous sediments, for which the existing correlations are not directly applicable.

3.2.2.2 Provision of strain gauge and pressure transducer

In order to obtain continuous and accurate measurement of membrane deflections, the dilatometer membrane assembly was changed. The concept of the new assembly was originally developed at the University of Adelaide (Auricht and Sheffield, 1989). It is based on a cantilever spring, capable of moving forwards and backwards depending on pressurisation or depressurisation of the membrane. On either side of the cantilever spring are two electrical strain gauges. Any movement of the spring causes a change in the length of the strain gauges, thereby changing the resistance, which causes a corresponding change in the output voltage, which is converted to a

digital read out to give a direct measurement of the membrane deflection. This is illustrated in Figure 3.1.

For the measurement of internal gas pressure corresponding to various deflections, an electrical pressure transducer was connected in the pressure line to the membrane and connected to the data acquisition system. Figure 3.2 shows a schematic of the modified dilatometer connections, together with the data acquisition system.

The modified dilatometer with such a modified membrane assembly is capable of emitting up to 100 intermediate readings of deflection and pressure for pressurisation as well as depressurisation. The exact number of these readings is based on the speed of the microcomputer.

3.2.3 Automation of DMT equipment

Jaksa (1990), and Jaksa and Kaggwa (1994) described the development of a data acquisition system at the University of Adelaide for the swift and automatic recording of CPT data. This data acquisition system uses a personal computer and a microprocessor interface together with the electric cone penetrometer. The CPT data comprising of cone tip resistance and sleeve friction values are obtained from the strain gauges of the electric cone penetrometer in microvolts, in the form of analogue signals and are received by the interface, where they are amplified and converted to digital values. Also part of the data acquisition system is the software which interacts with the interface in order to accomplish the following.

(a) The digital values sent by the interface between the range of 0 to 1023 is converted to the actual values of tip resistance (0 to 15 MPa), and sleeve friction (0 to 4000 kPa).
(b) This processed data is scrolled on the screen of the computer, mounted on the field truck, while the test is in progress.
(c) The processed data is saved on to a disc, at regular intervals or during the withdrawal of the cone from the soil, for post processing.

This data acquisition system has proved useful where a large number of tests are to be done and data is to be recorded at close intervals with precision. This CPT data acquisition system was modified for the automated DMT as a part of this research (Kaggwa, et. al. 1995). A number of changes to hardware and software (refer to

flow chart shown in Figure 3.3) of the CPT data acquisition system were undertaken, so that it could perform the following tasks:

(1) When the DMT blade is being jacked into the ground, q_d values are emitted from the load cell strain gauge every 5 mm of penetration, received by the microprocessor interface, converted to digital readings (0 to 1023), preprocessed by DMT software and displayed in numerical figures on the computer screen in the in the range of 0 to 15 MPa.

(2) When the jacking of the DMT blade is stopped and the membrane is pressurised, readings of deflection and pressure are emitted from the membrane strain gauges and received by the microprocessor interface at deflection intervals of 0.001 mm or as specified. These readings are converted from analogue to digital values (0 to 1023) in the microprocessor interface, preprocessed by the DMT software (deflection in the range of 0 to 1.1 mm and pressure in the range of 0 to 4000 kPa) and scrolled on the computer screen in numerical figures while test is in progress.

(3) The maximum deflection to which deflection and pressure readings are obtained is 1.1 mm, after which an audio signal is received, indicating pressurisation is to be stopped to prevent the membrane from permanent deformation.

(4) Immediately after hearing the audio signal, the pressure is released and recording of readings for depressurisation stage is done.

(5) From the computer screen display, it is determined whether the membrane deflection has completely ceased upon depressurisation or not, after which the DMT data is saved to the disc and penetration resumed.

(6) Every time penetration is resumed, the previous deflection and pressure readings are saved to a preformatted disc. Similarly, every time the membrane pressurisation is resumed, the previous q_d values are saved. This arrangement ensures that all readings are saved onto disc, at regular intervals.

(7) Since a large amount of data is to be recorded, which includes the depth of penetration, dilatometer blade tip resistance, membrane deflection, and dilatometer pressure, the data is saved at regular intervals, thereby making the

entire random access memory of the microcomputer available for the temporary data storage once again.

(8) The entire data is recorded on to the disc in the form of four vertical columns, ie. depth, dilatometer blade tip resistance, membrane deflection and pressure values.

(9) The data saved on the disc is readily transferable to IBM computer in the office for further cleaning, data reduction, plotting and interpretation of results.

3.3 Checks of modified dilatometer

3.3.1 Laboratory checks

The primary aim of the laboratory test checks of the modified dilatometer was to ensure that the software worked effectively in conjunction with the hardware and the signals for depth, dilatometer blade tip resistance, deflection and pressure, emitted from the respective strain gauges were received, processed, displayed and recorded correctly. This part of the test check was conducted in the instrumentation workshop by connecting the various components of the modified dilatometer assembly as shown in the Figure 3.2. The precision of the load cell and deflection strain gauges together with the pressure transducer were also checked and calibrated.

The first few tests were conducted by burying the modified dilatometer blade in sand and pressurising the membrane. The data displayed on the computer screen and recorded on the floppy disc was examined. After a few trials and necessary changes in the hardware and software the functioning of the modified dilatometer was found to be satisfactory.

3.3.2 Preliminary field checks for robustness

After satisfactory functioning of the modified dilatometer in the instrumentation laboratory, it was checked under field conditions. There are a number of problems linked with robustness of all components of any field testing device.

For the field test checks, the same site was used where the actual field tests were finally done. A number of modified dilatometer and standard dilatometer tests were conducted adjacent to each other. As both the dilatometers give pressure readings at

key positions of 0.05 and 1.1 mm membrane deflections, a comparative study of the pressure readings obtained from the two dilatometers was made possible. This also assisted in further calibration of the modified dilatometer membrane, as discussed in the following sections. Some of the points noted during the preliminary field test checks are as follows.

(a) The modified dilatometer required setting of the membrane to a fixed reference position prior to the commencement of any test, which is to be strictly followed in order to get all the deflection readings with reference to that zero position so that results from different test spots could be comparable.

(b) The zeroing of membrane deflection should preferably be done at underground temperature as the outside temperature is different to the underground temperature.

(c) When the contact and expansion pressure readings P_0 and P_1 obtained from the two dilatometers were compared, it was found that the expansion pressure readings were slightly lower in the case of modified dilatometer, compared to the normal dilatometer.

The above crucial aspects and differences of the modified dilatometer needed further improvements for which calibration of the modified dilatometer was done with the help of a sensitive micrometer and also calibration chamber tests were conducted in water.

3.3.3 Calibration with micrometer

For accurate calibration of the dilatometer membrane deflection, it was necessary to check the interface generated digital readings of deflection with an accurate micrometer. This was done in the instrumentation laboratory by putting the modified dilatometer blade on a horizontal surface in air and placing the micrometer on the dilatometer membrane in such a way that its tip made contact with the centre of the membrane. The membrane was pressurised and a set of deflection readings were recorded at regular intervals from the micrometer (0 to 1.1 mm) as well as the computer (0 to 1023). A plot of micrometer versus computer digital readings is shown in Figure 3.4. This graph shows that there is a non linear relationship between the computer digital readings and the actual micrometer deflection readings.

For solving this problem, a polynomial function was used to obtain a regressed curve (see Equation 3.1 below) expressing the relationship between the actual deflection and the computer read digital values of deflection.

$$y = A + B(x) + C(x^2) \qquad (3.1)$$

where, x = digital readings of deflection ranging between 0 and 1023
y = actual deflection reading in mm, measured by micrometer

The coefficients A = - 0.45, B = 0.0026 and C = 7.2 (10^{-7}) were experimentally determined. This equation was incorporated into the computer program so that the computer obtained digital values of deflection were automatically converted to the regressed values and any error in reading deflection was minimised.

Such a calibration of digital deflection readings, read through the computer, was made a routine feature as the same calibration may not hold good all the time and a variation in the coefficients of the equation may prove necessary after repeated use and wear and tear of the instrument.

3.4 Calibration chamber tests

Calibration chamber tests were conducted to check the functioning of modified dilatometer under water, subjected to known external pressures and for studying the membrane stiffness. The details of the calibration chamber, the method of testing and results are described in this section.

3.4.1 The calibration chamber

The details of the calibration chamber and its components is shown in Figure 3.5. The calibration chamber is basically a hollow steel cylinder, made up of 15 mm thick steel wall. It is possible to dismantle the calibration chamber into four parts, namely a top and a bottom pedestal serving as top and bottom covers and two cylindrical portions of equal sizes which together form the main cylindrical body.

The provision of dismantling assists in the placement of the dilatometer blade into the chamber. The inside clear dimensions of the chamber are 500 mm high and 300 mm diameter. The top pedestal consists of (a) a central hole of 35 mm diameter meant for dilatometer rod insertion, (b) a water inlet for filling the chamber with

water, (c) an inlet for compressed air for maintaining a required pressure within the chamber and (d) a safety valve which automatically opens and releases the pressure of the chamber in case the pressure exceeds a present maximum value of 900 kPa.

Also part of the calibration chamber is a pressure read out system in the form of dial gauges which read the pressure maintained inside the calibration chamber with an accuracy of 1 kPa. For pressurising the water of the chamber a gas bottle containing atmospheric air was used.

3.4.2 Test procedure in calibration chamber

The test procedure followed during the calibration chamber tests is described below stepwise.

(1) The calibration chamber was filled with water, the water pressure was increased slightly and it was checked for leakages.

(2) The modified dilatometer assembly and the data acquisition system were connected as earlier shown in the schematic diagram Figure 3.2.

(3) All the parts except the top pedestal were first bolted together with rubber seals in between. The dilatometer rod was inserted into the central hole of the top pedestal and the dilatometer blade was fixed to the connecting rod and the top pedestal bolted into position.

(4) The membrane was brought to a reference zero deflection position by pressing the centre of the membrane with a straight edge and rotating the screw provided in the RS232 port so that the deflection value displayed on the computer screen read zero. After zeroing of the deflection reading when the membrane is left free in air, it comes to its normal resting position, with respect to the adjusted zero position.

(5) The modified dilatometer blade, together with the top pedestal, is placed on top of the calibration chamber and bolted tightly. The aim of the calibration chamber tests is to determine the deflection versus pressure curve of the modified dilatometer membrane when subjected to a known external water pressure. The water in the calibration chamber was pressurised to a desired external pressure, say 100 kPa, and the membrane was pressurised from inside,

using a gas bottle, causing the membrane to lift off and expand horizontally up to 1.1 mm against the external water pressure. The deflection versus pressure readings were recorded using the data acquisition system. The test was repeated for a minimum three times for the same external pressure in order to check reproducibility of the results.

Similarly, the test was repeated for different values of external pressures varying between 0 to 250 kPa, every time repeating the test at least three times and recording the data on to a floppy disc.

3.4.3 Results of the calibration chamber tests

The test was conducted for external pressures of 50, 100, 150, 200 and 250 kPa and the membrane deflection - pressure readings were recorded onto a floppy disc. The saved data was used to obtain the deflection versus pressure curves. As the membrane stiffness is a very small value (usually in the range of 20 to 50 kPa), it is very sensitive to the recorded pressure readings. It is important to maintain the external pressure to an exact fixed value during any single test as any fluctuation in the external pressure may alter the internal membrane pressure readings, thereby changing the pressure versus deflection curves.

A typical pressure versus deflection curve is shown in Figure 3.7a, obtained for an external pressure of 100 kPa, under controlled conditions and further used for the evaluation of membrane stiffness in Section 3.6.

3.5 Standardisation of modified dilatometer testing procedure

After all the test checks it was possible to set a standard testing procedure for the modified dilatometer testing in order to minimise errors and obtain consistent results. Given below is a brief description of the standard procedure, for the modified dilatometer tests.

3.5.1 Field set up

The various components of the modified dilatometer are connected as shown in Figure 3.2. All the joints should be checked to ensure that there is no loose connections or gas leakage. The button provided at the back of the RS232 port

should be switched to DMT mode. This is particularly important as otherwise the data acquisition system would be in CPT mode.

3.5.2 Setting reference zero for membrane deflection and initialisation of dilatometer blade tip resistance

As mentioned before, it is important to bring the membrane deflection to a fixed zero position so that all the deflection values are recorded with reference to this reference position. For zeroing the membrane deflection to a reference zero position the following routine is performed prior to every test commencement.

(a) The blade is jacked into the ground and left for approximately 15 minutes to condition the strain gauges to the ground temperature.

(b) The computer is switched on and left for approximately the same time of 15 minutes for warming up, thereby avoiding any drift of readings later.

(c) After 15 minutes of computer warming up the system disc consisting of DMT software is inserted into drive A and another preformatted disc into drive B of the computer. The executable DMT program is run and from the menu, "*Port adjustment*" is selected. The computer screen then displays four readings corresponding to depth, dilatometer blade tip resistance, membrane deflection and pressure respectively. Separate screws are provided on the RS232 port for initialising the membrane deflection and tip resistance by rotating the relevant screw in either clockwise or anticlockwise direction.

(d) The DMT blade, already conditioned to ground temperature, is withdrawn from the ground and kept on a horizontal surface. A straight edge is placed over the centre of the membrane, pressed firmly with a thumb and the membrane depressed until it comes in contact with the inner steel surface. The deflection port screw is rotated slowly to get a zero deflection reading on the computer screen. This process is repeated three to four times to make sure that the computer consistently reads zero when the membrane is depressed.

(e) The load cell on the dilatometer is also initialised by standing the blade vertically in free air and rotating the tip port to read zero tip resistance.

(f) When these adjustments are complete, then modified dilatometer blade is set up, ready for jacking into the ground.

(g) Appropriate selection is made from the menu of the DMT software depending on whether the blade is being jacked or the membrane is being pressurised. As the blade penetration and membrane pressurisation alternates, the menu selection is changed accordingly, thereby also saving the data. Alternatively, menu selection could be such that only deflection and pressure readings are recorded, ignoring the tip resistance readings or vice versa.

(h) During the membrane depressurisation stage of testing, it was observed from the computer display readings that the membrane deflates very slowly upon depressurisation. Even after complete release of all the gas from the vent opening, the membrane continued deflating under natural pore water pressure for nearly 30 seconds. In order to record the entire depressurisation readings, it is therefore necessary to delay for nearly 30 seconds, or as required, before going to the penetration part of the test. This is particularly important for studying the pore water pressure response.

3.6 Reduction of modified dilatometer data

The reduction of modified dilatometer data mainly consists of two parts, namely the cleaning and corrections of raw data. The process of cleaning and correcting of raw or field obtained data is described below.

3.6.1 Processing of the raw data

The raw or field data recorded during the course of modified dilatometer testing consists of four columns; depth, dilatometer blade tip resistance, deflection and pressure. But the entire data is not of relevance. During the penetration stage only the first two columns, namely the depth and tip resistance are of significance and during the membrane pressurisation stage only the third and fourth columns, namely the deflection and pressure are of significance. Therefore the recorded data was cleaned and split accordingly so that (a) the first two columns gave the depth versus dilatometer blade tip resistance plot and (b) the last two columns gave the continuous deflection versus pressure plot.

The cleaning of data was done by deleting the unwanted parts of the columns. An example of the saved data file, as recorded directly on the field is shown in Figure 3.6, where the marked portions denote the data to be deleted.

3.6.2 Corrections to the processed data

Corrections are necessary to depth, non continuous blade penetration and membrane stiffness.

(a) Depth correction

The tip resistance values obtained from the load cell and the deflection and pressure readings obtained from the membrane assembly are from different depths. In order to match the two sets of readings, a depth correction is necessary. If the load cell position is taken as the start depth, the depths recorded against deflection and pressure readings will lag behind by a depth of 100 mm (the distance between load cell and centre of the membrane is 100 mm).

The depth correction to be applied to the depth readings depend on whether the dilatometer blade tip, the centre of the membrane or the load cell position is taken as the reference depth position, when specifying the start depth value initially. During the present field tests, the centre of the membrane was taken as reference position for depth recording and a negative correction (equal to the distance between load cell and membrane centre) was applied to the depth readings corresponding to the tip resistance.

(b) Non continuous penetration correction

During the course of modified dilatometer testing the tip resistance values are recorded in between two successive membrane pressurisations for which the penetration is halted at regular intervals. Due to this regular halting and resumption of penetration the first few readings of tip resistance drop to zero. This phenomenon was noticed during the course of cone penetration testing also while adding the drill rods and was attributed to the soil rebound or response of the electrical components (Jaksa and Kaggwa, 1994).

Although there is provision of automatically deleting two such readings using the software, examination of the tip resistance profiles revealed that it was necessary to

delete three to four such readings in the case of loose sand, in order to get a smooth profile of dilatometer blade tip resistance. Alternatively such can be avoided by conducting a few tests with the sole purpose of getting the tip resistance profile, without stopping intermittently for membrane pressurisation readings. (A few tests were conducted this way to get a quick profile of dilatometer blade tip resistance.)

(c) Correction for membrane stiffness

The pressure readings recorded during dilatometer testing are inclusive of the membrane stiffness. The aim of the dilatometer test is to determine the pressure required to push the soil horizontally, exclusive of the membrane stiffness.

In the case of normal dilatometer testing the membrane correction is done to pressure readings corresponding to 0.05 and 1.1 mm. But while using the modified dilatometer all the intermediate pressure readings need to be corrected for membrane stiffness and a continuous curve for membrane stiffness is therefore required.

The differential pressure (= internal membrane pressure required for expansion - calibration chamber water pressure), was plotted against the membrane deflection and is shown in Figure 3.7b. These curves were used for evaluating the membrane stiffness in the form of an equation by determining a regression curve through the data points and then working out its coefficients. Following two equations were worked out for the membrane stiffness corresponding to the pressurisation and depressurisation stages respectively.

$$y = A + B(x) + C(x^2) \quad (3.2a)$$

$$y' = A' + B'(x) + C'(x^2) \quad (3.2b)$$

where,

y = membrane stiffness during membrane pressurisation (kPa)

y' = membrane stiffness during membrane depressurisation (kPa)

x = corresponding membrane deflection (mm)

A, B, C = coefficients corresponding to membrane pressurisation

A', B', C' = coefficients corresponding to membrane depressurisation

The experimentally determined values of A, B and C were found to be 39.53, -6.68 and -12.29, respectively, and that of A', B' and C' equal to 71.40, -60.95 and -2.41, respectively.

For deflections less than the nominal membrane resting position (say 0.3 mm in free air), the stiffness was added to the field pressure values and for deflections greater than the nominal resting position, it was subtracted. The corrected pressure readings represent the pressure applied to the soil, and this was used to evaluate the modulus of elasticity and other soil properties.

During the depressurisation stage the membrane moves inwards from 1.1 mm to its normal resting position (say 0.3 mm deflection in free air) and has a tendency to come to its normal resting position by itself, so the membrane stiffness assists in the process of depressurisation. Hence, the correction should be opposite to that used during the pressurisation stage. Therefore, for deflection values lying between 1.1 and 0.3 mm (or whatever the membrane resting position is), the stiffness correction is positive. The case is the reverse for deflection less than 0.3 mm and the stiffness correction is negative.

3.7 Description of testing program

The main aim of this research is to evaluate the properties of calcareous sand with the application of field tests using cone penetration and dilatometer modulus tests. The validity of available DMT and CPT correlations, established on clean silica sand, are tested on calcareous sand based on laboratory evaluated results. Where necessary, the existing correlations are modified and then used for bearing capacity and settlement predictions.

For this purpose a uniform site of sand deposit was required which consists of a small percentage (10 to 25 %) of calcium carbonate and is therefore calcareous in nature. To enhance the value of this work, the aim was to select a site which would also be used for construction and would be useful to the community. By doing so it would also be possible to reassess the predicted settlement results from the actual field results.

The soils of the Port Adelaide area, South Australia, consist of calcareous sand. These soils have caused numerous problems with many old buildings in this area developing cracks. In the near future, one of the most important projects likely to be undertaken in Adelaide is the Multi function Polis (MFP), a portion of which is adjacent to Port Adelaide area. The aim is to build up a residential and business complex, to serve as a model for the modern age as to how people should live, earn and learn in the twenty first century.

Because of the importance attached to this project, wide ranging surveys, including geotechnical surveys, have been conducted, dealing with the soil stratigraphy, its properties and implications on the proposed project. Most of the required data related to this project is available in geotechnical reports by Coffey Partners International Pty. Ltd. and PPK Consultants Pty. Ltd, (PPK Consultants et. al., 1992; Coffey International, 1991) which were used to select a suitable field test site within the MFP zone.

3.7.1 The MFP site

The original MFP site comprised mainly of the Gillman and Dry Creek areas to the north of the city of Adelaide. Changes have been made in the original MFP core site from time to time and according to the latest proposal, the Greater Levels area has also been added to the original MFP core site. Figure 3.8 shows the original MFP core site and the latest additions. It is presently barren land, partly used as a dumping ground. The northern part of the MFP site is mainly marshy with mangroves. Port Adelaide river flows towards the west of this site. The eastern border is Main North Road and the southern boundary coincides with the Wingfield and Enfield council boundaries.

A major part of the western part of the MFP site is covered with tidal channel sand and marshy soils, transported by tidal action. The tidal channel sand areas, containing carbonates, are marshy with grass covering or bare ground. Therefore these areas were preferred for conducting the field tests.

3.7.2 Available MFP soil data

Borehole findings of MFP site

A study of borehole data logged by Coffey International (1991) reveals that the tidal channel sand areas are exclusively sand deposits, uniform and slightly calcareous in nature. The western part of the MFP site was found to be the most appropriate as it consists of a uniform deep deposit of sand with sea shells, carbonate sediments and calcrete.

Particle size distribution curves

The particle size distribution curves reported by Coffey International (1991) indicate that the tidal channel sand and sandy shore face locations of MFP site consist of uniformly graded sand with a slight percentage of fine gravel. In fact this gravel could be in the form of sea shells and calcrete crust. All the referred particle size distribution curves are almost identical in nature. The percentages of gravel, sand and silt obtained from the various particle size distribution curves, all within a radius of 500 metres from the present test location is tabulated below.

Table 3.1 Percentage of gravel, sand and silt in the soil of the test site (based on data of Coffey International, 1991)

Depth (m)	Silt (%)	Sand (%)	Gravel (%)
0.7 to 1.0	12	85	3
1.4 to 1.7	66	31	3
1.7 to 2.0	25	72	3
2.4 to 2.7	18	79	3
3.1 to 3.45	10	89	1

CPT data

The profiles of the Dutch cone soundings in the areas of interest indicate that cone resistance varies between 0 and 10 MPa, except at a few points, where values exceed 24 MPa. It is interesting to note that these unpredictable high values of cone resistance were associated with very low values of friction ratio. This could be an indication of calcareous sediments with a high degree of cementation, as found by Joustra and Gijt (1982) and discussed in Chapter 2.

Further, Dutch cone profiles and corresponding borehole logging details of Coffey International (1991) were collated. This matching showed that a calcareous layer existed where CPT profiles revealed high cone resistance and low friction ratio values. The maximum depth to which borehole logging details were shown was approximately 2 metres in most of the cases, indicating that there was a crust with a high degree of cementation at 2 metres making further boring difficult, as is the case with calcrete.

3.7.3 Field testing program

Priority was given to pinpointing an area inside the MFP site that would be used for construction. This would permit bearing capacity and settlement predictions of foundations on these soils to be used during the design stage. Keeping in mind aspects such as (a) construction location; (b) accessibility of the site; (c) absence of fill or dumped material; (d) presence of moderately calcareous sand; and (e) uniformity of soil profile, the western part of the MFP site was chosen for conducting the field tests.

The field tests were conducted on a slightly calcareous, uniform and virgin sand deposit, within the Rifle range area of the MFP site, by the side of the existing target mound which is located on the southern part of Gillman in Figure 3.8. The final selection of test locations was done after preliminary testing of soil samples, obtained from this area. The preliminary tests were done for the identification and description of the soil, thereby confirming its suitability for the current research work.

The field tests included cone, dilatometer and modified dilatometer penetration tests. These penetration tests were conducted up to a depth of approximately 6 metres using a truck mounted hydraulic device, which is capable of providing a reaction up to 4 tonnes when utilising anchors. The data from the CPT and modified DMT tests were recorded by a microcomputer and the data for the normal DMT were recorded manually.

The tests were carried out at two locations, 10 metres apart. At both locations a minimum of 3 CPTs, 2 DMTs, 2 modified DMTs and one continuous sampling were done so that the tests were conducted within a circle of 5 metres diameter. Conducting the tests in such a planned manner assisted in verifying the accuracy and reproducibility of each type of test and comparing their results.

The test locations and pattern are illustrated in Figure 3.9, which shows that three anchors fixed in a triangular pattern were used to provide the necessary reaction and to give three axes for the setting up of the test truck and subsequent testing. Along either side of the anchors and on each axis, two tests were conducted nearly half a metre apart with different combination of tests, so that one type of test was next to

the other type, enabling cross comparison of the results and also the reliability in predicting the soil stratigraphy.

The combination of adjacent CPT and DMT was helpful for the simultaneous evaluation of soil parameters. The DMT and modified DMT were conducted adjacent to each other so that the proper functioning of the modified DMT could be ascertained by matching the P_0 and P_1 profiles of the two tests. Similarly, adjacent CPT and modified DMT were helpful in the simultaneous evaluation of tip resistance and other soil parameters.

The distance between adjacent penetration tests was carefully considered to ensure that the disturbance due to the penetration of one test did not adversely affect the other, as well as to minimise any appreciable change in the nature of soil. The depth interval for DMT soundings was 200 mm and at every location, the DMT was conducted prior to the CPT with the side of the membrane orientated away from the adjacent test holes, so that the horizontal deflection versus pressure readings of the DMT membrane were not adversely affected due to adjacent tests.

While interpreting the results from the field data, an assessment of field density of the soil was required for the calculation of effective overburden pressure, as the chart suggested by Schmertmann (1986) could not be used directly. An assessment of field density was also required for preparation of laboratory specimens at the given density. Several samples were obtained from the site using a thin wall sampler, for determination of the field dry density. Although obtaining high quality samples in sand is generally difficult, it was possible to obtain a few good quality samples, partly due to the cementation of the calcareous sand. These samples were obtained at a depth ranging from 1.7 to 2.5 because the soil is fairly uniform below 1.5 metres.

Continuous sampling was also done to allow visual inspection of soil particles and determination of the variation of carbonate content and particle size distribution with depth below ground surface.

The test site consists of a 0.75 metre thick highly cemented crust between 0.75m and 1.5 m below the ground surface and penetrating through it was difficult. This crust frequently resulted in bending of the dilatometer blade and lifting of the truck, while testing at Location No. 1. Hence, at Location No. 2, it was decided to predrill a hole up to 1.5 metres deep and then commence the test from 1.5 metres downwards.

3.7.4 Laboratory testing program

According to existing correlations, many parameters of cohesionless soils can be evaluated from the DMT and CPT correlations. However, in this research emphasis was placed on determining the common parameters used in design. The laboratory testing program consisted of preliminary tests, used to help select a suitable site, and tests conducted on samples recovered at the test site, used as reference values for the soil parameters obtained from DMT and CPT.

Preliminary tests and results

These tests were conducted on reconstituted samples according to the Australian testing standards (Standards Association of Australia, 1977) and British testing standards (Head, 1990) in order to aid in the selection of the exact field test site and to determine the basic soil properties. These tests included, visual inspection, specific gravity, maximum and minimum dry density, in situ dry density, organic content and carbonate content. The preliminary test results determined for the selected test site are tabulated in Table 3.2.

Tests conducted on recovered samples

(a) Sieve analysis

Sieve analysis was done on samples from every half metre of depth in order to determine the particle size distribution curves, identify the soil and determine the relative percentages of gravel, sand and silt. These results were helpful in checking the soil stratigraphy predicted by in situ tests and also to determine whether the soil is well graded, uniformly graded, or poorly graded.

(b) Carbonate content determination test

This test was performed on samples to determine the percentage of carbonates in the sand at various depths. The calcareous sand was reacted with normal (1 Normal) hydrochloric acid, washed with distilled water, oven dried and the percentage decrease in the dry weight of the soil calculated, which directly gives the percentage of carbonate in the given sand. The reaction involved is represented by the following equation:

$$CaCO_3 + 2\,HCl \rightarrow Ca{\downarrow}Cl_2 + H_2O + CO_2{\uparrow} \qquad (3.3)$$

The variation of the carbonate content in the sand with depth represents the variation in the degree of cementation and is therefore helpful is examining the effects of cementation on the CPT and DMT parameters.

Table 3.2 Laboratory tests and results for description of soil.

Test	Sample Depth	Result / Remark
(1) Visual inspection	0 to 0.75 m 0.75 to 6 m	Mottled brown sand with shell fragments appearance of cement mortar/slurry with decomposed shells; sand particles are held together due to cementation; forms dry lumps on drying which can be broken by fingers with moderate strength.
(1) Particle size distribution curves	1m 2m	Poorly graded sand Poorly graded sand
(2) Carbonate content (reaction with Hcl)	1m 2m 2.2 m 3.2 m 4.2 m 5.2 m	23.00 % 23.56 % 12.90 % 12.35 % 16.67 % 17.72 %
(3) Organic content (heating upto 800°C)	1m 2m	5.31%, 11.87% 1.446%
(4) Minimum dry density	2 to 3 m	1.22, 1.29, 1.26 t/m^3
(5) Maximum dry density	2 to 3 m	1.62 t/m^3
(6) Field dry density	2 to 3 m	1.46 t/m^3
(7) Relative density	2 to 3 m	67%
(8) Bulk Density	0.00 to 0.90 m	1.728 t/m^3 (above water table)
(9) Specific gravity (at 21°C)	2m	2.66, 2.64

(c) Shear box tests

Shear box tests were conducted on samples from every half metre depth intervals to determine the angle of friction of the soil and to compare these values with those determined from the field tests. The angle of friction obtained by this test is for plane strain conditions.

These tests were conducted on saturated sand samples, immersed in water during testing in a 60 by 60 mm square shear box under drained conditions. It was noted that calcareous sediments, on exposure to air have a tendency to harden and form lumps and therefore if tested dry may not reflect the field conditions and may give altogether different values of friction angle. As the ground water table of the test site is at 0.9 metres below the ground surface and below that the sand remains saturated, the tests were conducted on samples saturated with tap water to prevent drying of the soil.

(d) Triaxial tests

Consolidated drained (CD) tests were conducted on saturated sand specimens, 38 mm in diameter, prepared directly on the triaxial cell pedestal. Specimen were prepared to the same field dry density, determined in the laboratory. A minimum of six tests were conducted. The tests involved three stages.

(a) Saturation stage, during which complete saturation of the specimen was ensured. The one stage back pressure elevation technique was used for saturating the specimen completely.

(b) Consolidation stage, during which the specimen was consolidated under drained conditions. The coefficient of volume change, m_v, was obtained during this stage which was used for the comparison of DMT obtained constrained modulus.

(c) Compression stage, during which the specimen was compressed axially under drained conditions in order to cause a shear failure.

From the CD tests, the modulus of elasticity and angle of friction of the calcareous sand were obtained. The results of all these tests are presented in Chapter 5 along with the DMT and CPT results.

3.8 Summary

The normal dilatometer was modified to study the nature of membrane expansion into the soil and investigate whether such expansion is linear or non-linear. The modification also permits better interpretation of soil parameters, particularly the modulus of elasticity, as continuous deflection versus pressure curves are used to

determine it, allowing greater accounting for the linearity or non-linearity of the test data. This is a significant improvement over the existing DMT and CPT correlations, which are empirical in nature and only examine the starting and end point of the test.

The second aim of modifying the dilatometer was to develop an instrument which could be used in the case of calcareous sediments, for which formulation of empirical correlations is difficult owing to the great deal of variation in them. Automation of the developed instrument was done to allow swift and accurate recording of data.

The selection of a proper test site consisting of slightly calcareous sand deposit was undertaken within the MFP site and preliminary testing was carried out on the soil samples to confirm the suitability of the selected site for the present research work. A field and laboratory testing program was designed for the research work involving field samples, continuous sampling, DMT, CPT and MDMT tests.

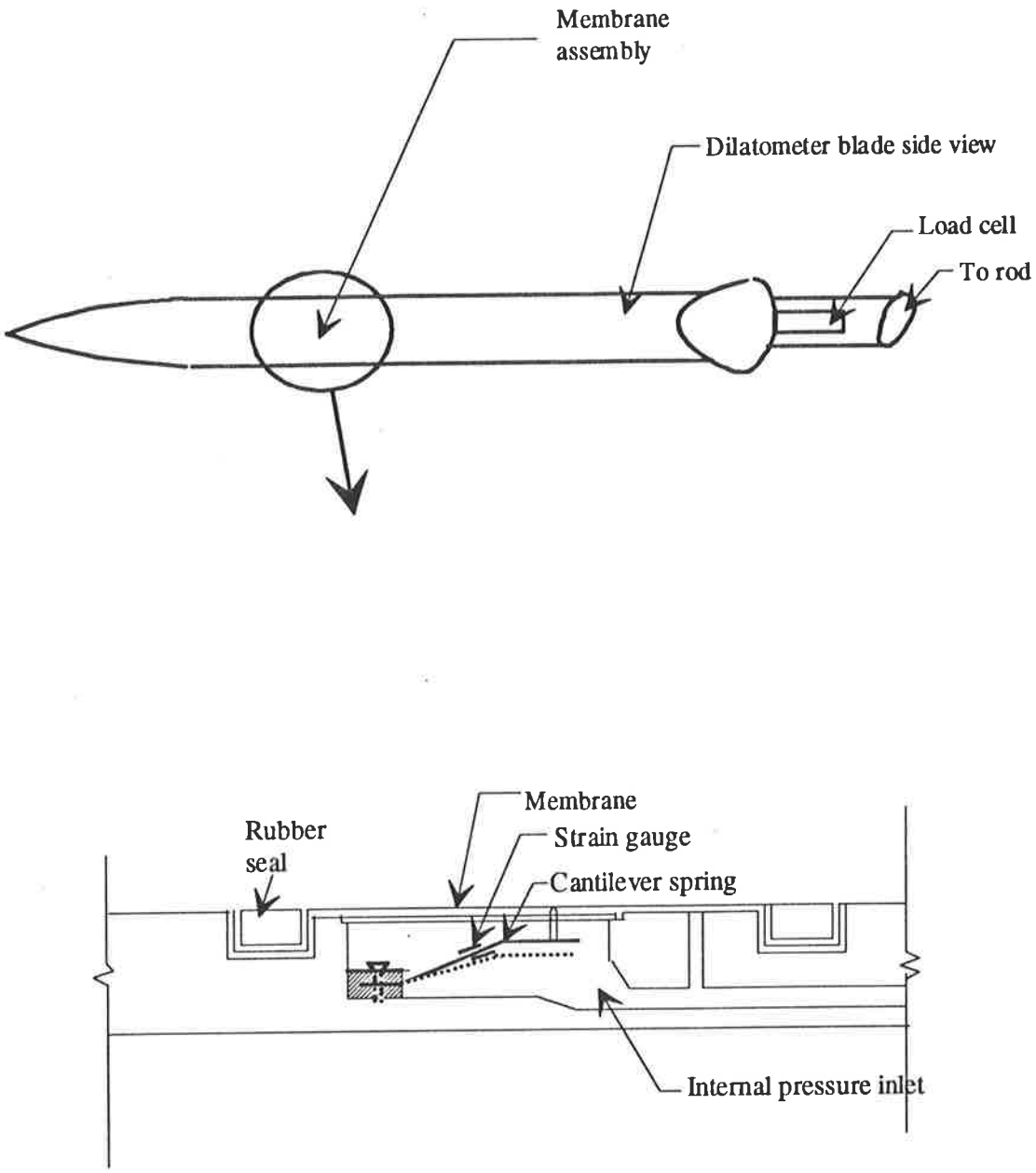

Figure 3.1 Internal modifications of the modified dilatometer blade

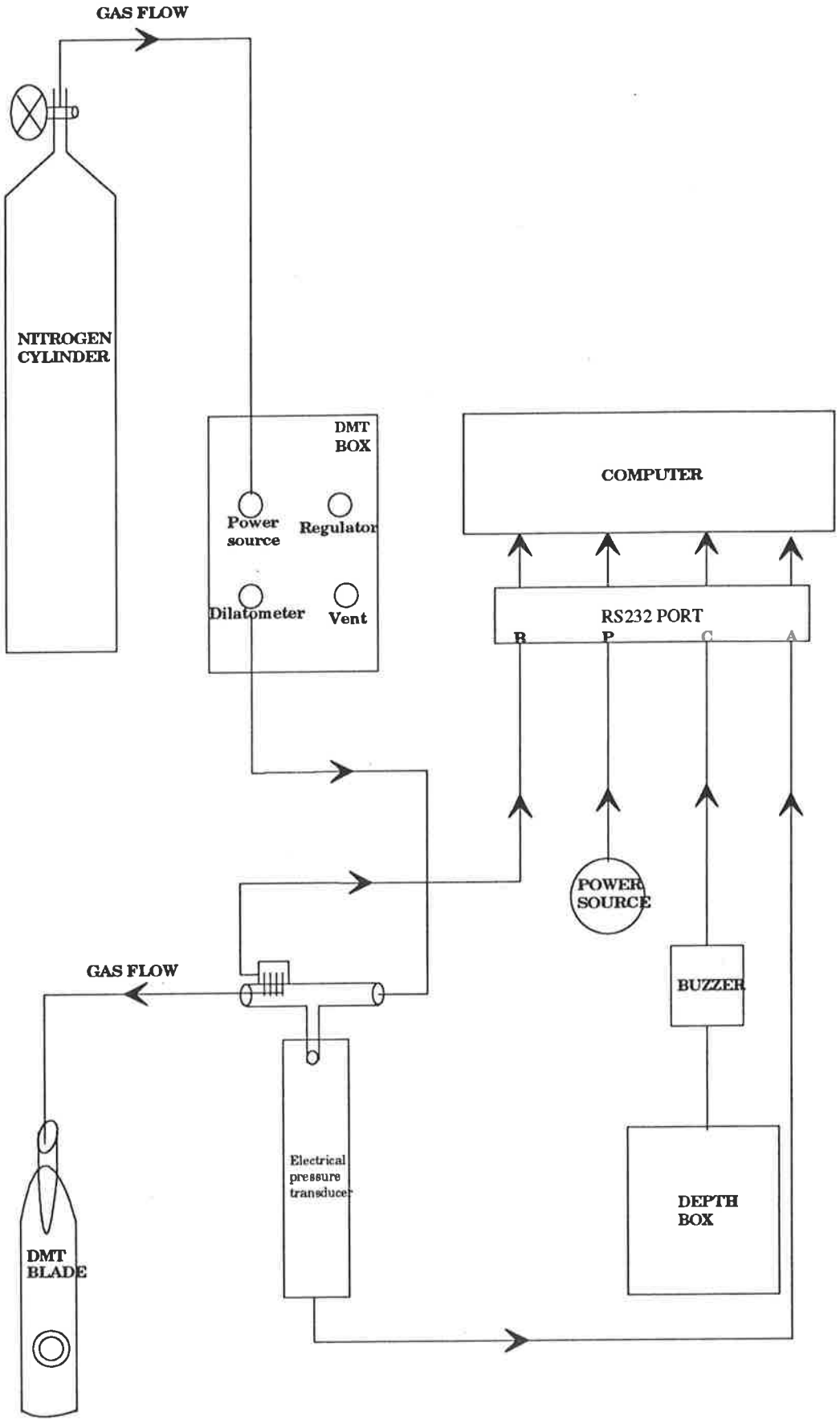

Figure 3.2 Schematic diagram showing the modified dilatometer connections

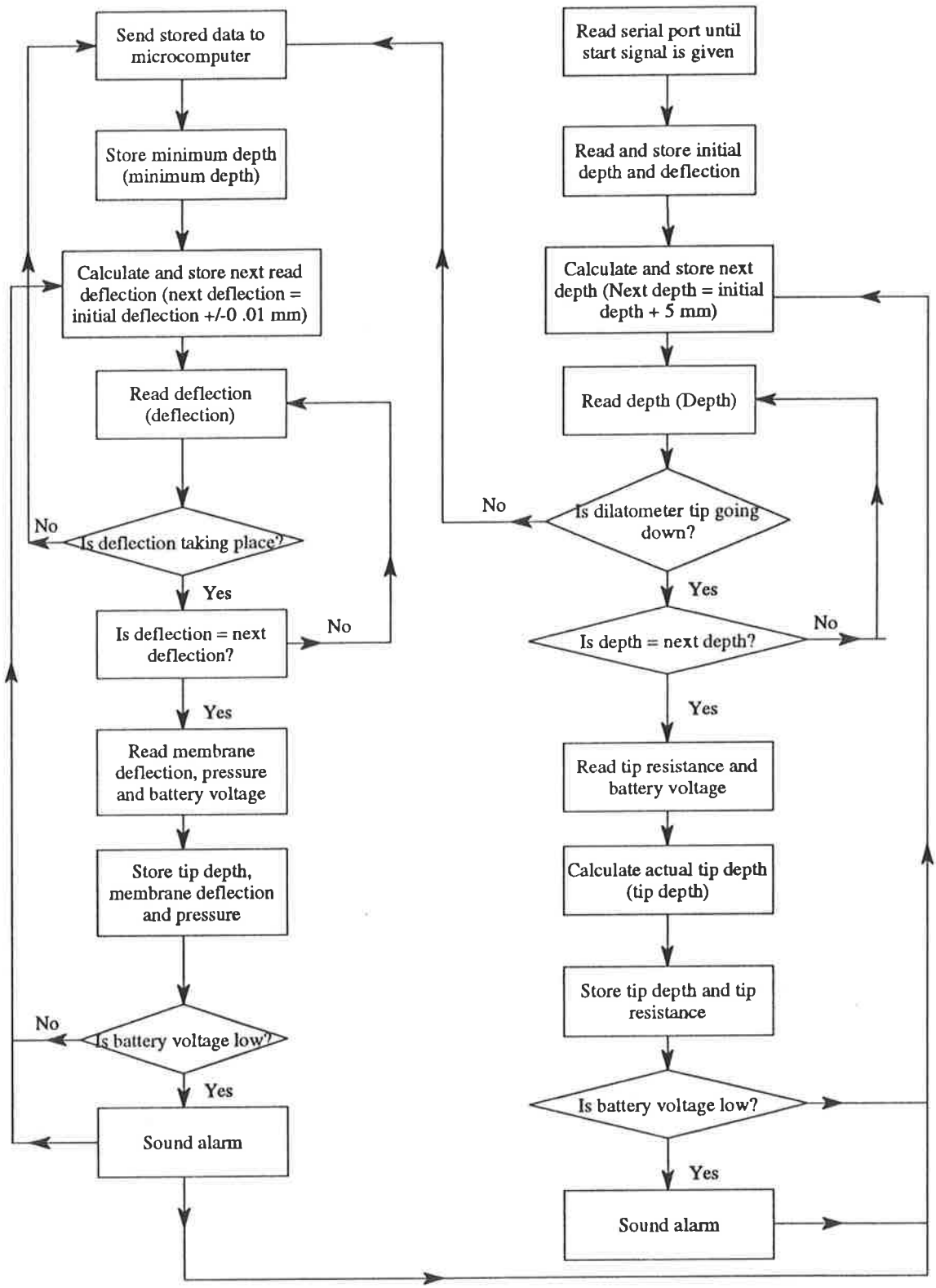

Figure 3.3 Flow chart of DMT software for data acquisition

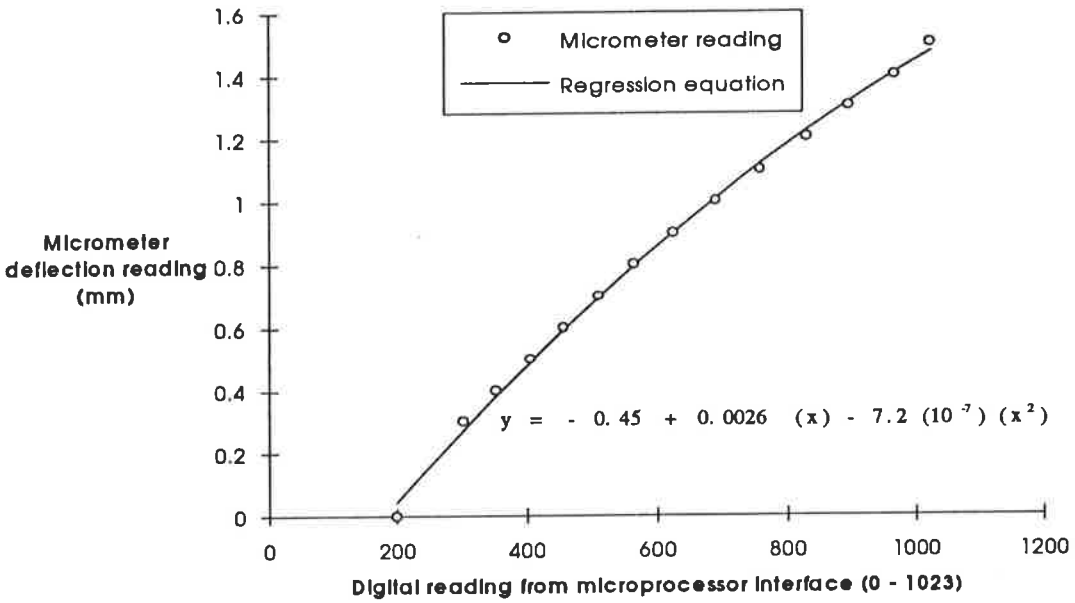

Figure 3.4 Calibration of membrane deflection using the micrometer

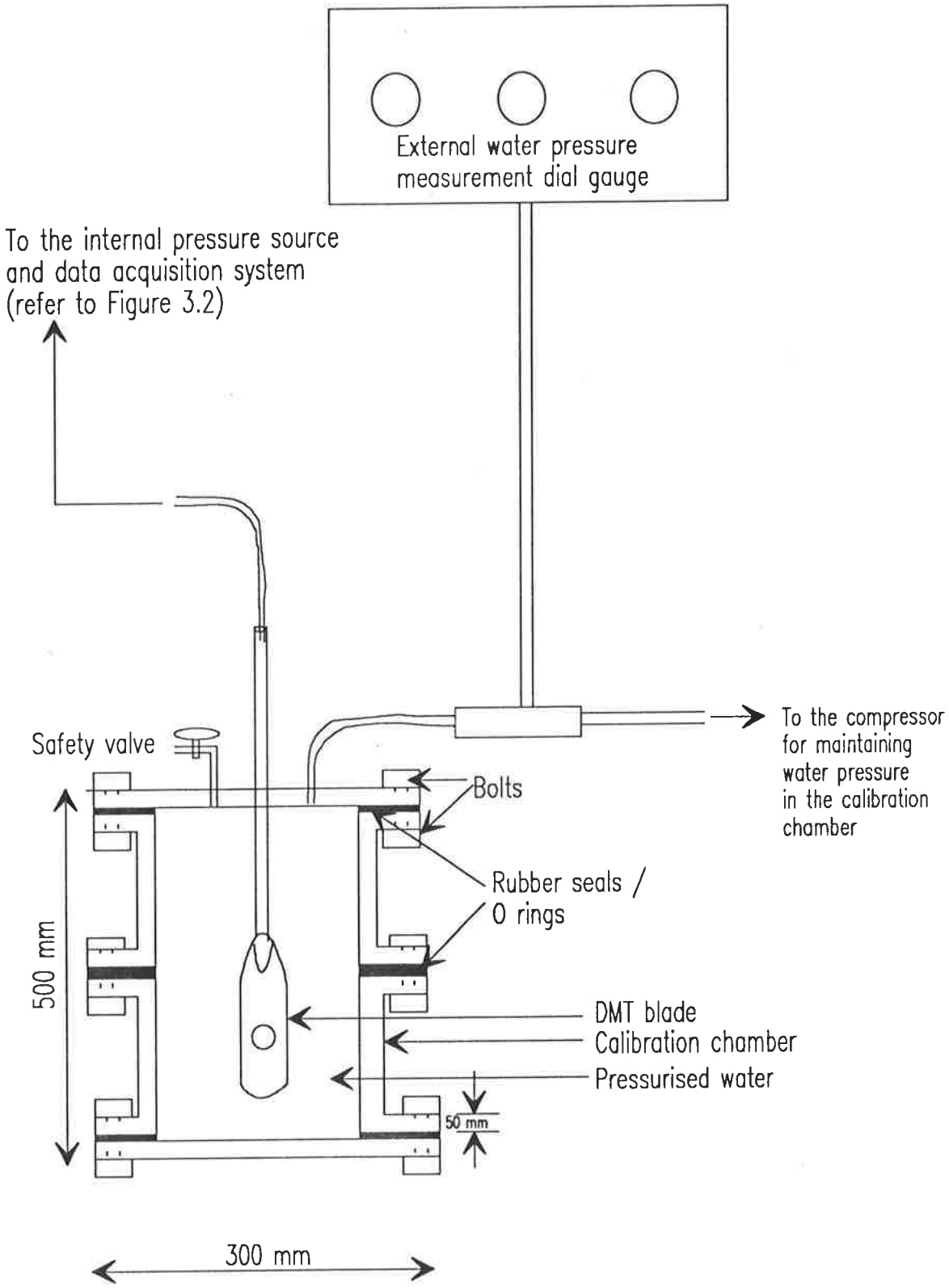

Figure 3.5 Details of set up of the calibration chamber

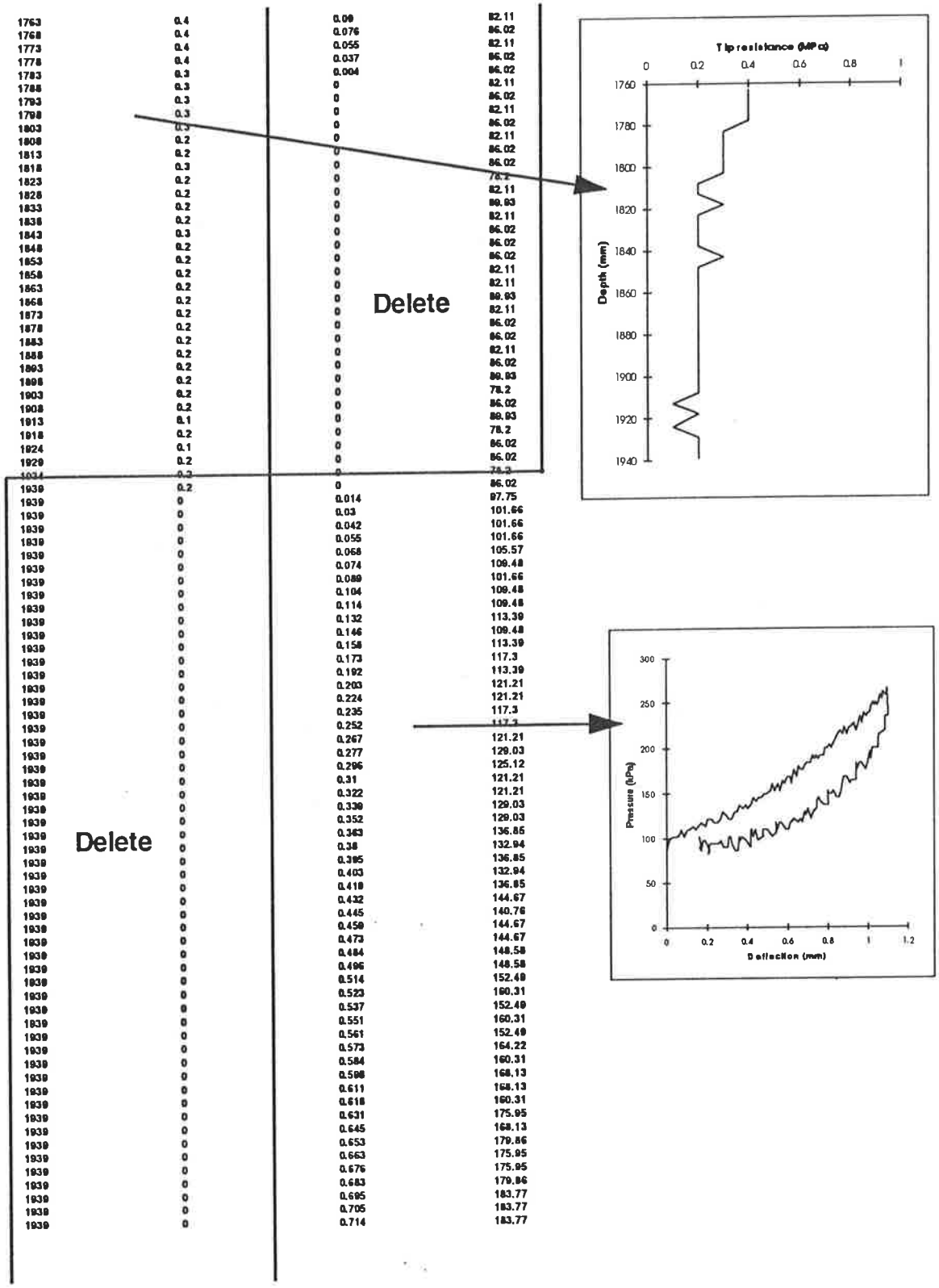

Figure 3.6 Computer obtained raw data from modified dilatometer

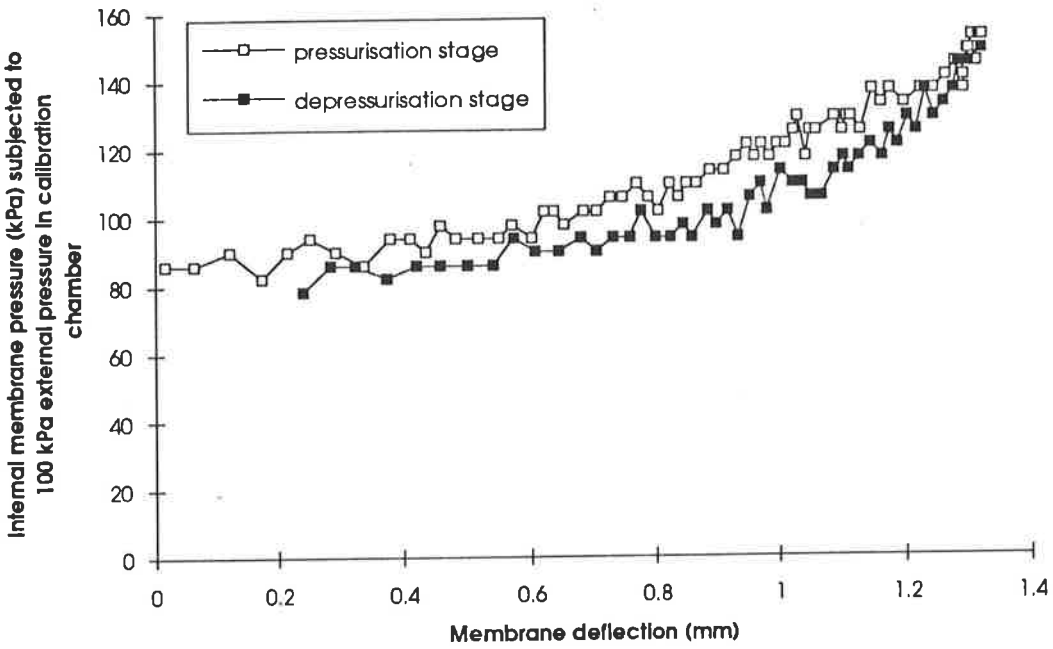

Figure 3.7 a **Modified dilatometer pressure versus deflection curve corresponding to 100 kPa external water pressure in the calibration chamber.**

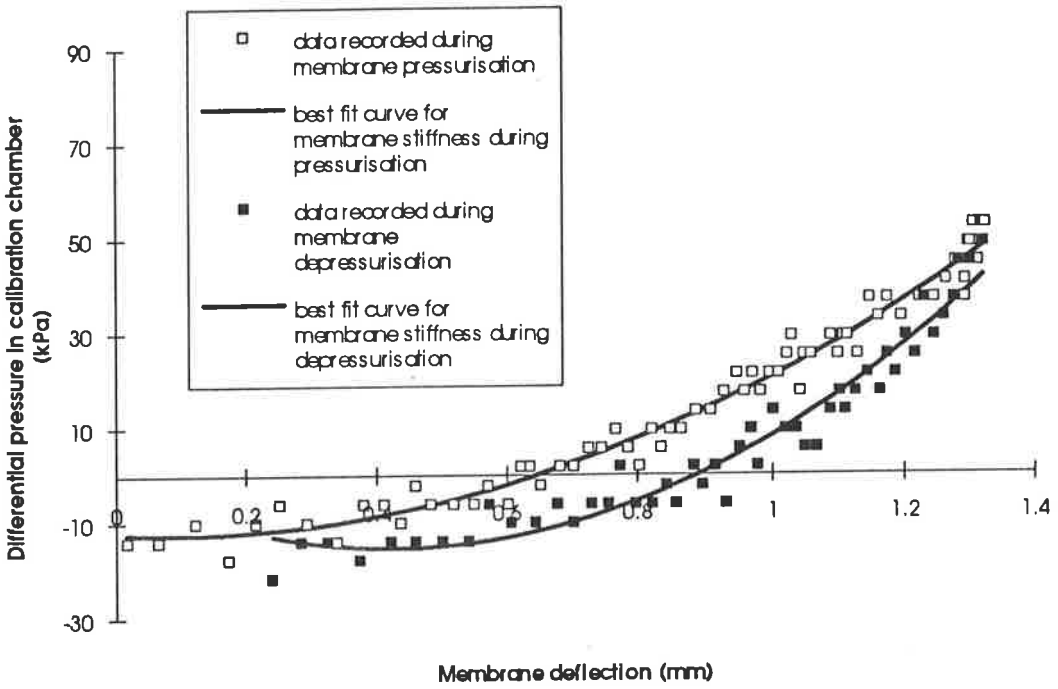

Figure 3.7 b Best fit curves for the membrane stiffness corresponding to stages of membrane pressurisation and depressurisation.

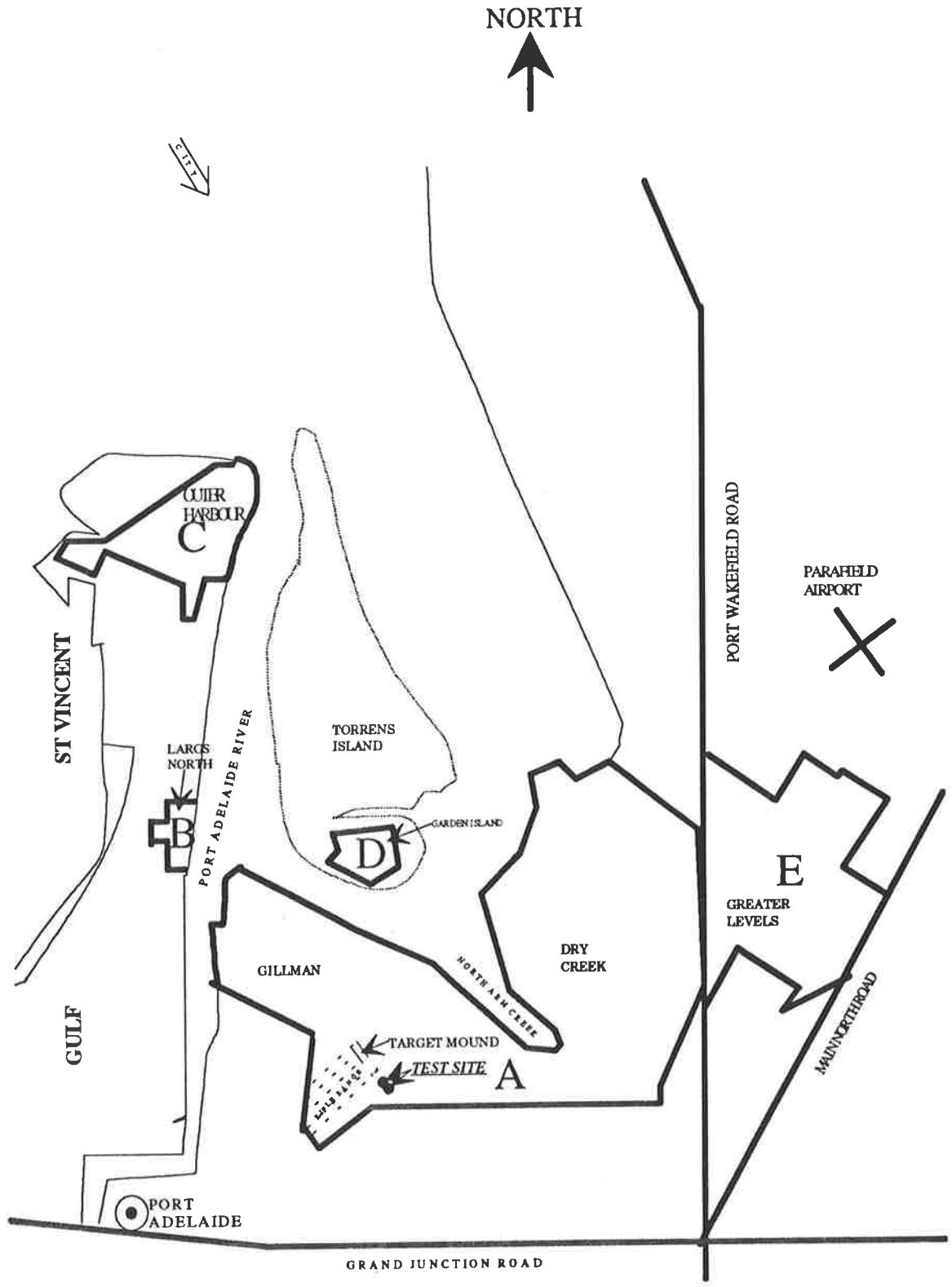

Figure 3.8 MFP lay out; A, B, C, D, - original MFP core site; E - 1994 added

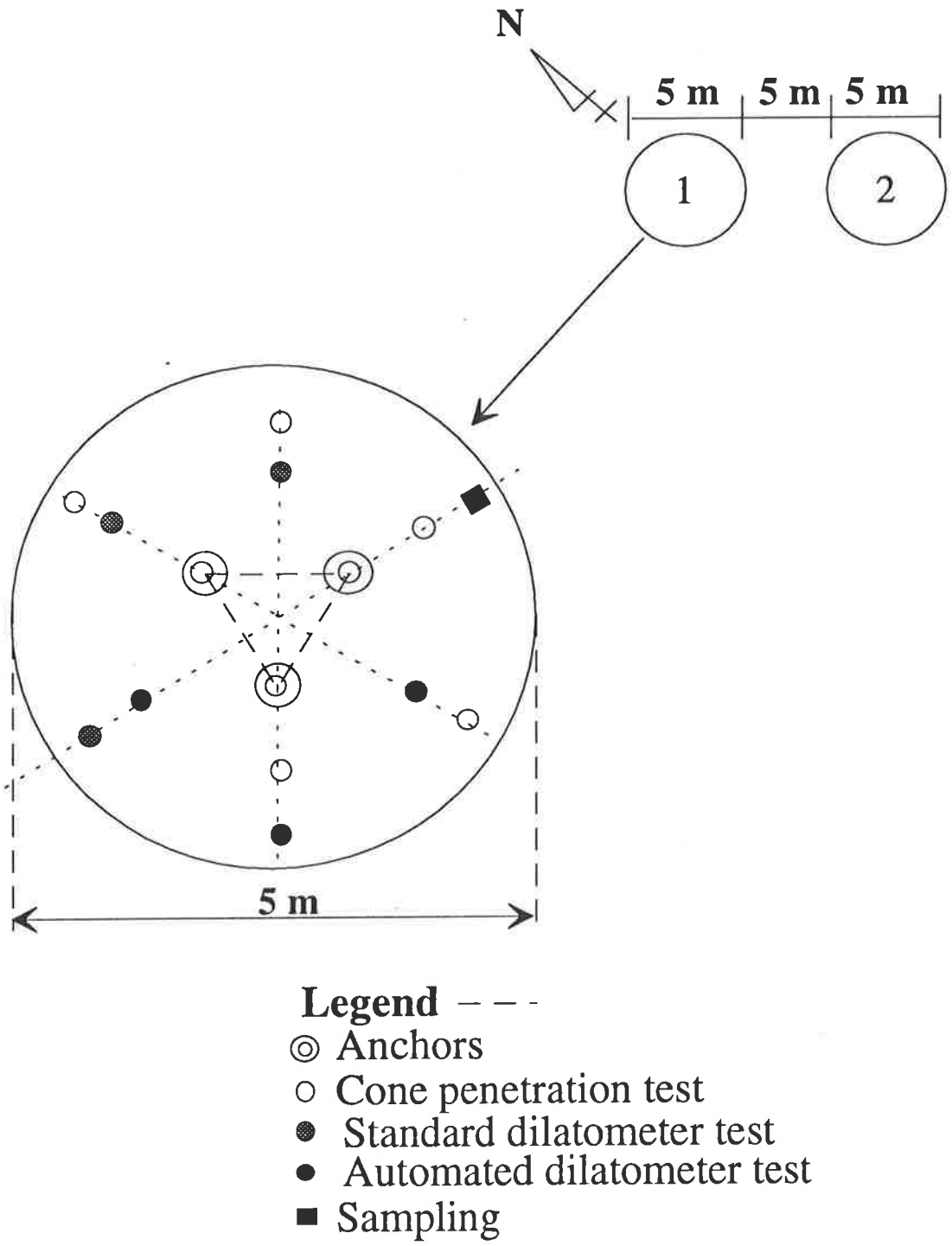

Figure 3.9 Field testing pattern

Chapter 4

ANALYSIS OF RESULTS OF MODIFIED DILATOMETER TESTS

4.1 Introduction

This chapter deals with the interpretation of results from the modified dilatometer test data. As described in Chapter 3, the modified dilatometer test gives continuous pressure versus deflection readings for horizontal membrane expansion into the soil and also the dilatometer blade tip resistance readings for the dilatometer blade penetration through the soil.

At the beginning of the Chapter the nature of some of the typical pressure versus deflection curves, obtained from the modified dilatometer test data are discussed and examined especially as to whether they are linear or non-linear. Subsequently, these curves are used for the direct evaluation of Young's modulus. The values of Young's modulus evaluated by standard and modified dilatometer tests are then compared to find out the difference between the two and ascertain whether the existing procedure for the evaluation of modulus of elasticity gives reasonable results.

A study of the pore water pressure is presented from the depressurisation stage of the pressure versus deflection curve. The pore pressure evaluated from the membrane depressurisation data is then compared with the pore pressure directly calculated from the ground water table. Whether the depressurisation of the DMT membrane is

capable of giving reliable data for the direct evaluation of in situ pore water pressure is ascertained from this study.

Finally, a comparative study of the dilatometer blade tip resistances with the adjacent cone tip resistances is done to determine whether the two are close enough and whether either of them could be used for the evaluation of angle of friction and coefficient of earth pressure at rest.

4.2 Typical pressure versus deflection curves

Figures 4.1 to 4.4 show some of the typical pressure versus deflection curves, corrected for membrane stiffness. Figures 4.1 represents a test depth greater than 3.5 metres, where the soil is relatively stronger or cemented. Figures 4.2, 4.3 and 4.4 are typical of the weaker soil layers and correspond to depths less than 2.2 metres below ground level.

These curves consist of five distinct portions in general, namely, OA, AB, BC, CD and DE. Figure 4.1 can be considered as a typical curve which shows that when the blade is jacked into the ground the membrane is pressed horizontally by the soil and the membrane remains seated on the metallic surface of the blade, corresponding to point O of the curve. On pressurisation, the membrane lifts off its resting position, up to point A of the curve and thereafter the pressure and deflection readings follow a linear trend up to point B.

How soon the first set of pressure and deflection readings are obtained after membrane pressurisation depends upon the membrane strain gauge setting. If the strain gauges are set to emit readings after 0.01 mm deflection intervals, the first set of readings will be obtained after 0.01 mm membrane movement into the soil.

The membrane pressure reading after which the curve shows a fairly linear trend (point A in Figure 4.1), is known as the lift off pressure and is of great significance as this is the minimum pressure required for the membrane to overcome the lateral pressure of the soil and is an indicator of the horizontal stress of the soil at that point. It is used to formulate the horizontal stress index, K_D, which in turn is correlated to parameters like K_o, ϕ, OCR and preconsolidation pressure. In different soils and in soils with different stress histories the lift off pressures are different. A relatively small value of lift off pressure is characteristic feature of sandy soils (Lacasse and Lunne, 1988), which is helpful in the prediction of soil stratigraphy.

The next region, AB, of the curve represents the deflection-pressure relationship during membrane expansion. It can be clearly seen that AB is a straight line only up to some deflection, corresponding to the low strain region, after which it tends to become concave downwards, showing that the deflection - pressure relationship is non-linear. The pressure difference between points A and B of the curve represents the work done by the gas on the soil in the horizontal direction and is used for the evaluation of modulus of elasticity of soil through the dilatometer modulus, E_D.

The point B of the curve corresponds to the maximum membrane deflection of 1.1 mm, at which the gas pressure is released. The portion BC of the curve shows that after the release of gas, the pressure starts decreasing immediately but not the deflection. It is only after the pressure drops to a certain extent that the membrane starts moving backwards appreciably. This could be either due to the unloading stiffness of the soil or due to a vacuum, caused by the membrane expansion and subsequent contraction, resulting in a suction pressure which restricts the backward movement of the membrane. When the membrane pressure drops appreciably, the outside suction pressure is overcome, enabling the membrane to deflate.

Beyond point C, there is a swift decrease in deflection with further decrease in pressure up to point D. The portion CD is also non-linear with concavity upwards. When point D is reached, almost all of the gas has escaped through the vent and the depressurisation is complete. The portion DE represents constant pressure but there is still a decrease in the membrane deflection, caused by the application of an external pressure, in the form of pore water pressure.

Under natural pore water pressures the membrane does not necessarily come to the pre adjusted zero deflection position. The point E denotes the final deflection position of the membrane to which it is pushed back under the influence of pore water pressure. But on being pushed to a new test depth the membrane is once again pushed back to the reference zero position by the lateral soil pressure and the new membrane pressurisation curve is obtained from the zero deflection position. However, in weak soils the lateral pressure is sometimes not sufficient to push the membrane back to its reference position and pressurisation commences with some deflection.

In stiff soils it is possible to record a small negative value of deflection corresponding to the starting position (see Figure 4.1, where the initial deflection is approximately -

0.1 mm). This is possible in two situations, (a) when the membrane is pressed inwards beyond the reference zero position, to which it was adjusted prior to test commencement and (b) due to a possible drift in the electronic digital readings towards negative or positive side. The later could be avoided by allowing for a suitable warm up time, necessary for the electronic components of the modified dilatometer.

The advantage of a variable initial deflection reading (which could be on either side of zero), is that it shows the relative intensities of the horizontal pressures onto the membrane prior to pressurisation. For example if the initial deflection reading at a depth of 1 m is 0.00 mm and that at a depth of 2 m is -0.05 mm then it shows that the soil at 2 metre depth exerts more pressure on the membrane compared to 1 metre depth. The initial deflections at different depths can therefore be used as an indicator of soft or stiff soil layers.

4.3 Modulus of elasticity determined from modified dilatometer data

The evaluation of the modulus of elasticity from the normal dilatometer is based on the assumption that the space surrounding the dilatometer membrane is formed of two elastic half spaces and the membrane expands within these elastic spaces. For this condition the equation proposed by Gravesen (Marchetti, 1980) is used for the calculation of dilatometer modulus, E_D, which in turn is related to the Young's modulus of the soil.

The calculation of the dilatometer modulus, E_D, from Gravesen's equation relies on membrane pressure readings at deflections of 0.05 and 1.1 mm, assuming a linear relation and leads to error as most of the pressure versus deflection curves (Figures 4.1 to 4.4) show a non-linear relationship between pressure and deflection. It is therefore proposed to calculate the dilatometer modulus, E_D, from the continuous pressure versus deflection curve, using a different approach, which involves the following steps.

(a) Apply membrane stiffness correction to the raw pressure-deflection data, as discussed in Chapter 3, and plot pressure versus deflection curves corresponding to each of the test depths.

(b) Examine each curve to determine the membrane lift off position and the initial portion of the curve, corresponding to the low strain region, where the curves show a fairly linear trend.

(c) Draw a straight line through the initial data points of the curve and determine its slope in terms of pressure/deflection. The plotting and inspection of all the curves, obtained from a number of modified dilatometer tests, reveal that these curves can be broadly categorised under four different types, namely:

- Curves from relatively stiff or cemented layers (Figures 4.1), where the slope is higher than the slope of the line joining points A and B.
- Curves from relatively weak or loose layers, where the slope coincides with the slope joining points A and B (Figure 4.2).
- Curves from marshy layers (Figures 4.3), where the slope is lower than the slope of the line joining points A and B.
- Curves from very weak soils, where no reading corresponding to point A is recorded (Figures 4.4). The modified dilatometer data is useful as there are a number of pressure and deflection readings, enabling an estimate of the Young's modulus.

(d) Calculate and substitute the value of modified slope in the Gravesen's equation and work out the new dilatometer modulus, $E_{D(new)}$. The original Gravesen equation is of the following form:

$$S_0 = \frac{2D\Delta P}{\pi} \cdot \frac{(1 - \mu^2)}{E} \qquad (4.1)$$

where,

$\frac{E}{(1 - \mu^2)} = E_D$ = dilatometer modulus,

E = Young's modulus of elasticity,

μ = Poisson's ratio,

S_0 = net membrane deflection = 1.1 mm,

ΔP = change of membrane pressure causing 1.1 mm deflection, and

D = diameter of membrane

Equation 4.1 can be rearranged to give the dilatometer modulus:

$$E_{D(new)} = \frac{E}{1-\mu^2} = \frac{2D}{\pi} \cdot \left(\frac{\Delta P}{S_0}\right) \qquad (4.2)$$

where,

$(\Delta P/S_0)$ = slope of the linear portion of the pressure versus deflection line corresponding to low strain.

For a membrane with diameter, D = 60 mm, Equation 4.2 becomes:

$$E_{D(new)} = 38.18 \text{ .(slope of the line)} \quad (4.3)$$

Various researchers have found that the standard dilatometer modulus, E_D, directly gives the Young's modulus of soil at 25% deviator stress level (eg Bellotti et al., 1985, 1986; Baldi et al., 1986; Campanella and Robertson, 1983; Jamiolkowski et al., 1988; Berardi et al., 1991). However, according to Leonards and Frost (1988), the Young's modulus hence predicted is towards the conservative side. This conservatism is possibly due to the non-linear relation between the membrane pressure and deflection and could be avoided if the new dilatometer modulus, $E_{D(new)}$, is used instead of E_D.

Even though independent examination of all the curves one by one, drawing of tangents, working out the slopes of the tangents and finally the evaluation of Young's modulus consumes more time than the standard approach, the results so obtained are more realistic and accurate. This method is particularly useful in the stiffer, cemented and over consolidated deposits, where the usual procedure using the standard dilatometer gives quite conservative values.

The E_{25} profiles evaluated from the modified dilatometer data using the two approaches (first one from the modified slope and second from the standard slope) are compared in Figure 4.5. The comparison indicates that the Marchetti (1980) method under predicts the Young's modulus, except for the weaker soil layers (between 1.5 and 2.5 metres of depth), where it gives reasonable predictions.

The profiles of E_{25} evaluated from the proposed method (using modified slope) are also compared with the standard dilatometer evaluated E_{25} (refer to Figure 4.6). It can be seen in Figure 4.6 that in cemented layers (between 3 and 6 metres of depth), the standard dilatometer modulus gives a maximum value of E_{25} = 35 MPa whereas the proposed method gives an increased maximum value of E_{25} = 45 MPa.

4.4 Pore pressure study from the modified dilatometer data

The membrane pressure should return to the atmospheric pressure after complete depressurisation of the dilatometer membrane, as the DMT box vent is opened to the atmosphere for the escape of all the gas. However, it can be seen from Figures 4.7a and 4.7b that the final membrane pressure upon depressurisation is not equal to the atmospheric pressure.

A comparison of three pressure versus deflection curves obtained from different test depths, shown in Figures 4.7a and 4.7b, indicate that the final membrane pressure upon depressurisation increases with the depth of the ground water table. The Figures show that the membrane pressure upon depressurisation is a minimum in the curve of the minimum test depth and a maximum in the curve of maximum test depth.

If the membrane pressure upon depressurisation is considered to be a true indicator of the in situ pore water pressure (Schmertmann, 1986), then the pore water pressures in the curves representing test depths of 0.62, 2.5 and 5.26 metres are around 0, 30, and 60 kPa respectively (Figure 4.7a), whereas the pore water pressures calculated directly from the ground water table are 0, 16 and 45 kPa, respectively, for the same depths. Figure 4.7b also shows a variation of nearly 60 kPa in the pore water pressure value for a change of nearly 5 metres in the test depth. The difference of 15 kPa is within the precision of the pressure transducer.

An examination of all the final pressure readings upon complete depressurisation indicate that the pore pressure so evaluated is not consistent with depth. This may be due to the fact that the present test site consists of calcareous sand which is not necessarily a free draining material and even though the DMTs were performed slowly, the time may not be sufficient to ensure the complete drainage of water, thereby giving inconsistent pore pressure values. However, in weakly cemented layers, good agreement is obtained between the depressurisation data and the values calculated from the ground water table position.

Before this method of evaluating pore pressure can be widely applied, further testing and study is needed. Modified dilatometer tests need to be carried out on pure silica sand to ensure complete drainage. The possibility of providing piezometer within the modified dilatometer membrane should also be explored for a more effective evaluation of pore pressure.

The third pressure reading upon membrane depressurisation, obtained from the standard dilatometer was found to be less reliable than the modified DMT as: (a) the DMTs were performed at close depth intervals and the pore pressure variation between two consecutive test depths was too small (approximately 2 kPa) to be directly read from the pressure measurement gauge and (b) the third pressure reading of the normal dilatometer is not corrected for the membrane stiffness, applicable for the depressurisation stage.

4.5 Comparative study of cone and dilatometer blade tip resistances

The standard DMT readings do not involve a bearing capacity failure reading and q_c values recorded from an adjacent CPT are used for the evaluation of ϕ and K_o. It is therefore worth examining whether the q_d values recorded during the course of DMT soundings could serve the purpose of q_c.

A comparative study of profiles of dilatometer blade tip resistance, q_d, and cone tip resistance, q_c, conducted at adjacent locations show that the two are not equal. Figure 4.8 shows that all three q_c profiles obtained within a 5 metre diameter circular area are essentially similar, whereas the q_d profiles obtained within the same area vary significantly, and are different from the adjacent q_c profiles. This difference between the two tip resistances is not in accordance with the American penetration testing experience (Schmertmann, 1986), according to which q_d nearly equals the adjacent q_c.

The difference between the adjacent q_d and q_c profiles suggest that the factors influencing the two resistances are different. A comparison of q_d profiles with the P_0 and P_1 (contact and expansion membrane pressures) profiles, recorded during the same sounding reveal that q_d profiles follow the same trend as the P_0 and P_1 profiles (refer to Figures 4.9a and 4.9b). That is, where P_0 and P_1 are low, q_d is also low, and where P_0 and P_1 increase so does the q_d. As the P_0 and P_1 pressures are direct indicators of horizontal soil stress, it can be inferred that q_d is influenced by the horizontal earth pressure. Similar comparisons of cone tip resistance, q_c, with the adjacent P_0 and P_1 profiles, as shown in Figure 4.9a and 4.9b, indicate that q_c profiles are quite consistent and do not follow the trends of P_0 and P_1 pressure profiles as well as the q_d profiles.

This suggests that if there is a variation in the horizontal stress of the soil, the dilatometer blade tip resistance will indicate it better than the cone tip resistance. This sensitivity of q_d to the horizontal stresses could be due to the shape of the dilatometer blade as all the other main factors influencing q_d and q_c values, such as the angle of soil friction, soil to steel friction and other in situ conditions, remain the same.

Research by Baldi et al. (1981) suggests that the soil properties can be better correlated to the in situ horizontal stress (represented by the membrane pressure readings in the case of DMT) of the soil rather than the vertical stress (represented by the cone tip resistance in the case of CPT) because the vertical stress changes less appreciably with the change in soil properties compared to the horizontal stress. It can be seen that within a relatively small test area there is appreciable variation in the dilatometer membrane pressures, P_0 and P_1, (Figures 4.9a and 4.9b) and dilatometer blade tip resistances, q_d, (Figure 4.8) whereas the cone tip resistance, q_c, (Figure 4.8) does not indicate this variation. It is due to this fact that the dilatometer is proving increasingly useful as a horizontal strength sensing device, for the in situ evaluation of soil properties.

As the above discussion confirms the sensitivity of q_d to the horizontal soil strength, it can be correlated to important soil properties. Large calibration chamber tests conducted upon the modified dilatometer which are capable of giving the q_d and P_0, P_1 values during the same sounding, would provide further data on this.

4.5.1 Evaluation of K_o and ϕ from dilatometer tip resistance

Cone penetration tests adjacent to dilatometer tests would not be necessary if the dilatometer blade tip resistance served as an alternative to the cone tip resistance. But the comparative study of the cone and dilatometer blade tip resistances show that the two differ and therefore use of q_d in place of q_c could lead to error, as the CPT-DMT K_o and ϕ correlations are developed with q_c values in mind.

However, as the dilatometer blade tip resistance, q_d, is found to be sensitive to the horizontal stress of the soil, it can be used as an alternative horizontal stress index (similar to K_D), for the direct evaluation of $K_{o(oc)}$. For exploring this possibility, the $K_{o(oc)}$ values evaluated from the dual scale chart (Baldi et al, 1986) or its analytical form, (excluding the data from the upper crust) were plotted against respective (q_d/σ'_v) (the new horizontal stress index) and a non-linear relation was found, shown

in Figure 4.10. Large scale calibration chamber tests are necessary for confirming the suitability of q_d for the assessment of K_o.

Attempts have also been made to use the adjacent q_d and q_c values for the in situ evaluation of the angle of friction of soil, based on D & M theory, as described in Chapter 2. Based on the parametric study of D & M theory, Schmertmann (1982) suggested the following equation for the evaluation of angle of friction of sand.

$$q_d/q_c = 2.03 - 0.04\ \phi'_{ps} \qquad (4.4)$$

where, ϕ'_{ps} is the angle of friction of sand for plane strain conditions.

During the course of field testing adjacent q_d and q_c values were recorded and the q_d/q_c ratio was used for the evaluation of ϕ'_{ps}, using Equation 4.4. The resulting profile of angle of friction tends to be too high for low q_d/q_c ratios (when $q_d/q_c < 0.5$) and too low for higher q_d/q_c ratios (refer to Figure 4.11), when compared to the laboratory evaluated values of angle of friction. A number of consolidated drained triaxial tests give an average value of $\phi'_{ax} = 32^o$ and shear box tests give an average of $\phi'_{ps} = 37^o$, which do not agree with the ϕ'_{ps} profile shown in Figure 4.11. Hence, it can be concluded that q_d/q_c changes due to factors other than the angle of soil friction and therefore this theory could not be relied upon for the evaluation of angle of friction.

4.6 Summary

The interpretation of the in situ Young's modulus of soil, based on membrane pressure readings, P_0 and P_1 leads to error and often gives conservative results. In loose sands this method may give reasonable predictions of the Young's modulus but in dense or cemented soils, with increased cementation or over consolidation, the Young's modulus is underestimated due to the non-linear relationship between the membrane pressure and deflection. This underestimation would be avoided if continuous readings of pressure and deflection are recorded from the modified and automated dilatometer.

The modified dilatometer data better indicates the variation in the in situ water pressure than the standard DMT. The present testing program was designed for calcareous sand deposits and further testing in free draining silica sand would be helpful in confirming the ability of the modified dilatometer for such a purpose.

Installation of a piezometer inside the dilatometer blade as well as the cone penetrometer shaft would be of additional advantage.

The dilatometer blade tip resistance has been found to be sensitive to the horizontal stress of the soil and attempts should be made to relate it to the important soil properties, mainly K_o and ϕ, so that DMT can be used independently.

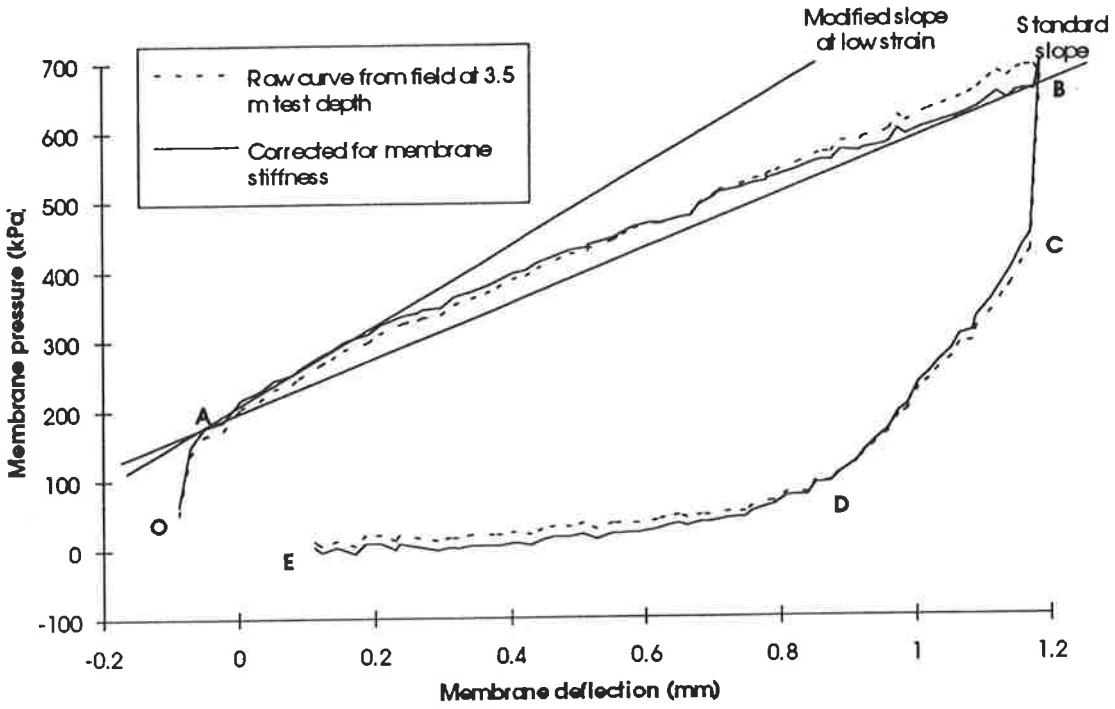

Figure 4.1 **A typical pressure versus deflection curve from the modified dilatometer.**

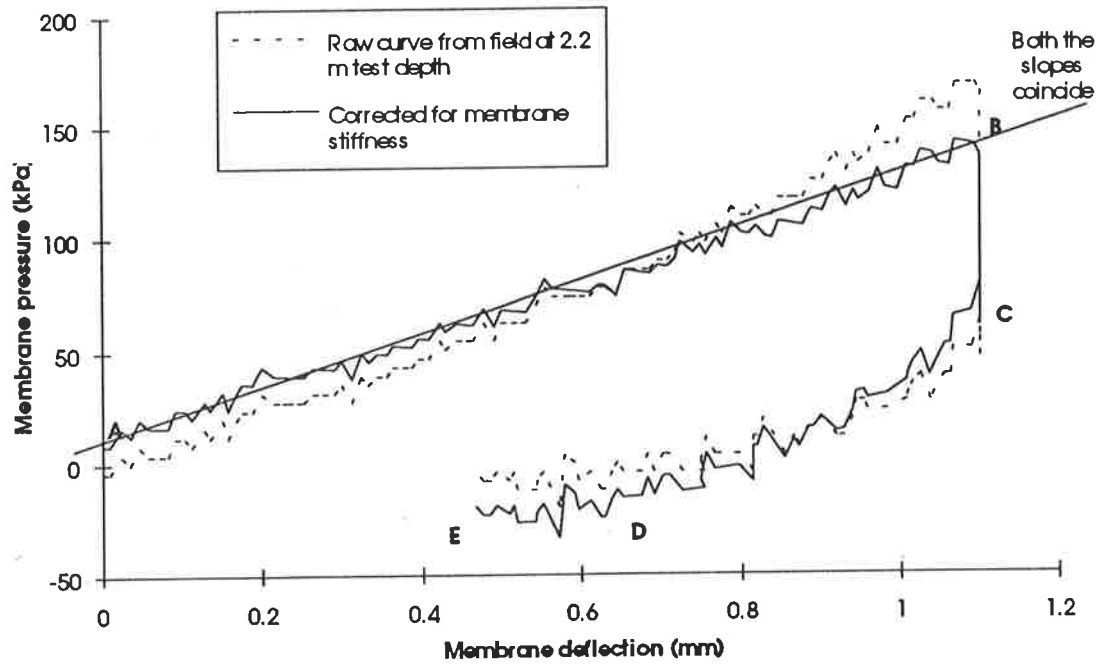

Figure 4.2 **Pressure versus deflection curve from loose silty sand, corresponding to 2.2 m test depth**

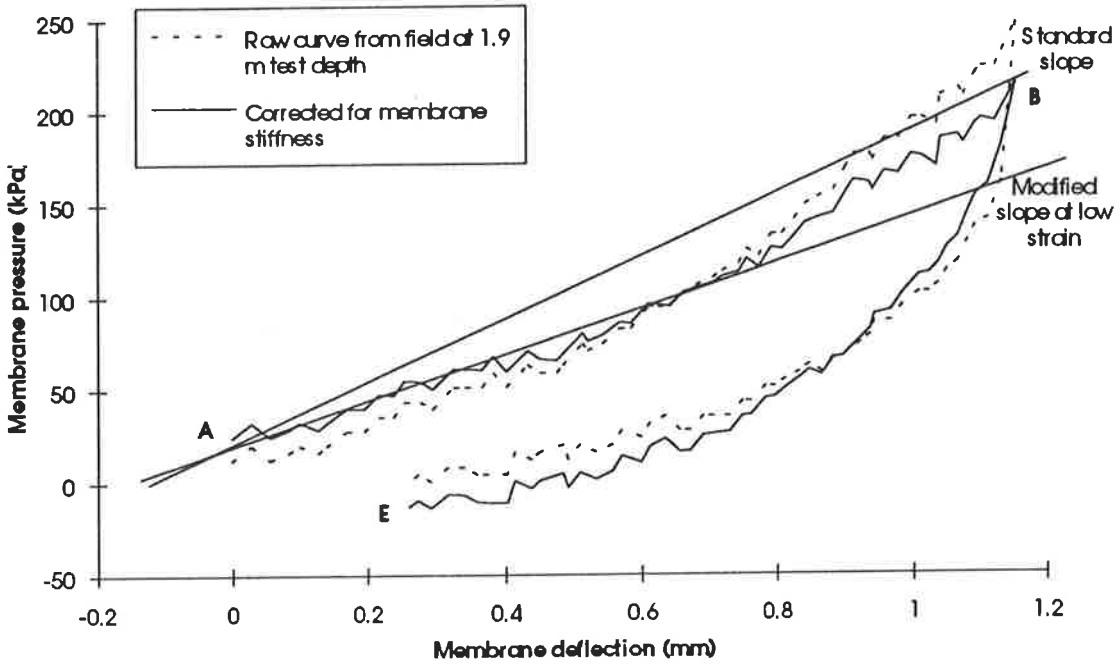

Figure 4.3 **Pressure versus deflection curve from marshy layer, corresponding to 1.9 m test depth.**

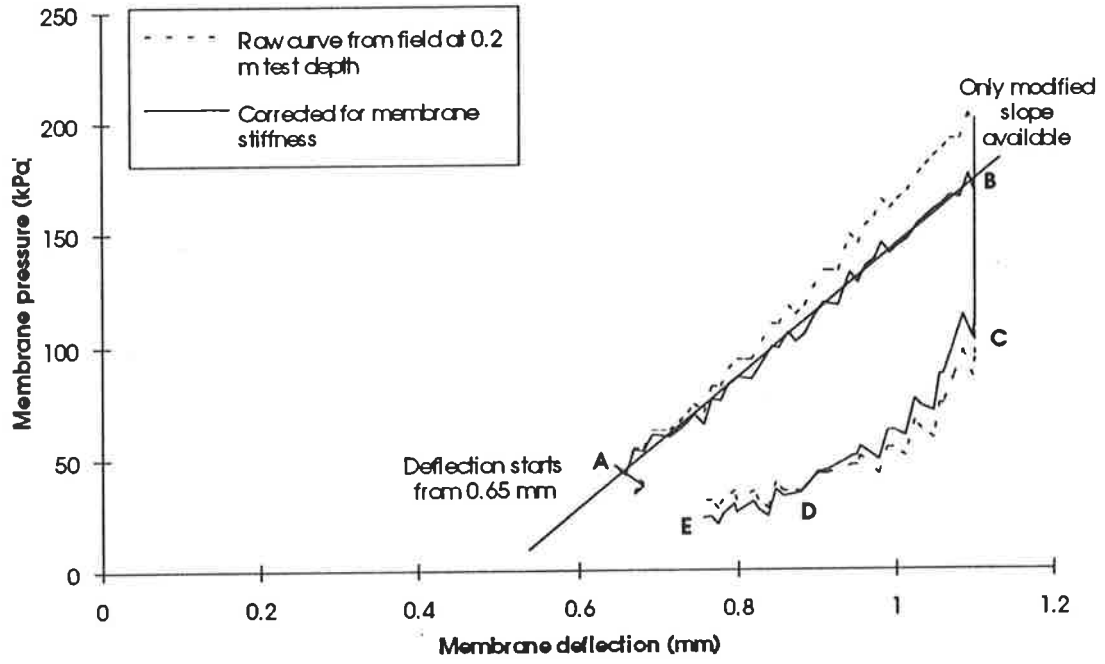

Figure 4.4 **Pressure versus deflection curve from very weak silty sand, corresponding to 0.2 m test depth**

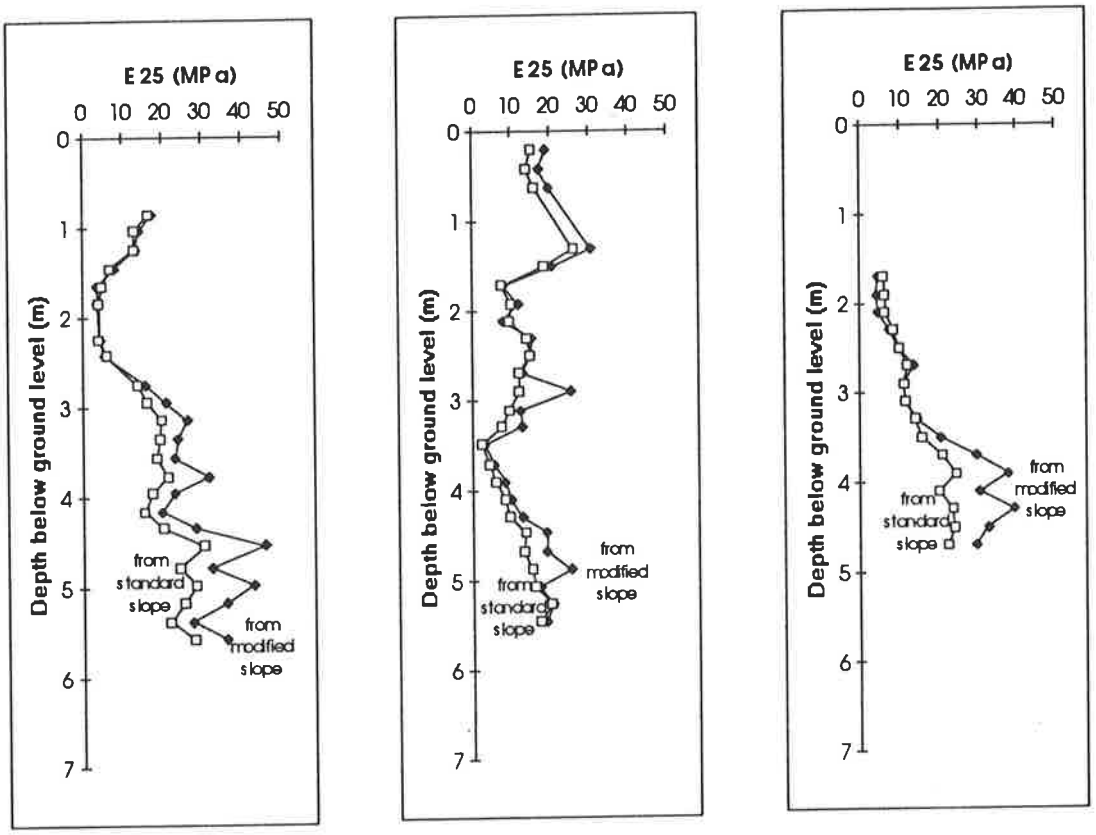

Figure 4.5 **Comparison of the Young's modulus (E_{25}) evaluated from the standard slope (Marchetti, 1980) and from the modified slope (both evaluated from the modified dilatometer data).**

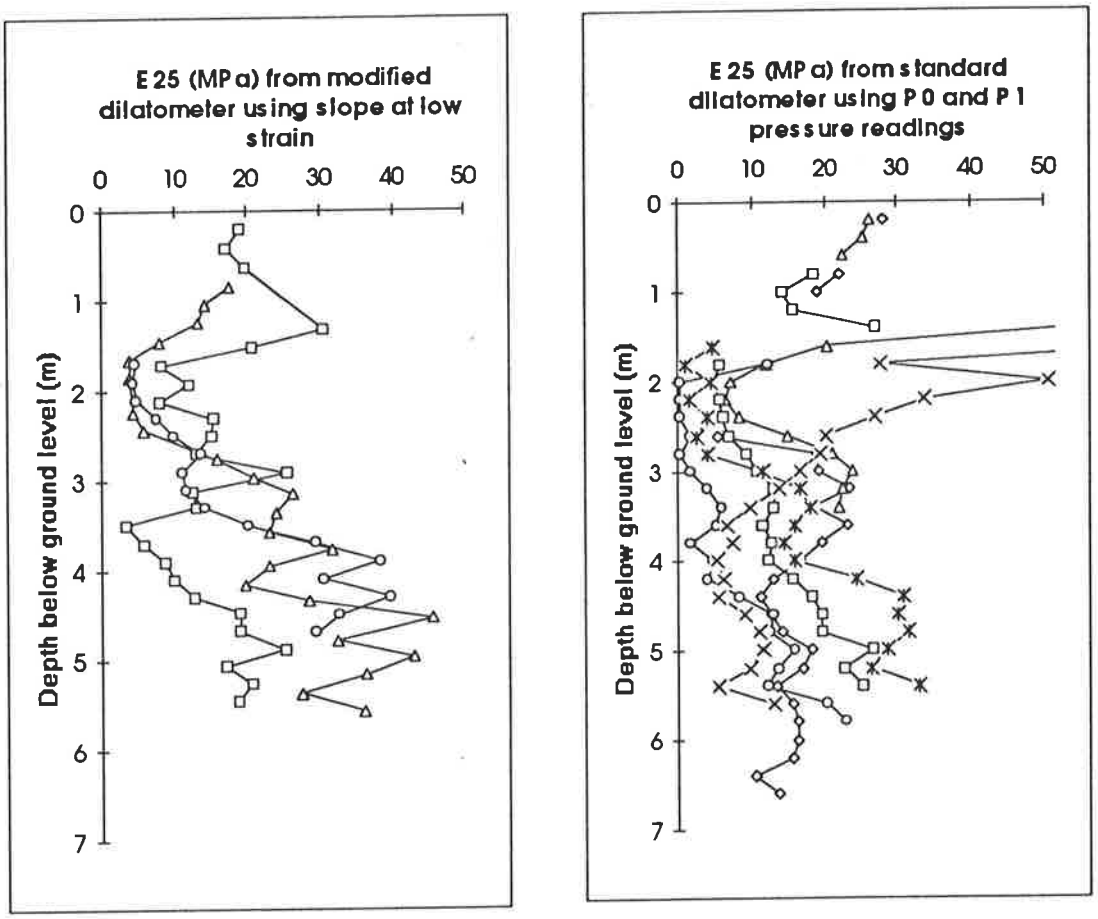

Figure 4.6 **Comparison of the Young's modulus (E_{25}) evaluated from the standard dilatometer modulus (using standard dilatometer data) and from the proposed method (using modified dilatometer data).**

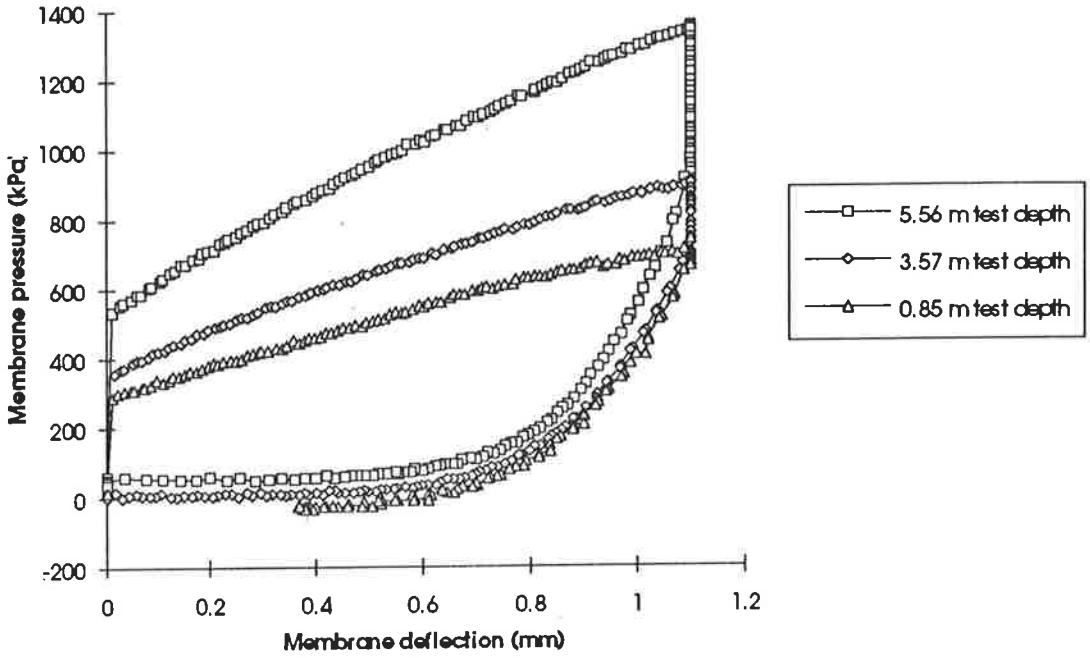

Figure 4.7a **Evaluation of pore water pressure from the depressurisation stage of the continuous curve, modified dilatometer sounding 1b.**

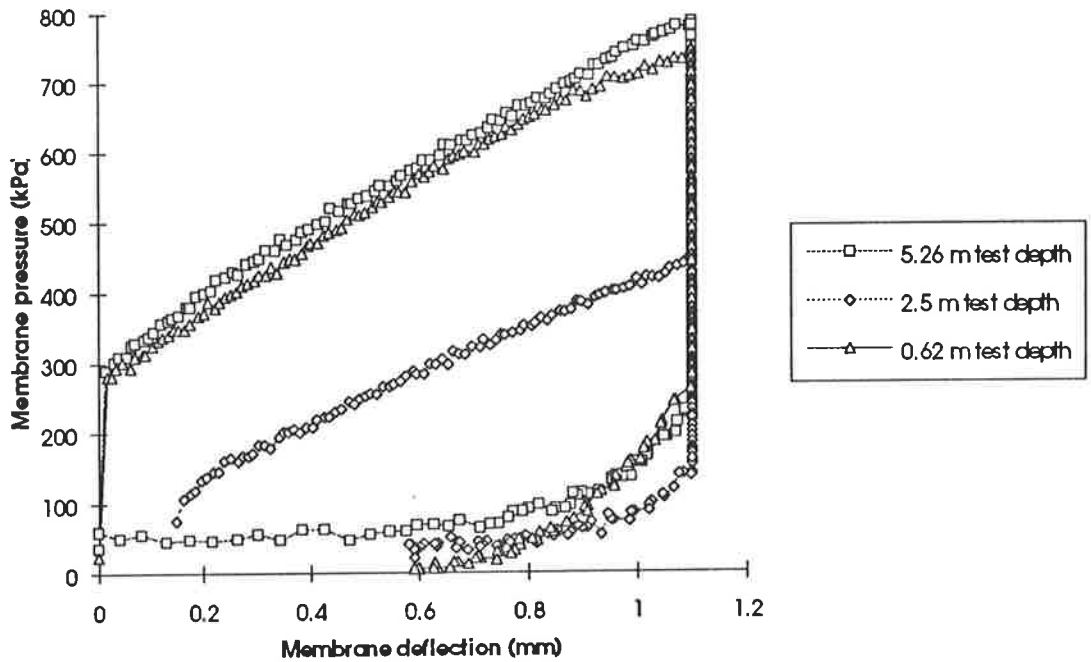

Figure 4.7b **Evaluation of pore water pressure from the depressurisation stage of the continuous curve, modified dilatometer sounding 1a.**

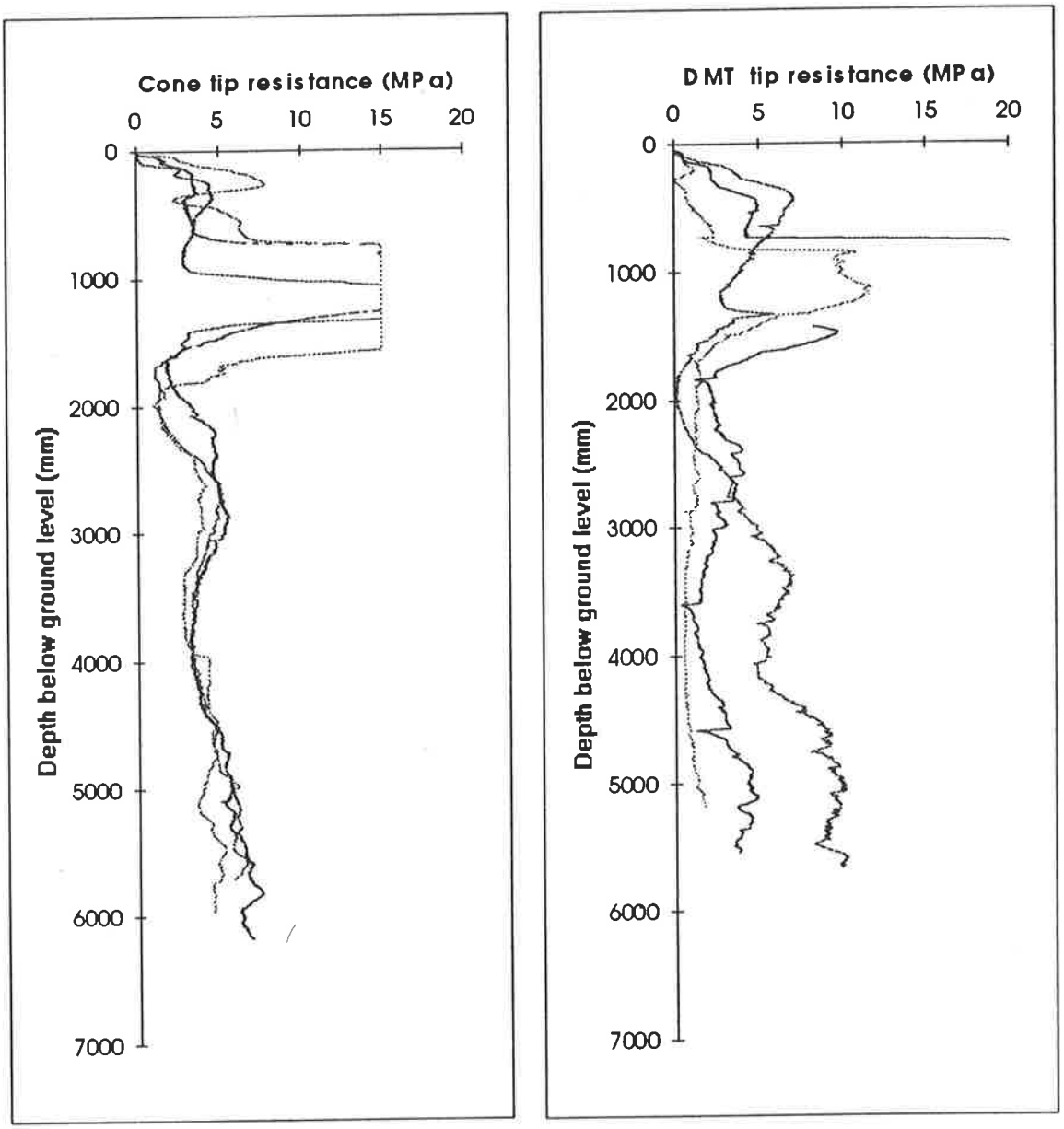

Figure 4.8 **Comparison of cone and dilatometer blade tip resistances, representing a 5 metre diameter circular area.**

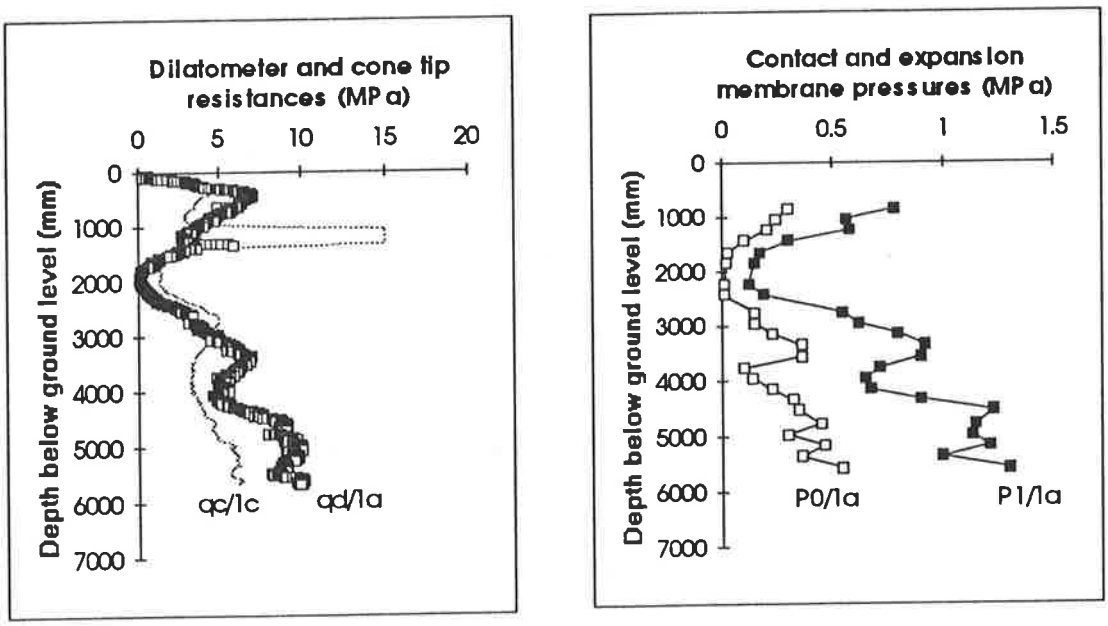

Figure 4.9a Comparison of P_0 and P_1 dilatometer membrane pressures with the dilatometer and cone tip resistances at Location 1a.

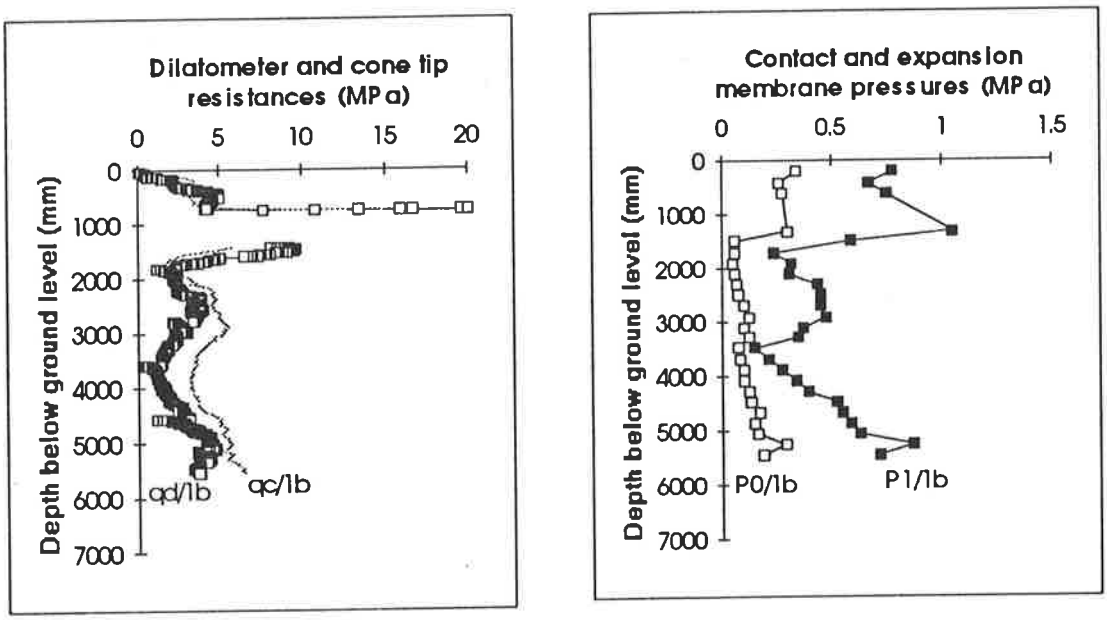

Figure 4.9b Comparison of P_0 and P_1 dilatometer membrane pressures with the dilatometer and cone tip resistances at Location 1b.

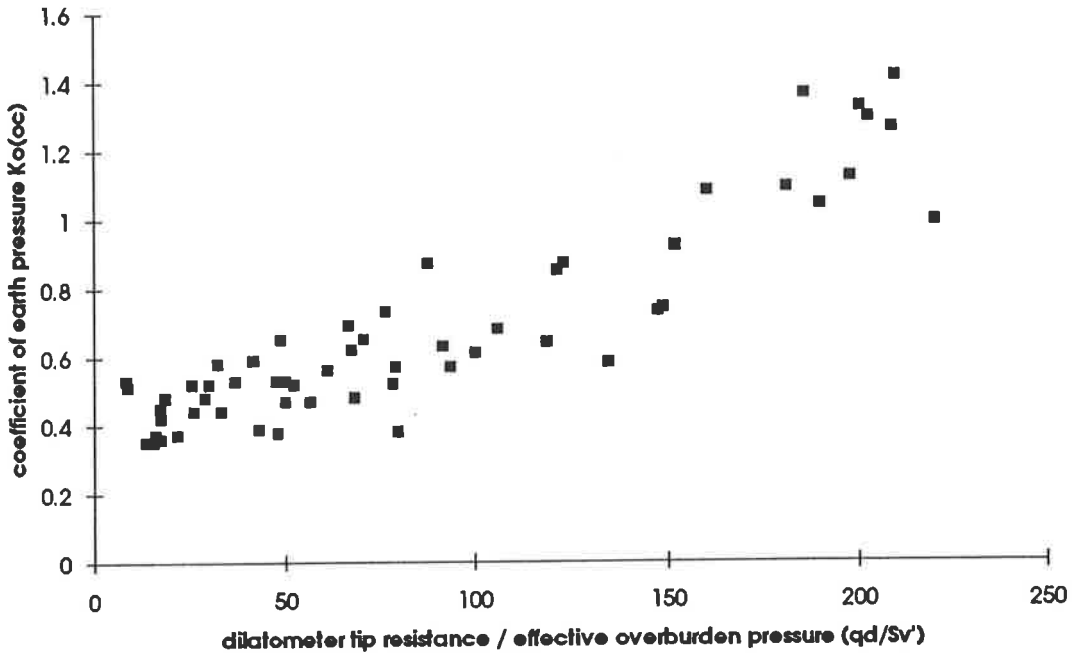

Figure 4.10 **Possible evaluation of coefficient of earth pressure at rest from the dilatometer blade tip resistance, q_d.**

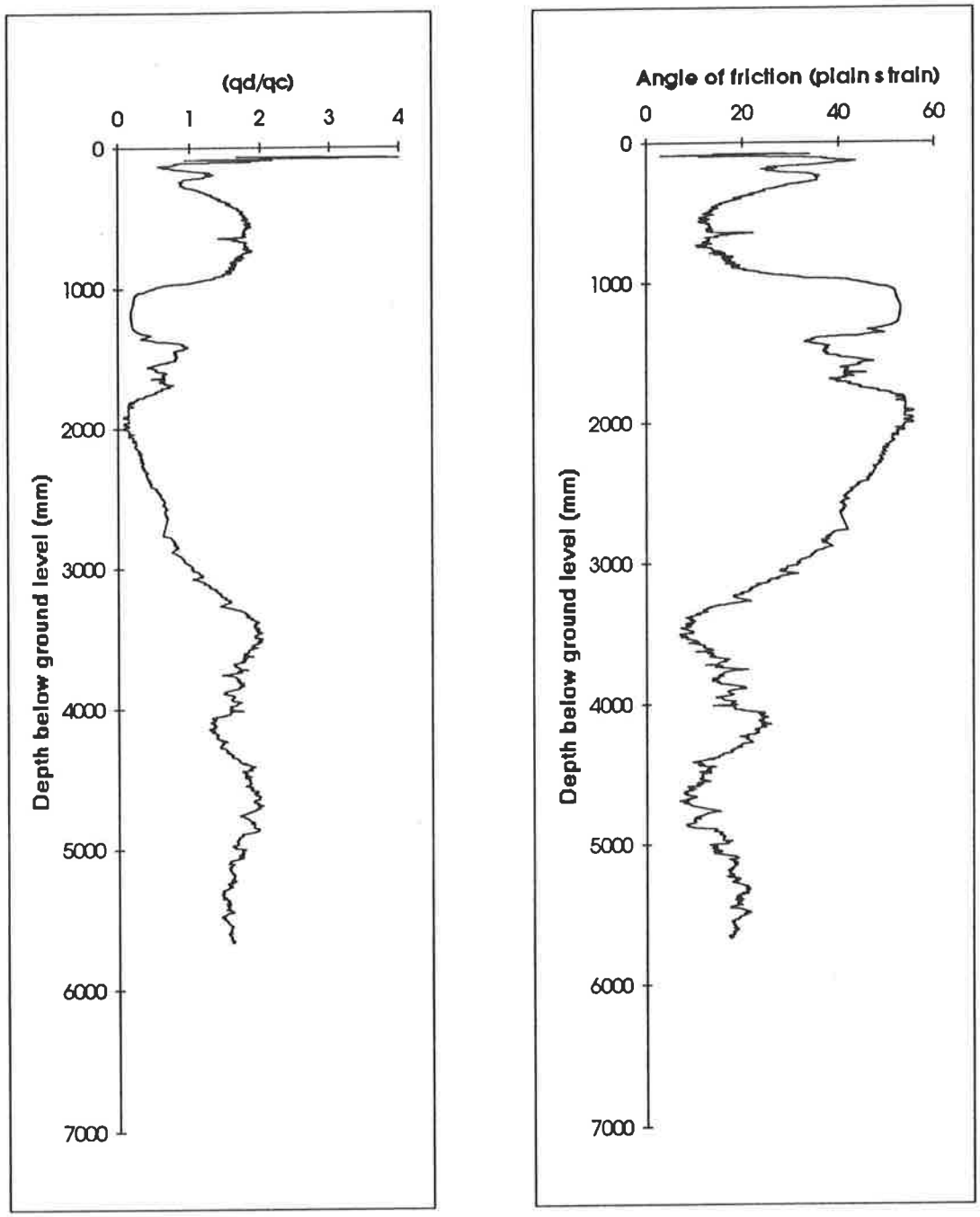

Figure 4.11 **A trial for the evaluation of angle of friction of soil based on q_d/q_c ratio; after Schmertmann (1982) method.**

Chapter 5

INTERPRETATION OF STANDARD DMT AND CPT RESULTS AND THEIR LABORATORY VERIFICATION

5.1 Introduction

This Chapter presents the reduction of normal DMT and CPT data, evaluation of important soil properties using the established silica based correlations, presentation of these properties in graphical form and their comparison with laboratory evaluated results. Various CPT and DMT correlations, discussed earlier in the literature review are summarised in Table 5.1 and used for the interpretation of in situ soil properties.

Since DMT and CPT correlations for cohesionless soils were proposed after a large number of field, laboratory and calibration chamber tests, it is more realistic to check in the laboratory the validity and suitability of these existing correlations with respect to slightly calcareous sand and suggest the most appropriate value for the local conditions, rather than attempt to propose new ones. This is particularly true in the case of calcareous sands as their properties tend to vary depending on their degree of cementation, chemical composition, depositional environment, age and biogenesis, making difficult the formulation of standard correlations. Therefore the existing correlations can be applied for the purpose, after proper laboratory verification and local field experience.

Table 5.1 Summary of existing DMT, CPT correlations used for interpretation of various soil properties.

Soil property	Device	Parameters	Reference(s)
Grain size or soil stratigraphy	DMT	I_D	Marchetti (1980)
	DMT	E_D, I_D	Schmertmann (1986)
	CPT	q_c, F_R %	Douglas and Olsen (1981)
			Campanella and Robertson (1983)
Bulk density (γ_b)	DMT	E_D, I_D	Marchetti (1980)
Relative density (D_r)	CPT	q_c, σ'_m (mean effective stress)	Jamiolkowski et al. (1988)
Constrained modulus (M)	DMT	I_D, E_D, K_D	Marchetti (1980)
	CPT	q_c, D_r	Mitchell and Gardner (1975)
			Vesic (1970)
Initial tangent modulus (E_i)	DMT	E_D	Robertson et al. (1988)
Modulus of elasticity (E_{25})	DMT	E_D	Baldi et al. (1986)
Coefficient of earth pressure at rest $K_{o(OC)}$	DMT, CPT	K_D, σ'_v, q_c adjacent	Baldi et al. (1986)
		K_D, q_d at the same spot, σ'_v	Schmertmann (1983)
Angle of friction (ϕ'_{ax})	DMT, CPT	$K_{(OC)}$, K_D	Schmertmann (1983)
	DMT, CPT	q_d,q_c adjacent	Schmertmann D& M method (1982)
Overconsolidation ratio (OCR)	DMT	$K_{(OC)}$, ϕ'_{ax}	Mayne and Kulhawy (1982) or, Schmertmann (1983)
Preconsolidation pressure (p'_c)	DMT	OCR, σ'_v	*

The CPT data comprising of cone tip resistance, q_c, and sleeve friction, f_s, is reduced to obtain friction ratio, F_R, and DMT data comprising of dilatometer blade tip resistance, q_d, and dilatometer membrane readings P_0 and P_1 reduced to obtain the three dilatometer indices, namely the dilatometer modulus, E_D, Material index, I_D, and Horizontal stress index, K_D, as described in the method of data reduction in Chapter 2.

At the beginning of this Chapter the DMT and CPT parameters are examined to find out their sensitivity to the presence of calcareous sediments and their effectiveness in detecting the degree of cementation of different soil layers. In subsequent sections some of the commonly used design parameters of soil, namely, the angle of friction, relative density and modulus of elasticity are evaluated by using the existing correlations and results verified by the laboratory tested results.

Further, the correlations are applied for the assessment of other important soil parameters, including coefficient of earth pressure at rest, overconsolidation ratio and preconsolidation pressure. Although it is comparatively difficult to correctly evaluate these parameters in the laboratory owing to sampling disturbance and loss of original stress conditions, an attempt is made to find out the maximum and minimum values of these parameters by examining the trends of these profiles and safe values are recommend for design purposes.

Finally, a conclusion is reached as to how the existing pure silica based correlations could be used for the safe evaluation of slightly calcareous offshore sand properties, especially for the purpose of bearing capacity and settlement calculations.

5.2 Soil stratigraphy

The prediction of soil stratigraphy is done by CPT as well as DMT, using cone tip resistance and friction ratio in the case of CPT, or E_D and I_D in the case of DMT. I_D is used to get an idea of the soil grain size and increases as the soil particles get coarser. The trend of P_0 and P_1 membrane pressure profiles can also be used to get a fair idea of the soil stratigraphy. A study is done to find out the response of these DMT and CPT parameters for the case of moderately calcareous sand and discussed one by one as below.

5.2.1 Soil stratigraphy from dilatometer material index (I_D) and dilatometer modulus (E_D)

The dilatometer material index, I_D, is calculated from P_0 and P_1 pressure readings using the formula, $I_D = (P_1 - P_0)/(P_0 - U_0)$, proposed by Marchetti (1980). Various researchers (Marchetti, 1980; Schmertmann, 1982; Lacasse and Lunne, 1986; Lutenegger and Kabir, 1988) concluded that the material index changes only with a change in the soil type and does not change if a change is brought about in the stress level of the same soil by the way of compaction, saturation or drying it.

Profiles of I_D representing six dilatometer tests, drawn in Figure 5.1, reveal that I_D values at Location 1 are invariably more than 1.8 and at Location 2 varies between 1 and 4 below 3 metres. According to Marchetti (1980), this is an indication of sand and silt. But at Location 2, I_D decreases to a value less than 0.6 above 3 metres of depth, which would indicate a clay layer if only the I_D value is relied upon for soil identification.

It is therefore preferable to use I_D together with another DMT index, E_D, for the purpose of soil identification, as proposed in the Schmertmann (1986) classification chart. Classification based on both I_D and E_D correctly indicates the presence of a highly compressible muddy or marshy layer between 1.8 to 3 metres of depth at Location 2, as E_D in this layer (shown in Figure 5.8) is less than 2 MPa. Therefore, it is necessary to use both I_D and E_D for identification of soil at the present test site, so that a compressible muddy or marshy layer is detected rightly and not misinterpreted as a clay layer.

At Location 2, one of the tests at spot o2a shows I_D (Figure 5.1) between 1 and 1.8 with the corresponding E_D (Figure 5.8) value more than 2 MPa, thereby suggesting that the test site consists of silt and silty sand layers also. Hence, according to I_D - E_D based identification the test site consists of sand and silty sand in general with few compressible and marshy layers.

In cemented layers P_0 and P_1 membrane pressure readings increase depending upon the degree of cementation, causing variations in I_D values, as the value of I_D is dependent upon P_0 and P_1 pressure readings. Hence, in case of cemented layers (between 1 and 2 metres at Location 1 and between 1.5 and 3 metres at Location 2), I_D values can not be relied upon for correct soil identification.

I_D values in the cemented layers can be unusually high or low depending upon whether the P_0 increases more than P_1 or vice versa. If P_0 increases more than P_1 then I_D decreases. On the other hand if P_1 increases more than P_0 then I_D increases. Both these cases have been experienced during the present testing. It is therefore advisable that an assessment of the soil stratigraphy be based on the trend of P_0 and P_1 profiles and their variation relative to overburden pressure with depth, as discussed in the following section.

5.2.2 Soil stratigraphy from P_0 And P_1 profiles

Lacasse and Lunne (1988) recommended the use of P_0 and P_1 pressure profiles and their respective positioning with respect to line of soil overburden pressure for getting a fair idea of the soil type. It was noticed (Marchetti, 1980; Lacasse and Lunne, 1988) that in the case of sand, the P_0 profiles nearly coincide with the line of soil overburden pressure, σ_v, and the P_1 profiles with that of 10 σ_v line.

During the present DMT testing, P_0 and P_1 profiles obtained from six standard dilatometer tests, all within a distance of 10 metres, are found to be close enough to the σ_v and the 10 σ_v lines, respectively, (refer to Figures 5.2, 5.3, 5.4), except at the depths where the soil was highly cemented. At these depths, both the P_0 and P_1 profiles tend to shift outwards beyond the σ_v and 10 σ_v lines, respectively. The greater the cementation the more is the shift of P_0 and P_1 profiles away from the expected positions.

An examination of P_0 and P_1 profiles in Figure 5.2 and Figure 5.3 indicate that the test site consists of a highly cemented crust between 1.2 and 1.7 metres, as the shift of the P_0 and P_1 profiles, away from the respective σ_v and 10 σ_v lines is quite pronounced. The cementation also increases at 3 and 5 metres of depth at location 1 (Figure 5.2). At location 2 (Figure 5.3), one of the three tests shows high cementation whereas the other two tests show no cementation, indicating that there are variations in cementation, even over short distances.

An inward shift of the P_1 profile, closer to the σ_v line, indicates an increase in the silt content. The more the inward shift of P_1 profile, the larger the content of silt in sand and more compressible the soil is. It can be seen from the Figures 5.2 and 5.3 that in some of the tests at location 1 (eg o1a, o1b at 2.2 metres) and also at location 2 (o2a and o2c after 3 metres), the P_1 profiles tend to get closer to the P_0 profiles, indicating

the presence of weak and compressible layers, with a possible increase in the silt content, devoid of cementation.

Figure 5.4 shows all the P_0 and P_1 profiles combined, obtained from both the test locations, indicating that the site consists of variable sand and silt with varying degrees of cementation.

5.2.3 Soil stratigraphy determined from CPT data

The prediction of soil stratigraphy from the CPT relies on the values of cone tip resistance, q_c, and friction ratio, F_R. Many CPT based classification charts have been proposed for the interpretation of soil stratigraphy (Douglas and Olsen, 1981; Campanella and Robertson, 1983; etc.). In the present study, the simplified and working version soil classification chart by Campanella and Robertson (1983) is used to determine the soil stratigraphy of the test site.

Figures 5.5 and 5.6 show the q_c and F_R profiles of the two test locations. According to the CPT classification system, both the test locations consist exclusively of sand except at the following depths, where it indicates silt or silty sand layers, as q_c drops below 3 MPa with corresponding increase in F_R.

at Location 1 (Figure 5.5):

soundings 1a, 1b, 1c	between 1.6 and 2.4 metres of depth
soundings 1a, 1b, 1c	between 3.5 and 4.2 metres of depth

at Location 2 (Figure 5.6):

sounding 2b	between 3.3 and 4.0 metres of depth
sounding 2a	between 3.8 and 4.1 metres of depth
sounding 2a	between 5.3 and 6.0 metres of depth

In general, the test site consists of sand and silty sand according to this classification system.

An examination of q_c and F_R profiles reveal that q_c increases considerably at places of high cementation whereas the corresponding F_R remains quite low, an indicator of cemented calcareous crust. For example, a value of 15 MPa was recorded during all the cone penetration tests and reflected in the q_c profiles between depths 0.75 m and 1.5 m below the ground surface. In fact q_c exceeds 15 MPa in this upper crust but

due to range of the CPT data acquisition system, a maximum of only 15 MPa is recorded and shown in the Figures.

5.2.4 Soil stratigraphy based on laboratory test results

Sieve analysis was done on samples recovered during continuous sampling to obtain the particle size distribution curves for the laboratory identification and classification of soil. Figure 5.7 shows all the particle size distribution curves obtained.

These particle size distribution curves indicate that the soil consists of gravelly sand with almost negligible silt content, contrary to the in situ predicted results. However, as the test site is variable in nature, more sampling and sieve analysis results could possibly confirm the presence of thin silty layers. The particle size distribution curves of Coffey International (1991), from the same location and discussed in Chapter 3, indicate the presence of a number of silty layers (up to 30 % silt content in some cases; mentioned in Table 3.1 of Chapter 3) and can be used as a justification of in situ predictions.

From the study of various DMT and CPT based classification systems and laboratory test results, it is concluded that the DMT and CPT give a reasonable idea of the type of soil and the degree of cementation of calcareous sand, but the prediction of soil stratigraphy should preferably be based on the trends and positioning of P_0, P_1, q_c and F_R profiles, instead of relying on the numerical values of I_D and E_D.

5.3 Deformation parameters

Three different types of deformation parameters can be evaluated from the DMT and CPT, namely, the constrained modulus, M, from the DMT, the constrained modulus from the CPT and Young's modulus of elasticity at 25 % stress level, E_{25}, from the DMT. The profiles of these deformation parameters are discussed below one by one.

5.3.1 Constrained modulus (M) from DMT

The DMT predicted M relies on Marchetti (1980) correlations, using DMT parameters I_D, E_D and K_D. A number of correlations have been proposed by Marchetti (1980) for the evaluation of M in soils of different types and selection of the relevant correlation is based on numerical values of I_D and K_D. If I_D is less than 0.6, which is indicative of clay, the correlation used is based on data exclusively from clayey soils.

On the other hand if I_D is more than 1.8, which indicates the presence of sand, then the correlation derived for sand is selected for evaluation of M.

However, as discussed under the soil stratigraphy, I_D can not be totally relied upon for the correct soil identification in calcareous sediments, making difficult the selection of appropriate correlation. For example, at Location 2, the I_D profile in Figure 5.1 gives a value of I_D less than 0.6, indicating clay, but the Schmertmann (1986) classification system and particle size distribution curves from the same depth reveal the presence of marshy and highly compressible sand. Hence, the selection of a suitable correlation based only on I_D value could give misleading values of M.

Moreover, Marchetti (1980) correlations for M were based on only few reference data points from sand and were mostly based on data from clayey soils. From recent research regarding the current status of DMT correlations, Jamiolkowski et al. (1988), suggests that M evaluated from Marchetti (1980) correlations may not give satisfactory results even in uncemented sand, due to the lack of sand data in the formulation of these correlations. However, profiles of M evaluated from Marchetti (1980) correlations and shown in Figure 5.9 give a value of 10 to 50 MPa at Location 1 and between 5 to 70 at Location 2, for depths more than 3 metres.

A comparison between M and E_D profiles was undertaken to examine effects of cementation, as both M and E_D are types of deformation parameters (M is the inverse of the coefficient of volume change, m_v; whereas E_D is related to Young's modulus of elasticity of the soil). A comparison of M profiles in Figure 5.9 with E_D profiles in Figure 5.8 reveals that in weakly cemented layers (o1a, o1b and o2c after 3 metres of depth) both M and E_D range between 10 and 20 MPa. However in more cemented layers (o2a at 1.8 metres of depth), the increase in M is more pronounced compared to E_D, as this layer gives a value of M = 180 MPa, compared to E_D = 70 MPa. This could be due to the fact that the correlations used for the evaluation of M uses the horizontal stress index, K_D, which is sensitive to horizontal strength of the soil and increases appreciably due to extra strength provided by cementation (refer to Figure 5.12 to see how K_D increases in the cemented layers).

For a reasonable prediction of M from the Marchetti (1980) correlation, it is therefore advisable that (a) a relevant correlation be applied after soil identification based on both E_D and I_D parameters (Schmertmann, 1986) rather than relying only on I_D, (b) values of M evaluated from relatively less cemented layers should be used, as cementation results in overprediction of M and (c) for the present test site a design

value between 10 and 20 MPa (after 3 metres of depth) should be taken for settlement calculations.

5.3.2 Constrained modulus from CPT

A simple correlation, $M = 2.5\ q_c$, was proposed by Mitchell and Gardner (1975) for an approximate estimate of in situ M. Other researchers (Vesic, 1970; Dahlberg et al., 1974; Lunne and Kleven, 1981; Baldi et al., 1982) proposed that the value of 2.5 was applicable to normally consolidated sand and the constant could vary significantly in the case of overconsolidated soils. The selection of the constant is very difficult and up to now a wide range of constants ranging between 2.5 and 13, have been proposed depending upon the value of OCR (Campanella and Robertson, 1983). Due to wide variations of OCR in cemented soils, selection of a proper coefficient is difficult, but as the site appears to be normally consolidated (discussed in following sections), an evaluation of M is based on the correlation $M = 2.5\ q_c$.

Profiles of M, obtained from the above correlation are shown in Figure 5.10 and give a value between 5 and 20 MPa below a depth of 2 metres. A comparison of this figure with the E_D profiles, Figure 5.8, shows that the two agree and give an average of 10 to 20 MPa below 3 metres of depth, except for the layers of relatively high and low cementation.

As the dilatometer membrane senses the horizontal stress directly, DMT predicted E_D values are more susceptible to changes in horizontal stress when compared to the CPT predicted M. For example one of the tests (spot o2c) in a highly compressible layer at a depth of 2.0 m gives a value of $E_D = 0.1$ MPa (Figure 5.8), compared to $M = 1.5$ MPa in Figure 5.10. On the other hand at spot o2b, $E_D = 30$ MPa due to increased horizontal stress whereas $M = 22$ MPa, proving better ability of DMT in sensing the soil compressibility. Due to this horizontal strength sensing ability of soil, it is beneficial to use the DMT predicted dilatometer modulus, E_D, for the direct evaluation of Young's modulus, as discussed in the following section.

5.3.3 Young's modulus of elasticity (E_{25})

Due to the uncertainty in the DMT and CPT evaluated constrained moduli, M, attempts have been made to evaluate the modulus of elasticity corresponding to 25% stress level, E_{25}, directly from the dilatometer modulus, E_D. This is a better option as evaluation of E_D relies directly on the membrane pressure readings required to push

the soil horizontally and does not involve a number of complicated correlations, the right selection of which is difficult.

According to Campanella and Robertson (1983), E_D approximately represents the value of Young's modulus of soil at 25% stress level, E_{25}, in cohesionless soils. If this is assumed to be correct, then the E_D profiles shown in Figure 5.8 can be directly used for an estimate of the E_{25} profiles.

Figure 5.8 shows that after a depth of 3 metres E_D varies between 10 and 30 MPa at Location 1, and between 5 and 35 MPa at Location 2. Near 1.5 metres of depth, where a cemented crust exists, the value of E_D increases up to 70 MPa at Location 2, and 60 MPa at Location 1. This shows that the cementation tends to increase the modulus of elasticity of soil.

An examination of all the profiles combined shows that o2c is the least cemented spot which gives the minimum value of modulus of elasticity, ranging between 5 and 20 MPa after a depth of 3 metres. Between 2 and 3 metres, where a muddy or marshy layer exists, the o2c profile gives modulus of elasticity as low as 0.1 MPa. All the other profiles also show a substantial decrease in E_D for this highly compressible layer.

Standard dilatometer calculated E_{25} also has limitations as it is evaluated from E_D which considers pressure readings at only two membrane deflection positions and assumes a linear relationship between membrane pressure and deflection. As the pressure versus deflection curves obtained from the modified dilatometer tests and described in Chapter 4, show a non linear relationship between pressure and deflection, it is advisable to evaluate the modulus of elasticity after inspection of pressure versus deflection curves, as suggested in Chapter 4.

Consolidated drained (CD) triaxial tests were conducted in the laboratory to compare in situ E_D with the laboratory evaluated E_{25} values. Recovery of undisturbed samples from cemented layers proved difficult and samples were obtained from 2 m depth, where there was low cementation. A number of CD tests were conducted on 38 mm diameter specimens, reconstituted at the field dry density. The tests were conducted for different values of effective cell pressures ranging between 25 and 75 kPa and the values of Young's modulus corresponding to 25% of the failure deviator stress were evaluated. The results are presented in Table 5.2:

Table 5.2 Results of consolidated drained (CD) triaxial tests

Effective cell pressure (kPa)	25 kPa	50 kPa	75 kPa
E_{25} (MPa)	6.20 MPa	13.04 MPa	6.23 MPa

The CD tests give E_{25} values between 6 and 13 MPa for different values of effective cell pressures. This compares with the in situ E_D profiles which also give values up to 10 MPa for different test locations (refer to E_D values at 2 m test depth, Figure 5.8)

Effective cell pressures between 25 and 75 kPa during the CD tests are close to the in situ stress conditions as the estimated effective vertical overburden pressure, σ_v', varies between 20 and 70 kPa and the effective horizontal earth pressure, σ_h', varies between 10 and 35 kPa for depths between 2 and 7 m. The estimate of σ_h' is based on the formula, $\sigma_h' = K_o \cdot \sigma_v'$ (Jaky, 1944). An estimate of σ_v' can be made from the field and laboratory evaluated bulk densities and K_o is assumed to be nearly 0.45 for the test site (in Section 5.4 it is shown that the values of K_o evaluated from weakly cemented layers are close to 0.45). Thus σ_h' can be estimated for different test depths.

As the laboratory tests were conducted on reconstituted samples, which are devoid of the original cementation, the laboratory evaluated E_{25} is lower than to the in situ E_D, especially in strongly cemented layers. Therefore, it appears logical to rely on field profiles of E_D rather than the laboratory results as it is difficult to simulate field conditions during laboratory tests.

In summary, reasonable estimates of Young's modulus, E_{25}, can be made from the standard dilatometer test data. However, for a more realistic evaluation of Young's modulus the modified dilatometer modulus $E_{D(new)}$ should be used based on the slope of pressure versus deflection curves (discussed in Chapter 4), as it takes into account the non linear relationship between the membrane pressure and deflection.

5.4 Coefficient of earth pressure at rest

Evaluation of K_o is based on the dual scale chart or its analytical form, using the relationship between K_0 , K_D and (q_c/σ_v'), proposed by Baldi et al. (1986). According to the K_0 , K_D and (q_c/σ_v') correlation, K_O increases with the horizontal stress index, K_D, and decreases with increase in the factor (q_c/σ_v').

As K_o evaluated from the K_0 , K_D and (q_c/σ_v') correlation is dependent upon K_D and the later changes appreciably due to cementation (Figure 5.11 shows that K_D increases due to cementation), an increase in K_D due to cementation results in an increased K_o. On the other hand (q_c/σ_v') also increases with cementation thereby decreasing K_o to a certain extent.

An examination of K_D profiles in Figure 5.11 and corresponding K_o profiles in Figure 5.12 show that whenever K_D increases, there is a corresponding increase in K_o, except for the highly cemented crust where, even though K_D is high, the (q_c/σ_v') factor increases substantially, due to very high cone tip resistance, beyond 15 MPa, resulting in an overall decrease in the K_o values.

The accuracy of K_o predicted from the K_0 , K_D and (q_c/σ_v') correlation depends on the selection of the coefficients for K_D and (q_c/σ_v'). Due to great variations in calcareous sand, a definite set of coefficients can not be proposed and the existing correlation may over predict or under predict the K_o values.

Hence, in calcareous sediments it is recommended that the spots with least cementation should be selected for the evaluation of K_o. Profiles of P_0, P_1 or K_D can be utilised for detecting the least cemented spot, as discussed earlier in Section 5.2. In the present case, spots o1a, o1b and o2c are the least cemented and K_o profiles at these spots, as shown in Figure 5.12, give values between 0.4 and 0.5, suggesting a normally consolidated deposit. This is acceptable, as the site consists of soft sand barring a few hard crusts. At other spots o1c and o2b, where the P_0, P_1 or K_D profiles show increased cementation, the K_o profiles give higher K_o values, going up to 1.5.

An evaluation of K_o is also done from the angle of friction obtained in the laboratory from the shear box tests, using the correlation $K_0 = 1 - \sin\phi$ (Jaky, 1944) and

treating the site as a normally consolidated sand deposit (field profiles from the least cemented spots o1a, o1b and o2c give $K_o \simeq 0.45$). A number of shear box tests give average $\phi'_{ps} = 37°$ which is equivalent to $\phi'_{ax} = 35°$ when converted to axial strain conditions using Equation 2.13a. Its substitution in to Jaky (1944) correlation, gives $K_o = 0.43$, indicating a normally consolidated sand deposit.

A number of consolidated drained triaxial tests give an average of $\phi'_{ax} \simeq 31°$, which when used with the Jaky (1944) correlation gives K_o of 0.48, indicating once again a normally consolidated young sand deposit.

In summary, the K_o evaluated by Baldi (1986) correlation indicates the presence of normally consolidated deposit at spots of least cementation. Hence K_o obtained from low cemented spots should be referred to for a true prediction of K_o in calcareous sediments.

5.5 Angle of friction

The value of K_o evaluated from the dual scale chart is substituted into the Schmertmann (1983) K_0 - K_D - ϕ correlation, to evaluate the angle of friction. Figure 5.13 shows that the angle of friction for axi-symmetric conditions, ϕ'_{ax}, obtained from the above method ranges between 32° and 39°, for depths greater than 2 metres at both locations. In the upper crust (between 0 and 2 metres of depth), ϕ'_{ax} ranges between 39° and 45°.

The least cemented layers at o2c gives ϕ'_{ax} values ranging between 32° and 37°. The more cemented layers (o2b after 3.5 metres of depth) give values between 35° and 37°. Another highly cemented layer (o1c, up to 3 metres) with a high value of K_D and K_O, gives ϕ'_{ax} between 34° and 4. Hence, it appears that the effect of cementation in increasing the angle of friction is taken into account by the K_0 - K_D - ϕ correlation and a reasonable estimate of ϕ'_{ax} is obtained. The simple correlation of Jaky (1944), valid for normally consolidated soil, gives erroneous results in the cemented layers, as the value of K_o or K_D increases considerably with cementation.

The values of ϕ'_{ax} predicted by the Schmertmann (1983) method (between 32° and 39° after 2 metres of depth) agree with the shear box test results (average $\phi'_{ps} = 37°$ which is equivalent to $\phi'_{ax} = 35°$ as $\phi'_{ax} = \phi'_{ps} - (\phi'_{ps} - 32) / 3$ for $\phi'_{ps} > 32°$; refer to Equation 2.13a) and consolidated drained triaxial test results (average $\phi'_{ax} = 31°$). It

is further recommended that the angle of friction evaluated from the least cemented layers (o1a and o1b at location 1 and o1c at location 2), where ϕ'_{ax} profiles give values between 33° and 37°, should be used for design purposes so as to obtain conservative estimates of footings.

As the values of angle of friction determined from laboratory tests fall within the range of the Schmertmann (1983) method, this method can be used for an assessment of angle of friction in moderately calcareous deposits. This method of evaluating ϕ'_{ax} is preferable over others (Holden, 1976; Baldi et al., 1981; Veismanis, 1974; Villet and Mitchell, 1981 etc.), as the effect of cementation and overconsolidation is taken into account by the horizontal stress index, K_D.

5.6 Relative density

Relative density, D_r, is evaluated based on the CPT cone tip resistance, q_c, and mean effective overburden pressure, σ'_m, making use of the Jamiolkowski et al. (1988) correlation. This correlation is preferable over others (Schmertmann, 1976; Villet and Mitchell, 1981; Parkin and Lunne, 1982; Baldi et al., 1982; Lancellota et al., 1983; Jamiolkowski et al., 1988) as it minimises the error caused by chamber size effects. As all the CPT tests give almost identical q_c profiles, the profiles of D_r shown in Figure 5.14, using these q_c values are similar.

Within the highly cemented crust (between 0.75 and 1.5 metres) a high value of relative density (up to 100%) is obtained as q_c in this layer is more than 15 MPa. Beneath this crust, due to the presence of a compressible / marshy layer (mostly between 1.8 and 2.2 metres of depth), the relative density decreases to a value as low as 10% (the cone tip resistance at this layer is found to be less than 1 MPa, as shown in Figure 5.5). On the whole an average of D_r = 40% is obtained in all the profiles in Figure 5.14 beyond a depth of 3 metres.

It is rather difficult to make an assessment of relative density in the laboratory due to difficulties in correctly evaluating the values of maximum, minimum and field dry densities. The laboratory determination of field dry density is difficult because the insertion of even a thin walled sampler disturbs the in situ conditions and causes an increase in the calculated field density through compaction or compression. The laboratory determination of maximum dry density is also difficult as compaction of calcareous sand causes disintegration of shell fragments, which changes the grain size distribution.

A number of laboratory tests (conducted on samples at depths between 2.5 and 3 metres) give values of 1.22, 1.46 and 1.62 t/m^3 for the minimum dry density, field dry density and maximum dry density, respectively. This corresponds to D_r = 67%, which is an overprediction, when compared to the average of D_r = 40% from the field tests.

Even though these profiles can not be relied upon for an exact assessment of relative density, they can be used as a reference as to how the relative density changes with depth. The profiles clearly indicate the presence of a stiff layer between 0.75 and 1.5 metres followed by a 1 metre deep compressible layer, after which the value of relative density stabilises giving an average of 40 to 50 % relative density.

5.7 Overconsolidation ratio (OCR)

After the evaluation of effective angle of friction, ϕ_{ax}', an estimate of OCR was undertaken based on the Schmertmann (1983) correlation which is a modification of the Mayne and Kulhawy (1982) correlation. The Schmertmann (1983) correlation is of the following form:

$$OCR = \left[\frac{K_{o(OC)}}{1 - \sin\phi'}\right]^{\frac{1}{0.8\sin\phi'}} \qquad (5.1)$$

From Equation 5.1 it is clear that OCR is dependent upon ϕ_{ax}' and $K_{o(oc)}$. As the in situ ϕ_{ax}' evaluated from the weakly cemented layers were comparable to the laboratory values, they have been used in Equation 5.1.

Figure 5.15 shows profiles of OCR evaluated from the Schmertmann (1983) correlation, based on the in situ evaluated $K_{o(oc)}$ and ϕ_{ax}'. From the profiles it can be seen that in the less cemented layers (o1a and o1b at location 1 and o2c at location 2), the values of OCR range between 1 and 2 below a depth of 3 metres. For tests at Location o2a increased cementation results in an OCR between 2 and 4, whereas the maximum cemented layers at location o1c and o2b give OCR values exceeding 10.

After a comparative study of high and low cemented locations, it appears practical to adopt values between 1 and 2 for OCR, as representative of the weakest and the least cemented layers.

5.8 Preconsolidation pressure (P_c')

The in situ preconsolidation pressure, p_c', is evaluated using the correlation, $p_c' = OCR \times \sigma_v'$. A suitable value of bulk density of (1.6 t/m^3) has been adopted for the calculation of σ_v', after comparing the in situ predicted values of bulk densities with the laboratory evaluated values.

As discussed in Section 5.7, the values of OCR are sensitive to cementation and for layers with least cementation OCR ranging between 1 and 2 is considered to be reasonable. Therefore, the in situ OCR values evaluated from the least cemented spots can be substituted in the above equation for a reasonable assessment of preconsolidation pressure. o1a and o1b are the least cemented spots at location 1 and o2c at location 2, where p_c' profiles indicate a value between 10 and 100 kPa, after 3 metres (shown in Figure 5.16). For layers with increased cementation (spot o2a), p_c' shows slight increase and ranges between 100 and 200 kPa, whereas the layers with maximum cementation, at o1c and o2b, give values up to 400 kPa.

For settlement predictions in sand, the preconsolidation pressure is an important parameter. Even though cementation tends to increase the apparent preconsolidation pressure, it is preferable to ignore the cemented layers when calculating the maximum possible settlement and design the foundation for the worst case. In the present case the minimum value of preconsolidation pressure, obtained from 6 parallel DMT and CPT tests, is found to be between 10 and 100 kPa for depths between 3 and 6 metres and is further used for settlement computations in Chapter 6.

5.9 Summary

Due to the inherent high degree of variability, it is difficult to formulate standard correlations for calcareous sediments. The laboratory evaluation of design parameters of calcareous sediments is equally difficult due to sampling disturbance, loss of cementation and loss of original stress history. Therefore, the best option is to evaluate the various soil parameters from the existing silica based correlations and choose a correct value based on local conditions and experience.

Examination of a number of parallel DMT and CPT parameters prove the effectiveness of these devices in detecting layers of relatively high and weak cementation by inspecting the P_0, P_1, K_D and q_c profiles. In order to evaluate the

parameters of calcareous sediments using silica based correlations, it is necessary to identify the weakly cemented layers. The response of these spots is nearer to cohesionless soils, owing to the relative absence of cementation, thereby making best possible use of the existing silica sand correlations. It should be borne in mind that these correlations are capable of giving an idea of the maximum and minimum values of the various soil properties, rather than the exact values.

As most of the soil design parameters, eg, relative density, Young's modulus, coefficient of earth pressure at rest, angle of friction, overconsolidation ratio, preconsolidation pressure etc. are interrelated and in situ evaluation of one parameter requires the substitution of others, it is advisable to examine the basic DMT and CPT profiles, eg., q_c, f_s, F_R, P_0, P_1, I_D, E_D and K_D and identify the weakest and the least cemented layers within a given area. Thereafter the soil parameters of these should be evaluated progressively by data reduction.

A number of DMT and parallel CPT tests prove that the calcareous sand in the Port Adelaide region is variable in nature and within a very small distance there can be stiff as well as very weak layers. A summary of DMT and CPT evaluated design parameters is shown in Table 5.3. These values refer to depths greater than 3 metres below ground level and are representative of the least and most cemented layers. However, the evaluated results from the weakest layers are recommended for foundation design.

Table 5.3 DMT and CPT evaluated design parameters of calcareous sediments for depths greater than 3 m below ground level.

Soil properties	Minimum values (from weakly cemented layers) below 3 metres	Maximum values (from highly cemented layers) below 3 metres
Bulk density	1.6 t/m^3	1.7 t/m^3
Modulus of elasticity	10 MPa	30 MPa
Relative density	40 %	50 %
Coefficient of at rest earth pressure	0.45	1.1
Angle of friction	33°	38°
Overconsolidation ratio	1	8
Preconsolidation pressure	40 kPa	400 kPa

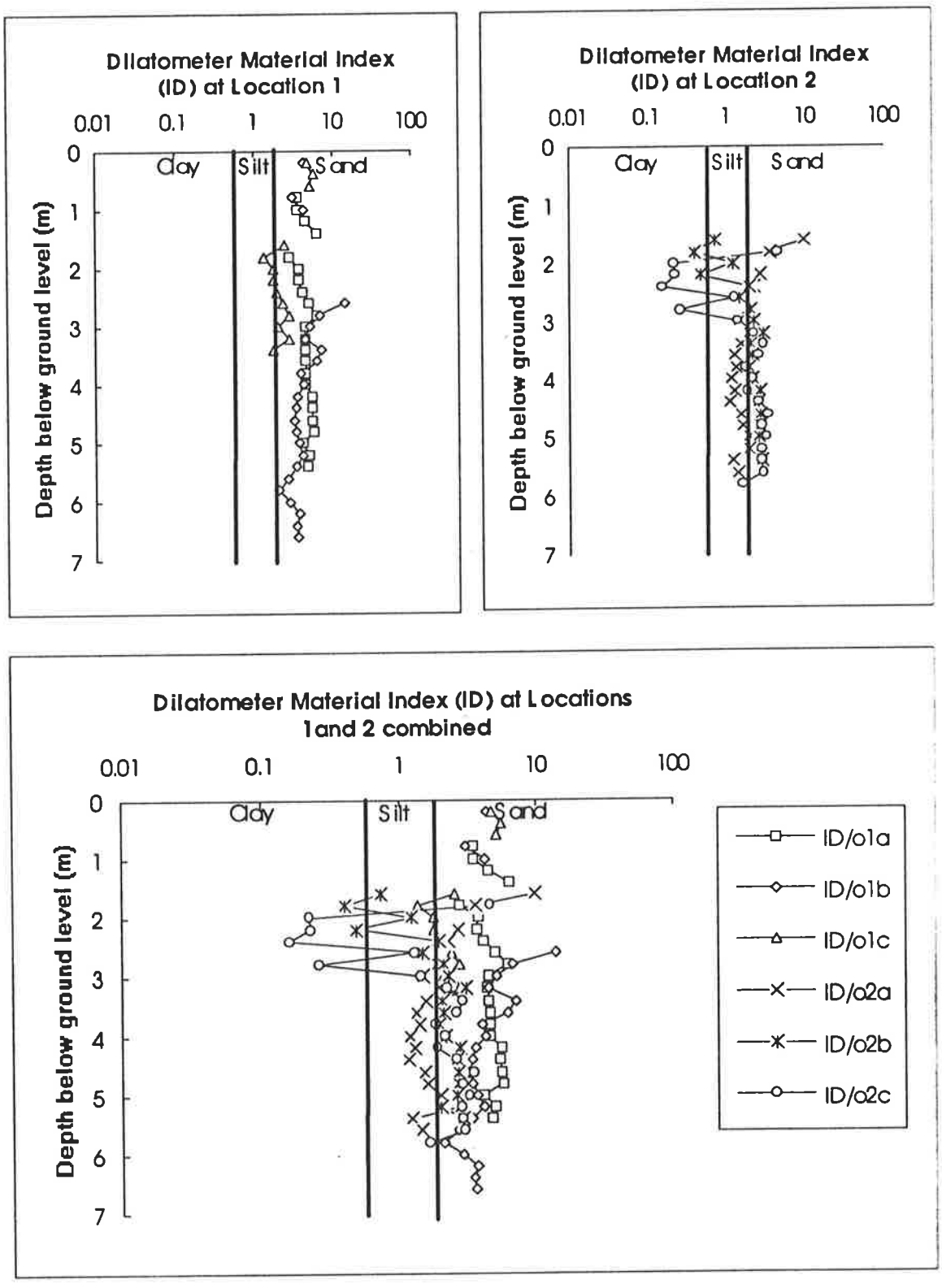

Figure 5.1 Profiles of dilatometer material index, I_D at the test Locations.

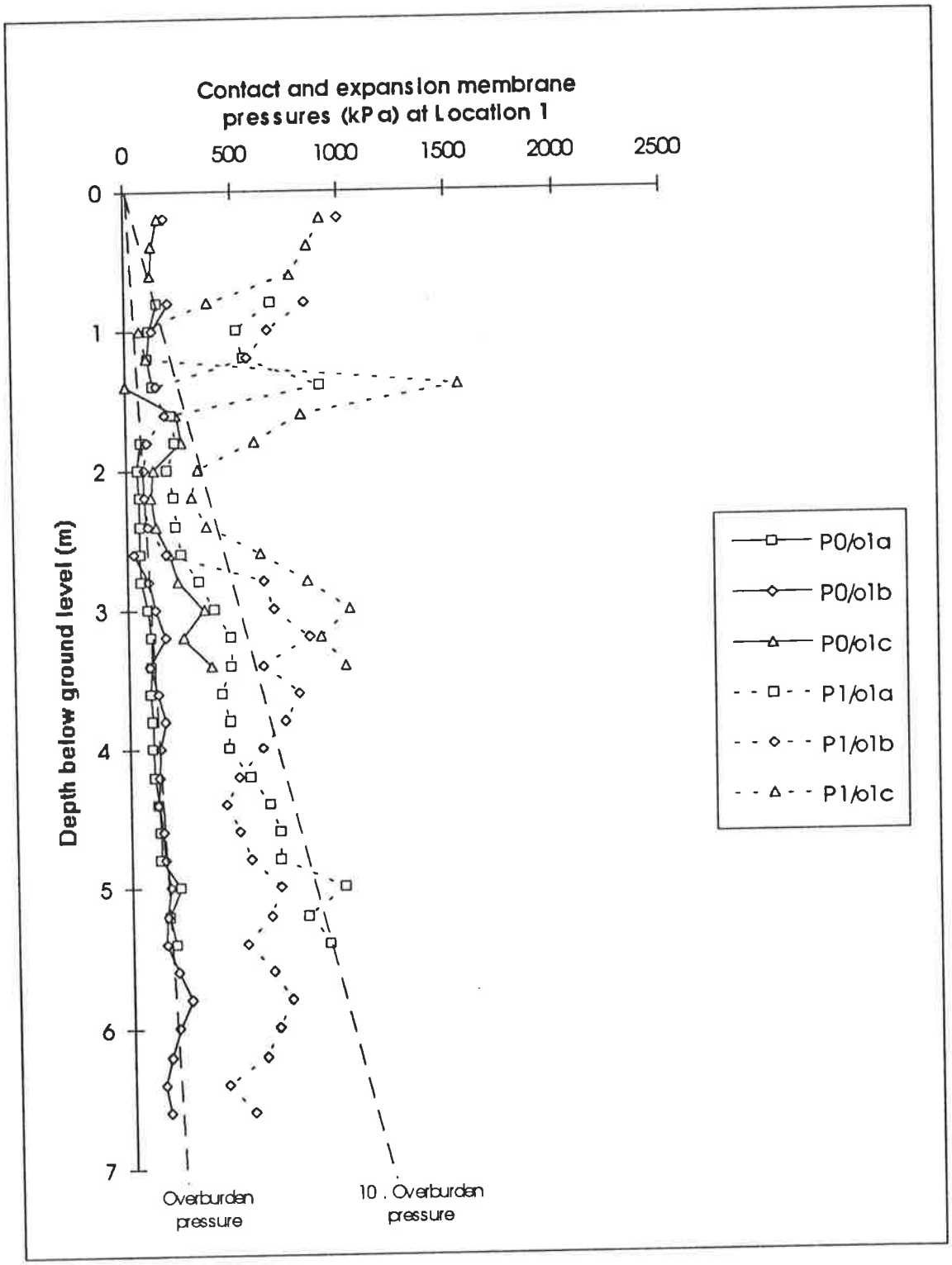

Figure 5.2 **Profiles of contact and expansion membrane pressures at Location 1.**

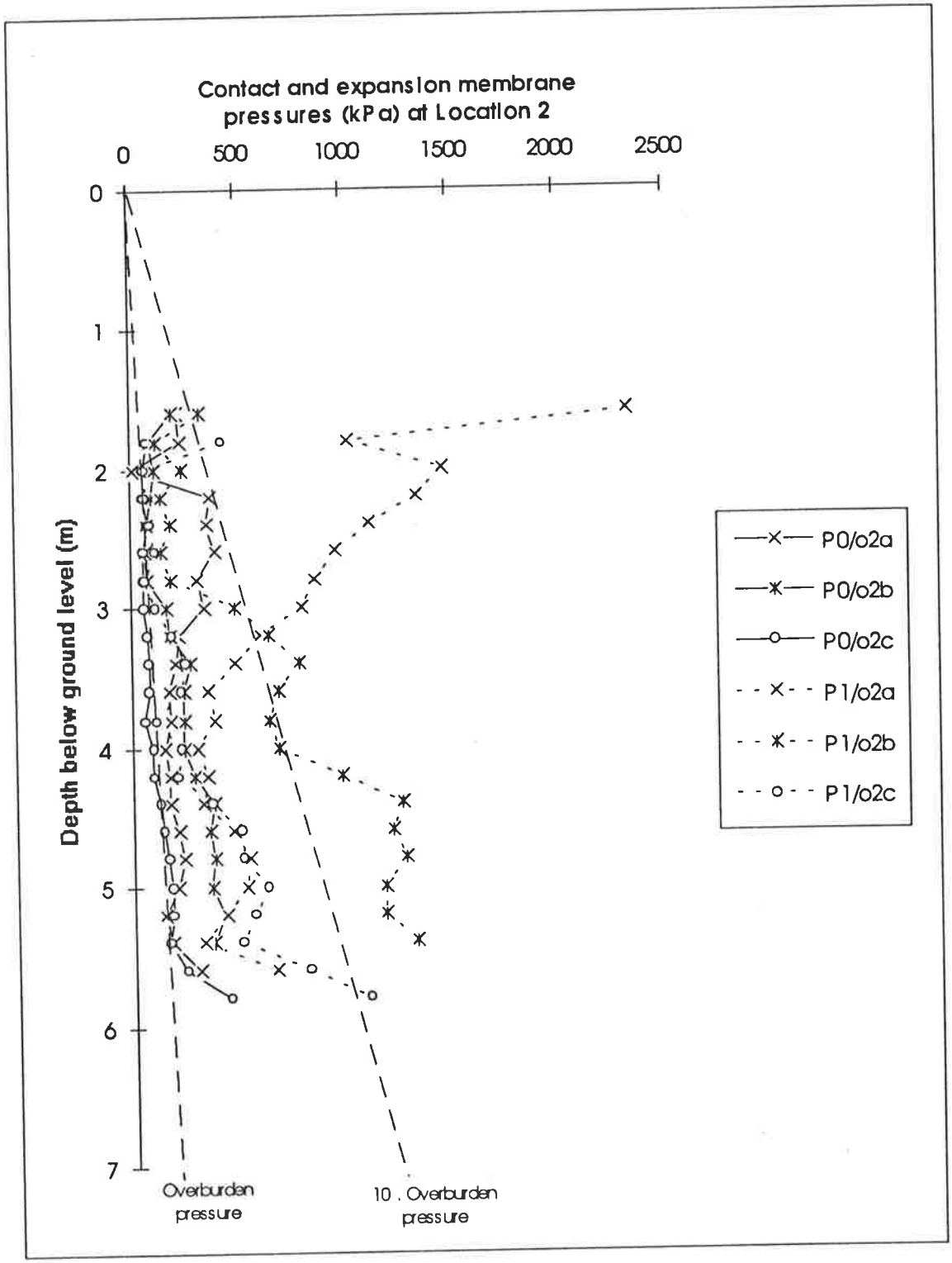

Figure 5.3 **Profiles of contact and expansion membrane pressures at Location 2.**

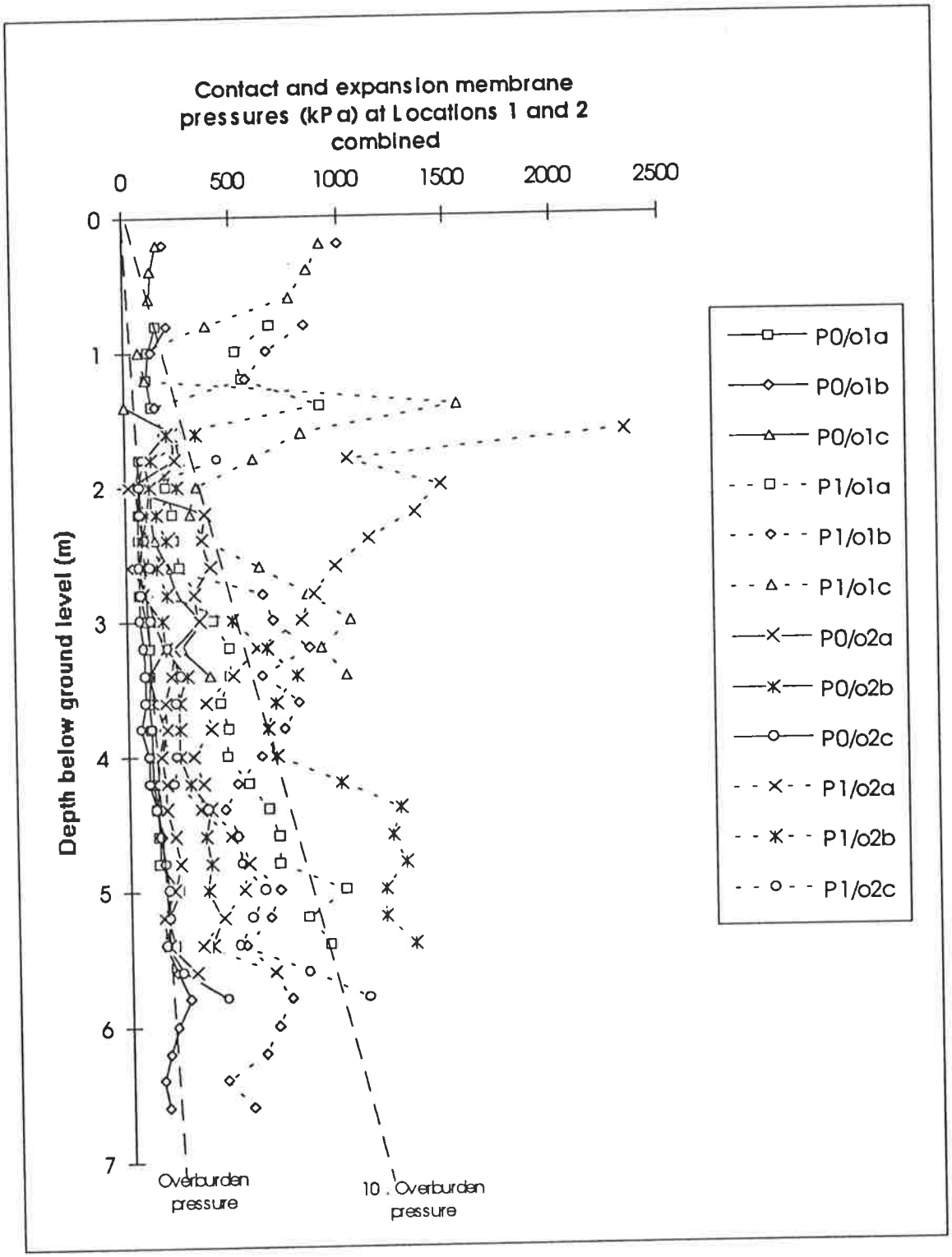

Figure 5.4 **Profiles of contact and expansion membrane pressures at Locations 1 and 2.**

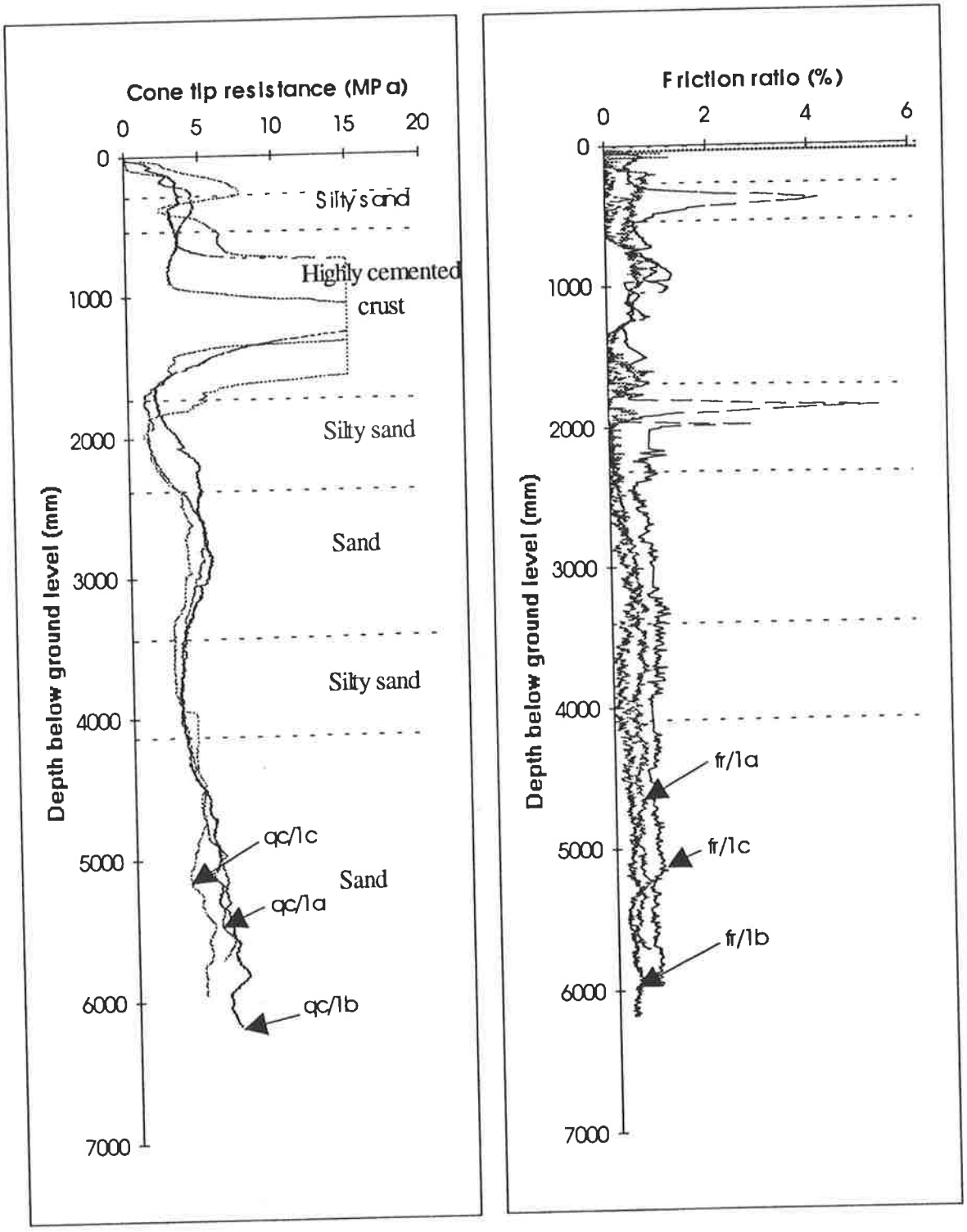

Figure 5.5 **Soil stratigraphy from the profiles of cone tip resistance, q_c, and friction ratio, F_R, at Location 1, based on Campanella and Robertson (1983) classification chart.**

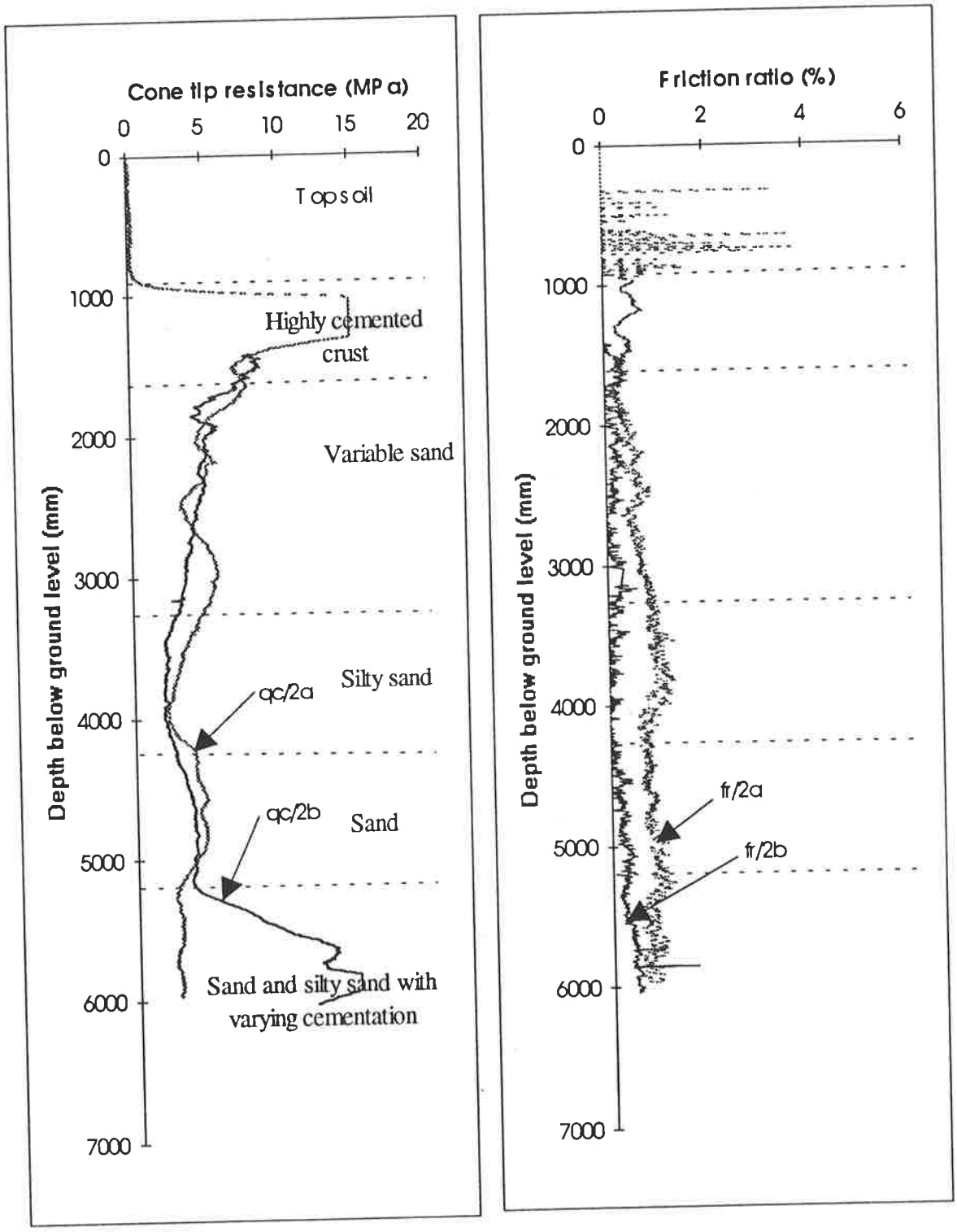

Figure 5.6 **Soil stratigraphy from the profiles of cone tip resistance, q_c, and friction ratio, F_R, at Location 2, based on Campanella and Robertson (1983) classification chart.**

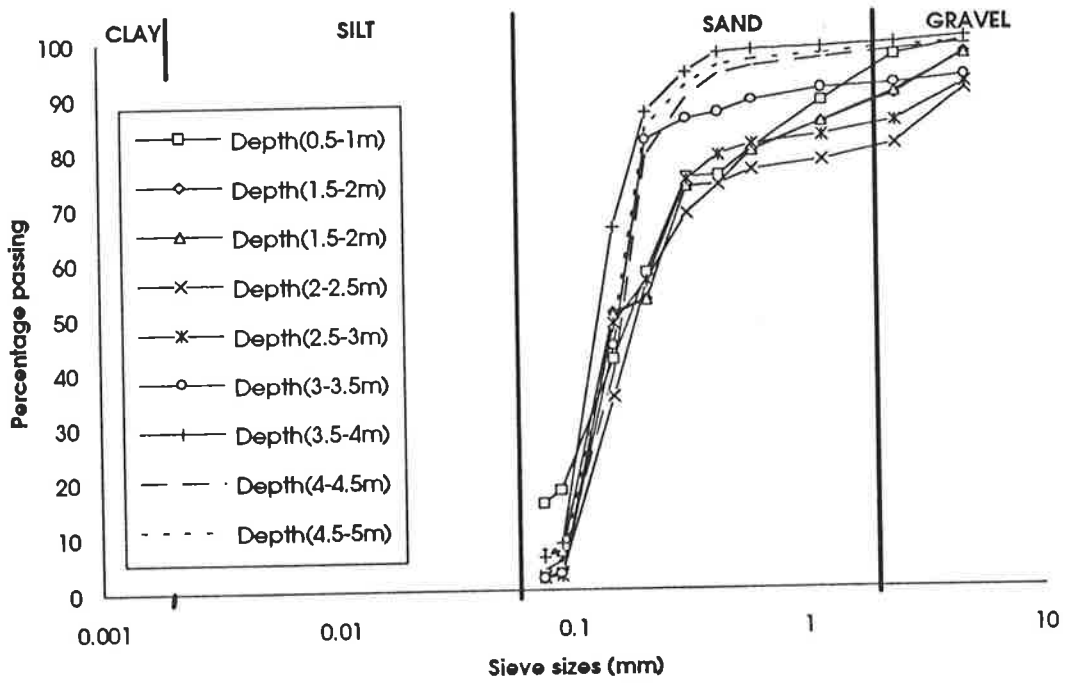

Figure 5.7 **Particle size distribution curves on soil recovered from the test site at depths between 0.5m to 5.0 m.**

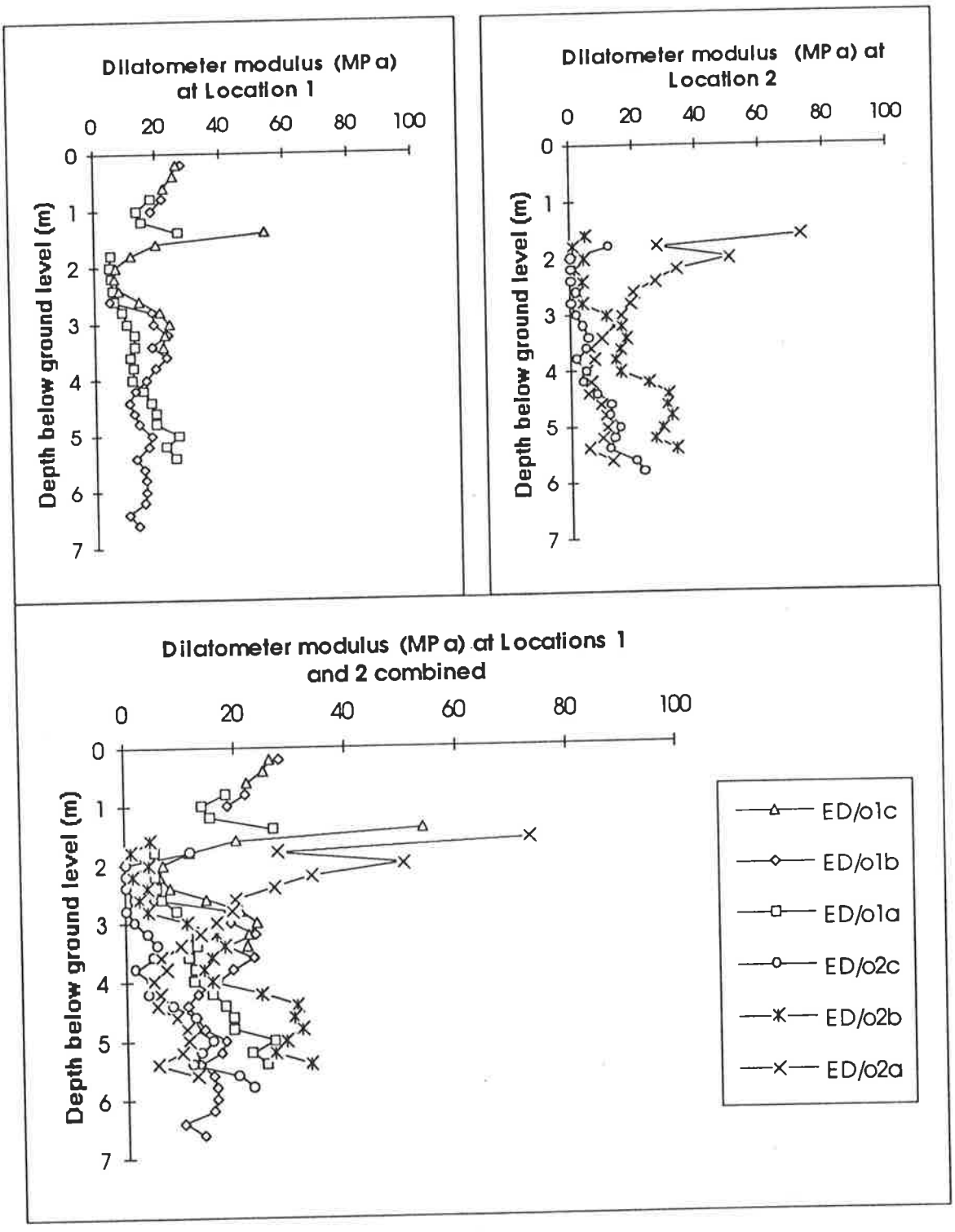

Figure 5.8 **Profiles of dilatometer modulus, E_D, based on Schmertmann (1986) correlation.**

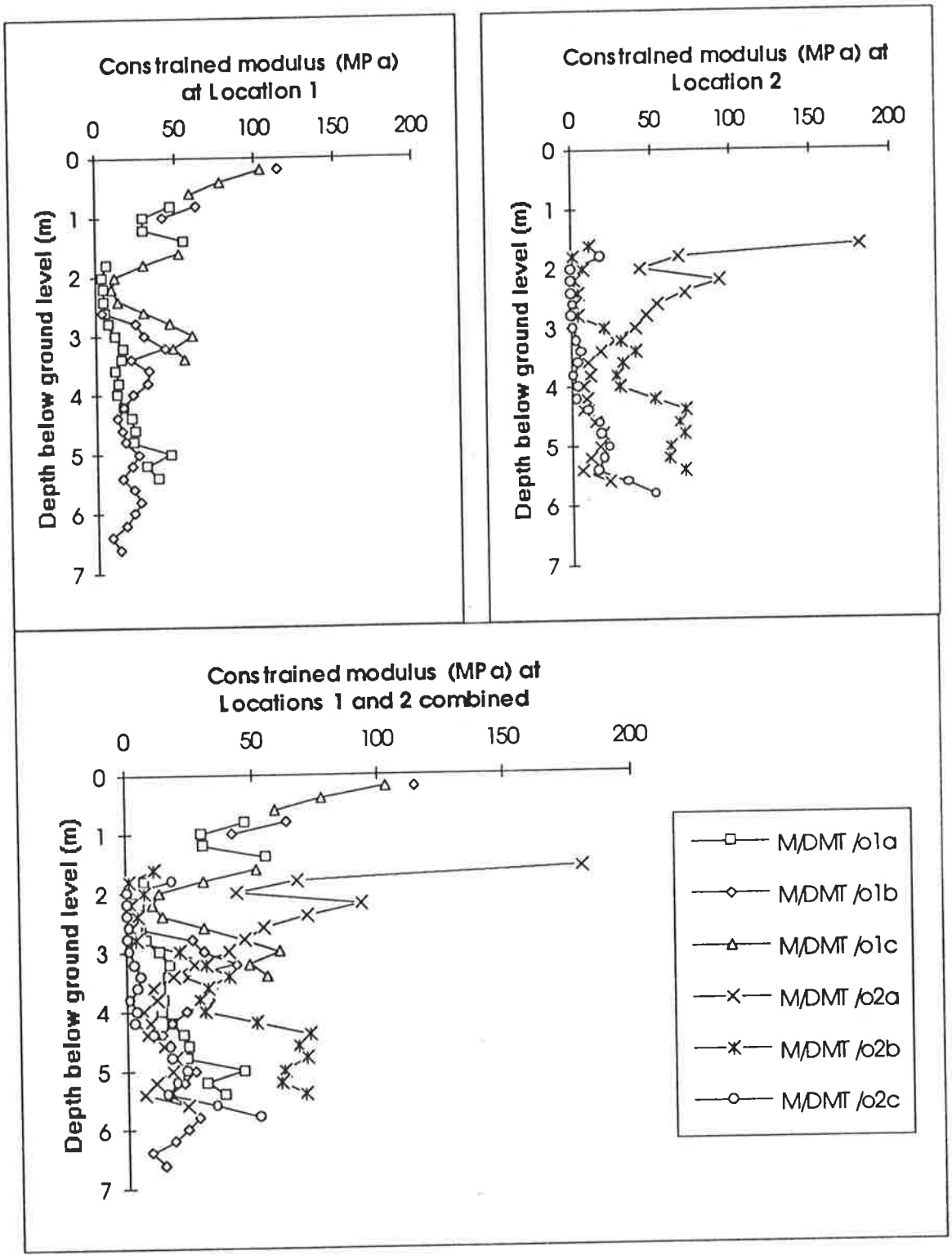

Figure 5.9 **Profiles of DMT evaluated constrained modulus, M, based on Marchetti (1980) correlations.**

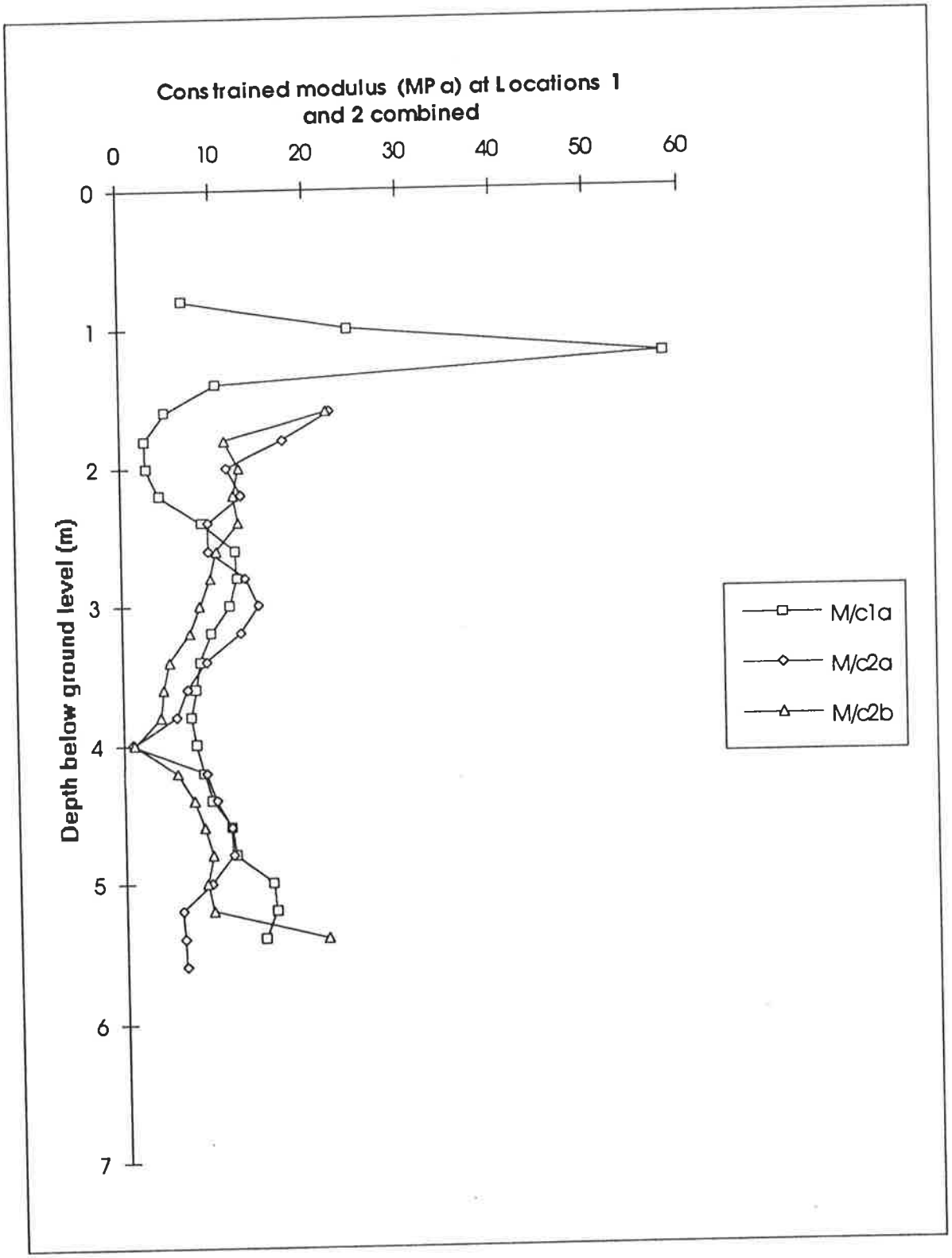

Figure 5.10 **Profiles of CPT evaluated constrained modulus, M, based on Mitchell and Gardner (1975) correlation.**

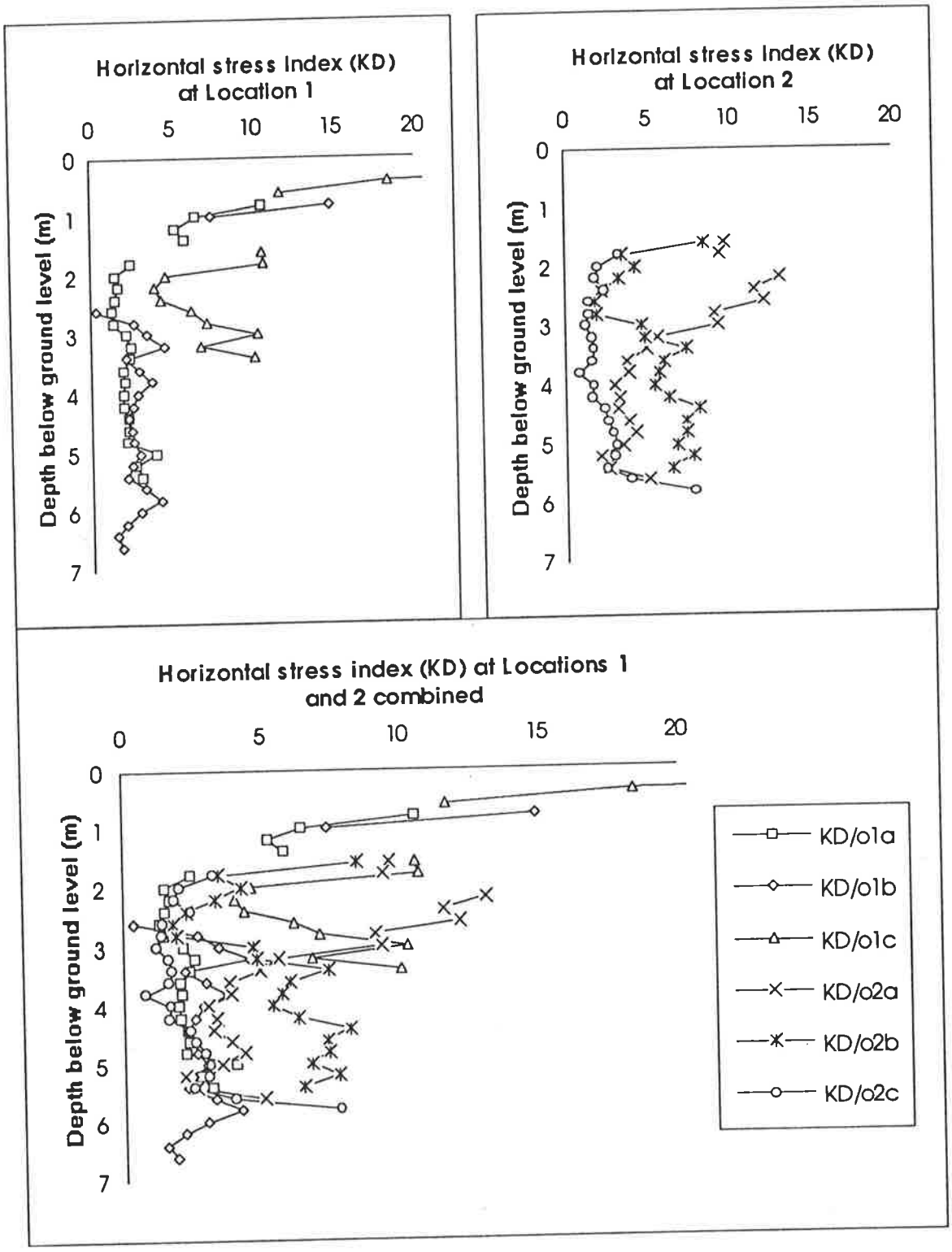

Figure 5.11 **Profiles of dilatometer horizontal stress index, K_D, based on Marchetti (1980) correlation.**

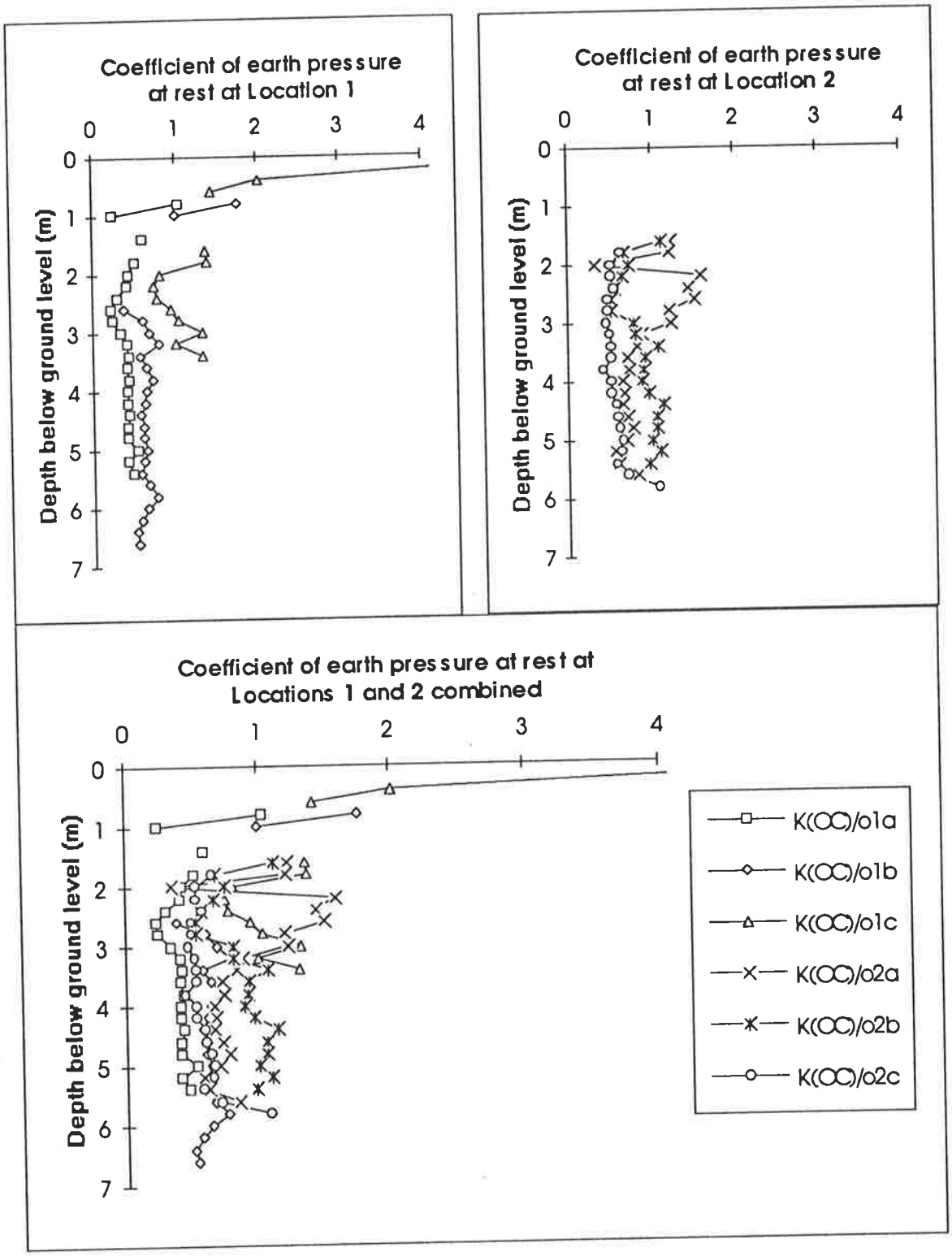

Figure 5.12 **Profiles of coefficient of earth pressure at rest, $K_{o(oc)}$, based on Baldi et al. (1986) correlation.**

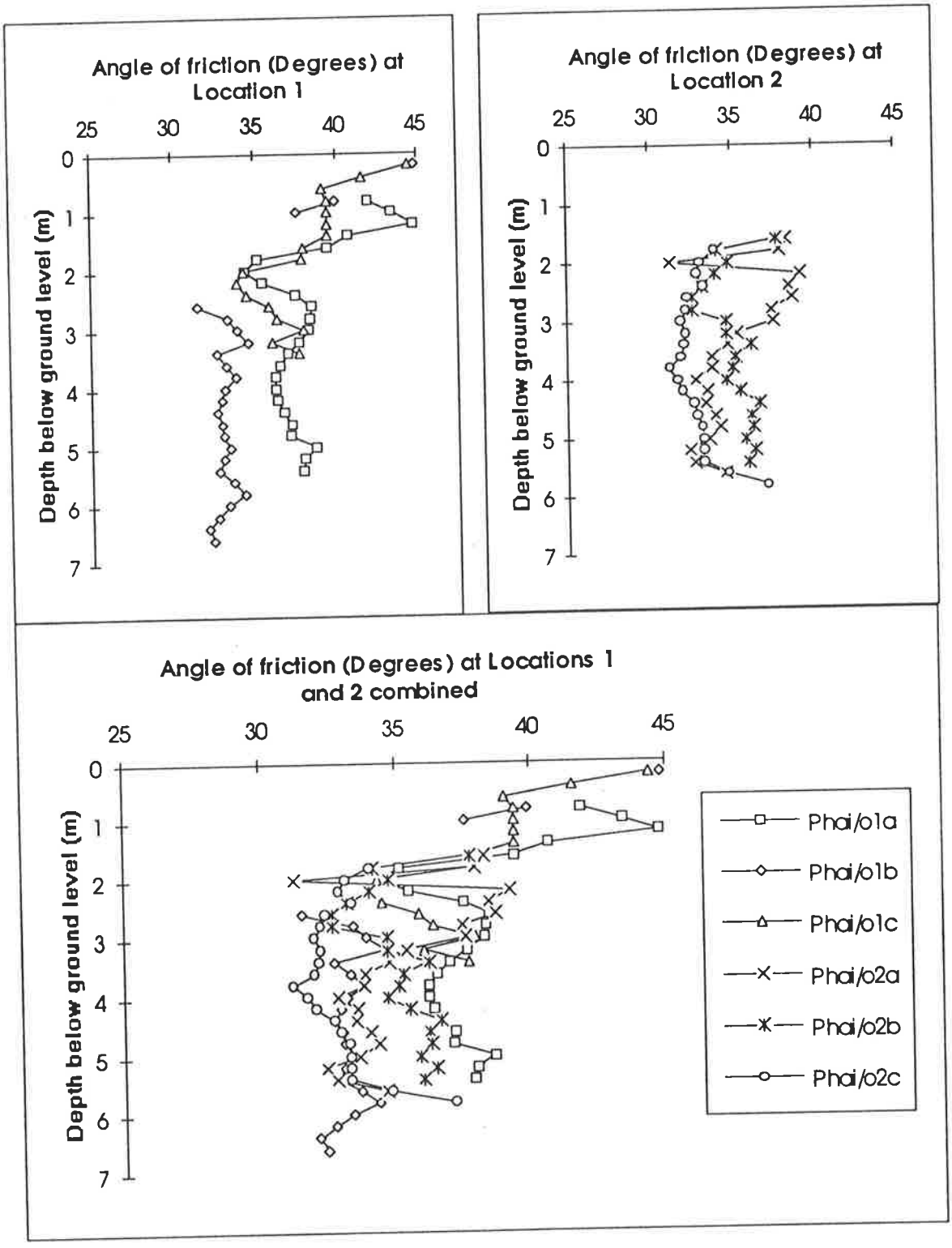

Figure 5.13 **Profiles of angle of friction, ϕ'_{ax}., based on Schmertmann (1983) correlation.**

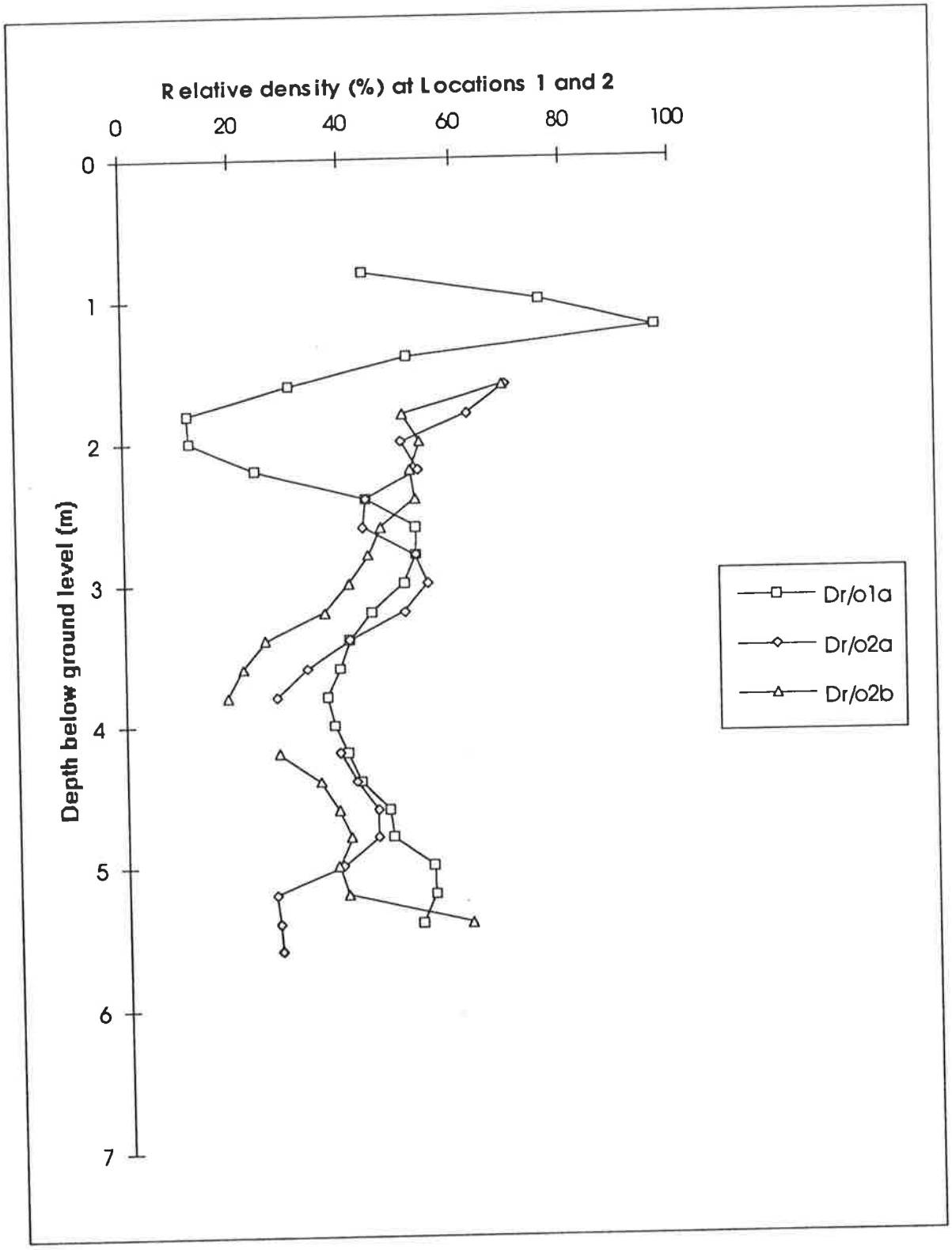

Figure 5.14 **Profiles of relative density, D_r, based on Jamiolkowski et al. (1988) correlation.**

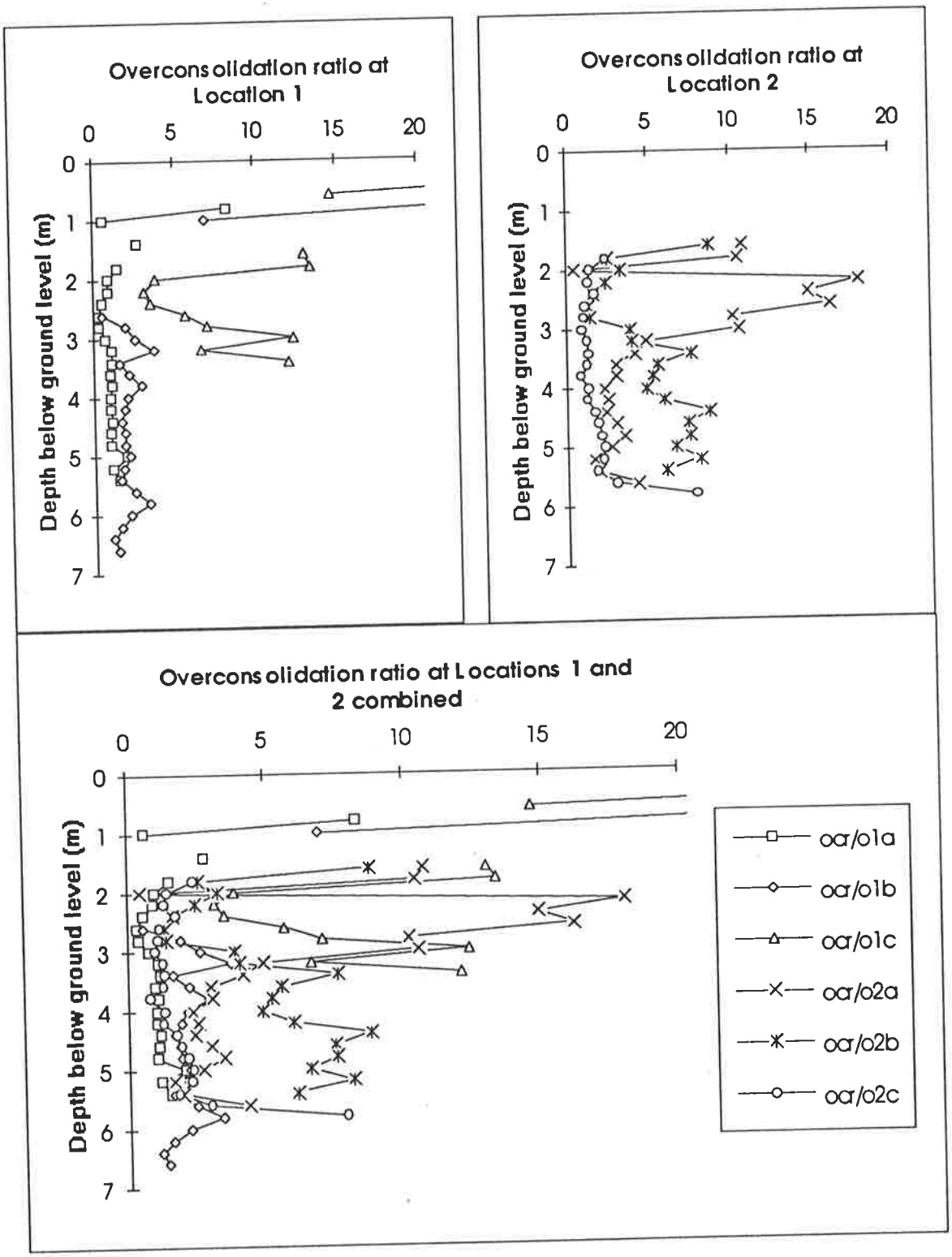

Figure 5.15 **Profiles of over consolidation ratio, OCR, based on Schmertmann (1983) correlation.**

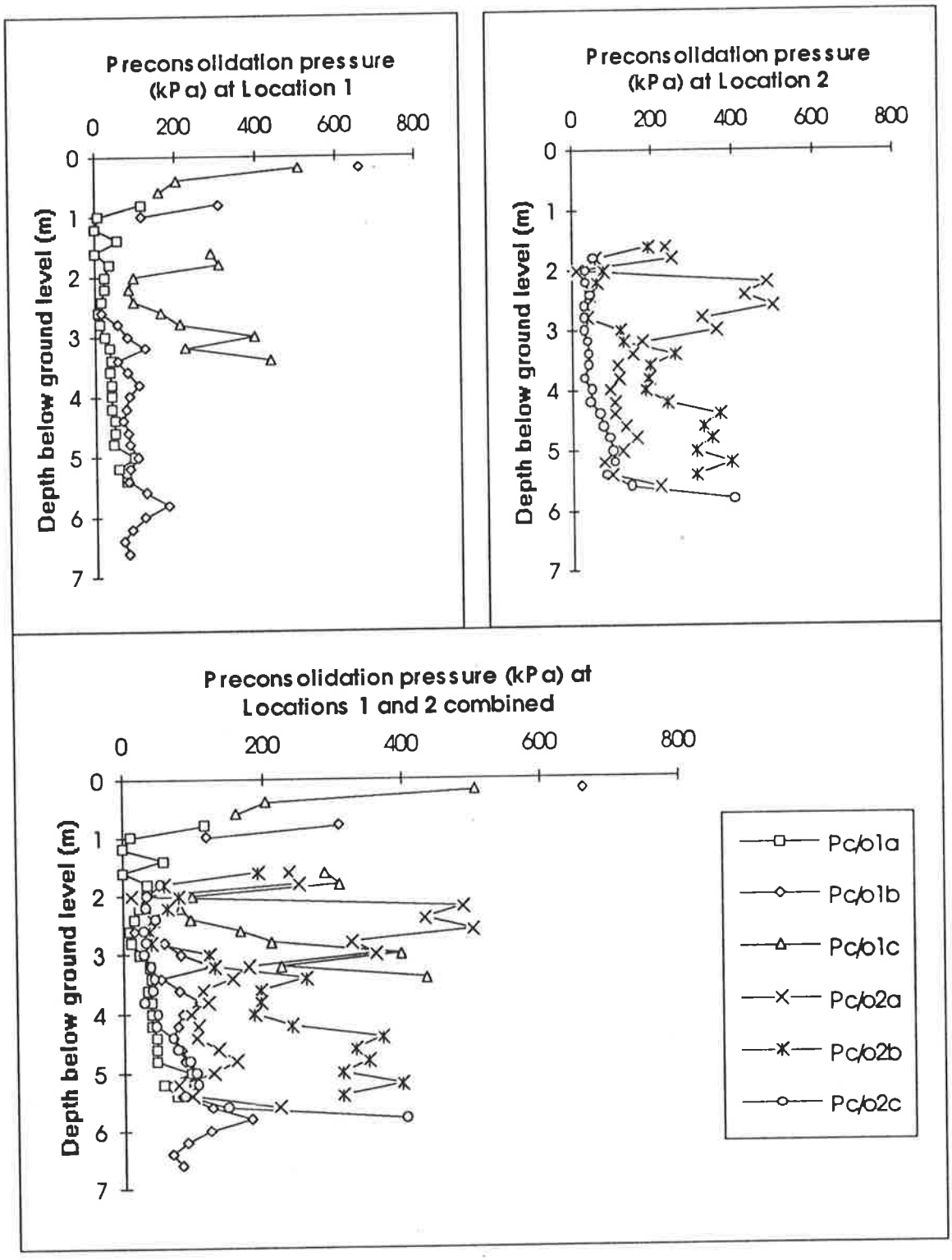

Figure 5.16 **Profiles of pre consolidation pressure, p_c', based on Leonards and Frost (1988) method.**

Chapter 6

APPLICATIONS OF RESULTS FOR DESIGN PURPOSES

6.1 Introduction

This chapter presents the application of the test results evaluated during the present research work. The bearing capacity and settlement calculations are done for some of the typical foundations, based on the DMT and CPT evaluated results. Settlement calculations are carried out with both the standard DMT data and the modified DMT data in order to find out the difference in the calculated settlement and prove the usefulness of the modified dilatometer data for a more realistic assessment of foundation settlement.

In the beginning some of the widely accepted bearing capacity theories are discussed and used for the assessment of the allowable bearing capacities of some of the typical foundations. Thereafter, settlement calculations are done for the same foundations, subjected to different loading intensities. The values of settlement, thus calculated, are examined as to whether they are within tolerable limits from the criteria of maximum allowable settlement. Finally, an assessment is made regarding the most suitable foundations and loads they can carry.

6.2 Bearing capacity

Bearing capacity is the pressure the soil can be subjected to without causing shear failure. Ultimate bearing capacity is the least contact pressure which causes a shear failure in the soil. Allowable bearing capacity is the maximum pressure which can be imposed on a given soil without causing shear failure or excessive settlement (Craig, 1987; Bowles, 1988).

When the contact pressure acting on the soil exceeds the ultimate bearing capacity, failure surfaces develop beneath the foundation. These failure surfaces spread from the bottom edges of the foundations and move downwards and then sidewards, in the shape of a wedge, to reach the ground surface. In general, three types of failures have been noticed.

(a) General shear failure, where the failure surfaces emerge from the edges and moves downwards and then sidewards to reach the ground surface as the plastic equilibrium is reached. This type of failure is accompanied by heaving of the adjacent ground and is characteristic of dense or stiff soils.

(b) Local shear, where the failure surfaces form but do not propagate fully and do not reach the ground surface. This type of failure is accompanied by only slight heaving of the adjacent ground and is characteristic of compressible soils.

(c) Punching shear, where the failure surfaces do not develop at all but the foundation starts sliding vertically under load. This type of failure is not accompanied by any heaving of the adjacent soil and is found to occur in highly compressible soils or in cases where the foundations are located at great depths.

Based on the different modes of wedge failure and model tests, bearing capacity theories have been postulated and several equations proposed for the assessment of the bearing capacity of soil. The first bearing capacity equation was proposed by Terzaghi, based on the theory of plasticity, which was the modification of Prandtl bearing capacity theory (Terzaghi, 1943). The Terzaghi (1943) bearing capacity equation is of the following form:

$$q_{ult} = c\,N_c\,S_c + q\,N_q + 0.5\,\gamma B\,N_\gamma\,S_\gamma \qquad (6.1)$$

where,

N_c, N_q, N_γ	= bearing capacity factors given by Terzaghi equations,
c	= unit cohesion,
q	= effective overburden stress per unit foundation width,
γ	= bulk density,
B	= foundation width,
S_c, S_γ	= shape factors.

Terzaghi's bearing capacity equation was formulated mainly for the shallow foundations, where depth of the foundation is less than the width of the foundation.

Meyerhof (1951, 1963) modified the Terzaghi (1943) bearing capacity theory by introducing another shape factor S_q for the term N_q and also introduced depth factors d_c, d_q, d_γ and inclination factors i_c, i_q, i_γ to be used together with the bearing capacity factors N_c, N_q, N_γ, respectively. Meyerhof also proposed his own equations for the calculation of all these factors depending on the size, shape and depth of the foundation.

Hansen (1970) extended the bearing capacity theory further by accounting for the possibility of the foundation being tilted with respect to the horizontal surface or a foundation on a slope, by introducing the factors g_c, g_q, g_γ and b_c, b_q, b_γ respectively, together with the bearing capacity factors N_c, N_q, N_γ. Hansen (1970) too gave his own set of equations for the calculation of various factors, which are more complicated than the previous ones.

Vesic (1973) carried on further work and came out with slightly different values for some of the variables. There is not much difference between Vesic and Hansen factors excepting for few changes, so that Vesic factors give less conservative results compared to those of Hansen.

The main drawback with all these bearing capacity equations is that they are mostly theoretical in nature and there is less practical validation based on model tests. The tests conducted on small models do not match their full scale prototypes, which are very expensive to conduct. Therefore, for the evaluation of bearing capacity one of these equations has to be relied upon.

6.2.1 Bearing capacity of foundations at the test site

Bearing capacity calculations have been undertaken for three different types of foundations, namely, square, rectangular and strip foundations of different sizes in order to find out which one offers the maximum allowable bearing capacity. The different types of foundations and their sizes, considered for the study of bearing capacity of the test site, are listed below:

Square	10m by 10m
	4m by 4m
	2m by 2m
	1.5m by 1.5m
Rectangular	10m by 20m
	4m by 8m
	2m by 4m
	1.5m by 3m
Strip	4m wide
	3m wide
	1.5m wide

All these foundations are assumed to be resting at a depth of 2 metres below ground level (D = 2.0m). The following data, as evaluated during the course of the field and laboratory tests, are used in the calculations:

effective angle of friction, ϕ'_{ax}	$= 33^\circ$
field dry density	$= 1.6$ t/m^3
depth of water table	$= 0.9$ m
moisture content, m (assumed)	$= 15$ %

The value of $\phi'_{ax} = 33^\circ$ was evaluated from the weakly cemented layers and is used for the evaluation of allowable bearing capacity. The shear box tests give an average of $\phi'_{ps} = 37^\circ$, for plain strain case, which when converted to axial strain condition using Schmertmann (1983) correlation, gives $\phi'_{ax} = 35^\circ$. A number of consolidated drained triaxial tests give $\phi'_{ax} = 31^\circ$. Therefore average value of $\phi'_{ax} = 33^\circ$, obtained from the

weakly cemented layers during the course of in situ testing is considered suitable for the evaluation of bearing capacity.

In the present case, the bearing capacity calculations are done from the Vesic (1973) equation, which is as written below.

$$q_{ult} = c\, N_c\, S_c\, d_c\, i_c\, g_c\, b_c + q\, N_q\, S_q\, d_q\, i_q\, g_q\, b_q + 0.5\, \gamma B\, N_\gamma\, S_\gamma\, d_\gamma\, i_\gamma\, g_\gamma\, b_\gamma \qquad (6.2)$$

where,

N_c, N_q, N_γ	= bearing capacity factors,
S_c, S_q, S_γ	= shape factors,
d_c, d_q, d_γ	= depth factors,
i_c, i_q, i_γ	= inclination factors for loads not passing vertically,
g_c, g_q, g_γ	= factors for tilted foundation, and
b_c, b_q, b_γ	= slope factors.

In Equation 6.2 the first term becomes zero, as c = 0 in cohesionless soils. As the considered problem does not involve conditions of inclined load, tilted foundation or sloping ground, their respective factors get eliminated and Equation 6.2 reduces to the following simpler form.

$$q_{ult} = q\, N_q\, S_q\, d_q + 0.5\, \gamma B\, N_\gamma\, S_\gamma\, d_\gamma \qquad (6.3)$$

For the calculation of the remaining factors in Equation 6.3, the table and equations proposed by Vesic (1973) are utilised. In case of a square foundation, 4m by 4m in size, the following values are worked out for the various factors.

$q = 2.58$ t/m^3	$B = 4.0$ m
$N_q = 26.09$	$N_\gamma = 35.19$
$s_q = 1.649$	$S_\gamma = 0.6$
$d_q = 1.205$	$d_\gamma = 1.205$

These values are substituted in Equation 6.3 to get q_{ult} = 1.80 MPa. If a factor of safety = 3 is considered, then the allowable bearing capacity = 1.80/3 = 0.60 MPa. Hence according to Vesic (1973) bearing capacity equations, the test site offers an allowable bearing capacity of 0.60 MPa for a 4m by 4m square foundation.

Similarly, the allowable bearing capacities for all the foundations are calculated in similar manner with the results tabulated in Table 6.1.

Table 6.1 Bearing capacity and settlement results for different types of foundations

Type of foundation	Size of foundation	Allowable bearing capacity (MPa)	Contact Pressure (MPa)	Foundation settlement (mm) using $E_{D(new)}$
Square	10m by 10m	0.84	0.84	235.74
			0.40	106.37
			0.20	48.09
			0.10	18.95
	4m by 4m	0.60	0.70	187.00
			0.60	157.00
			0.40	99.90
			0.30	70.77
			0.20	41.64
			0.13	20.00
			0.10	12.50
	2m by 2m	0.56	0.56	132.27
			0.40	85.36
			0.20	27.08
			0.15	12.51
	1.5m by 1.5m	5.80	5.80	1645.00
			2.00	539.00
			1.00	247.85
			0.50	102.16
			0.25	29.31
			0.23	***22.03***
			0.20	14.74
			0.15	0.71

Rectangle	10m by 20m	0.98	0.98 0.40 0.20 0.10	277.18 107.30 49.02 19.89
	4m by 8m	0.62	0.62 0.40 0.20 0.10	167.06 102.96 44.68 15.54
	2m by 4m	0.50	0.50 0.40 0.30 0.20 0.10	122.96 93.82 64.68 35.54 6.41
	1.5m by 3m	4.70	4.70 2.00 1.00 0.50 0.30 ***0.20*** 0.15	1339.00 552.62 261.24 115.55 57.27 ***28.14*** 13.57
Strip	4m wide	0.59	0.59 0.40 0.30 0.20 0.10	160.00 106.00 77.00 47.73 18.59
	3m wide	0.51	0.51 0.40 0.30 0.20 0.10	137.69 104.76 75.63 46.49 17.35
	1.5m wide	3.58	3.58 1.50 0.60 0.40 0.20 0.15 0.10	1027.00 420.00 158.00 99.81 41.53 26.96 12.39

The results indicate that usually the allowable bearing capacity decreases with decrease in the length and breadth of the foundations. However, when the breadth of foundation is reduced to less than the depth of the foundation (D/B >1), there is an abrupt increase in the allowable bearing capacity due to increase in depth factor d_q. For example, a square foundation of size 10m by 10m and D/B ratio < 1 gives allowable bearing capacity = 0.84 MPa, whereas a much smaller square foundation of size 1.5m by 1.5m and D/B ratio > 1 gives allowable bearing capacity = 5.8 MPa. Similarly, the rectangular and strip foundations with D/B ratio > 1 also give increased values of allowable bearing capacities.

6.3 Settlement calculations

The allowable bearing capacities of foundations of different sizes and shapes, as obtained from the above calculations, can be considered to be safe if the settlement caused due to these pressures do not cause excessive settlement of the soil layers. Hence, settlement calculations are carried out for all these foundations, considering that the foundations transmit contact pressures equal to the allowable bearing capacities.

For the calculation of foundation settlement it is necessary to know the deformation parameter of the soil, such as the Young's modulus or constrained modulus. During the field testings these values were evaluated from the combined use of the DMT and the CPT. However, the DMT and CPT evaluated results of constrained modulus are empirical in nature and their applicability for moderately calcareous sand is doubtful. Therefore, the best option is to use the modified dilatometer modulus, $E_{D(new)}$, as discussed in Chapter 4, because it does not depend on complicated correlations and is a direct evaluation, based on the continuous readings of pressure versus deflection.

The method proposed by Leonards and Frost (1988), as discussed in Chapter 2, makes use of the dilatometer modulus along with the DMT-CPT predicted preconsolidation pressure, p_c', and is therefore considered suitable for the purpose. The other methods, such as Janbu (1963, 1967, 1985) and Schmertmann (1986a) use the constrained modulus, M, and have not been used due to uncertainty in the evaluated M values. The profiles of preconsolidation pressure, p_c', presented in Chapter 5, show great variations due to actual variation in the degree of cementation of the test site. However, as recommended in Chapter 5, the values of p_c' obtained

from weakly cemented layers are suitable for settlement calculations, in order to design for the worst case.

It has been shown in Chapter 4 that the standard dilatometer modulus, E_D, gives conservative values of Young's modulus in cemented soils, compared to the modified dilatometer modulus, $E_{D(new)}$, due to non-linearity of the pressure versus deflection curve. In loose or uncemented layers both moduli give similar results. Settlement calculations are therefore done from E_D as well as $E_{D(new)}$, in order to find out the extent of the difference in the predicted results.

6.3.1 Example of settlement calculation from DMT, CPT data

An illustration of foundation settlement calculations using Leonards and Frost (1988) with the DMT and CPT data is given below. A square foundation, 4m by 4m in size, and a loading intensity of 0.60 MPa (equal to the allowable bearing capacity) is considered for the purpose. The details of the foundation and soil data are shown in Figure 6.1. The settlement calculations involve of the following steps.

- Divide the soil below the foundation into a number of layers depending upon the depth intervals at which DMTs were performed (in the present case approximately 0.2 m).

- Work out the effective vertical overburden stress, σ_v', at the centre of each layer.

- Calculate the stress increase, $\Delta\sigma_v'$, at the centre of each layer assuming 2 vertical : 1 horizontal stress distribution beneath the foundation (Fang, 1991). For example, if a square foundation, 4m by 4m in size, is carrying a load intensity of 0.60 MPa then at a depth of 0.2 m below the foundation the same pressure will be distributed over an area of (4 + 0.2) m by (4 + 0.2)m size. Hence, the net increase due to 0.60 MPa pressure will be $[0.60(4\times4)]/[(4+0.2)(4+0.2)] = 5.44$MPa. This method of calculating the stress increment is fairly simple and widely accepted.

- Calculated the final stress, σ_f', at the centre of each layer by adding σ_v' and $\Delta\sigma_v'$.

- Work out the values of preconsolidation pressure, p_c', for each layer through the data reduction procedure, as described in Chapter 2 and 5. For the present

calculations a profile of p_c', evaluated from weakly cemented layers is directly taken from Chapter 5.

- Determine the portion of the load increment that falls in the OC range $[R_Z(OC)]$ and the NC range $[R_Z(NC)]$ by the following equations.

$$[R_Z(OC)] = \left(\frac{p_c' - \sigma_v'}{\sigma_f' - \sigma_v'} \right) \qquad (6.4\ a)$$

$$[R_Z(NC)] = \left(\frac{\sigma_f' - p_c'}{\sigma_f' - \sigma_v'} \right) \qquad (6.4\ b)$$

- From the values of dilatometer modulus, E_D, work out the values of $E_Z(OC)$ and $E_Z(NC)$ using equations $E_Z(OC) = 3.5\ E_D$ and $E_Z(NC) = 0.7\ E_D$ respectively. In the case of using the modified dilatometer data replace E_D with $E_{D(new)}$.

- Work out the values of strain influence factors, I_Z, for every layer using the modified influence factor diagram (Schmertmann, 1978).

- Calculate the settlement of individual layers, S_i, using the following equation.

$$S = c_1\, q_{net}\, I_Z\, \Delta_h \left[\frac{[R_Z(OC)]}{[E_Z(OC)]} + \frac{[R_Z(NC)]}{[E_Z(NC)]} \right] \qquad (6.5)$$

where,

q_{net} = surface load excluding excavated earth,
S = estimated settlement,
c_1 = embedment correction,
q_{net} = surface load - load of the excavated earth,
Δ_h = height of the sublayer,
E_D = dilatometer modulus.

- Add the settlements caused due to each layer to find out the total settlement below the footing.

The calculations in Table 6.2a show that for a loading intensity of 0.60 MPa, there will be a settlement of 156 mm when using the modified dilatometer modulus, $E_{D(new)}$, and 311 mm when using the standard dilatometer modulus, E_D, (Table 6.2b). As the

maximum settlement in sand should not be allowed to exceed more than 20 mm (Skempton and Mc Donald, 1956), the allowable bearing capacities determined from the strength considerations have to be reduced to meet the constraint of maximum allowable settlement. For doing so, the contact pressures are reduced gradually and each time the settlement calculation is repeated until the calculated settlement comes within 20 mm.

Table 6.2a Settlement calculations for a square footing (4m by 4m) with a contact pressure of 0.60 MPa, (using modified dilatometer modulus, $E_{D(new)}$; after Leonards and Frost, 1988 method).

Depth (m)	E_D (MPa)	σ_v' (kPa)	$\Delta\sigma_v'$ (kPa)	σ_f' (kPa)	p_c' (kPa)	$R_z(OC)$	$R_z(NC)$	I_z	Δ_z (m)	$E_z(OC)$ (MPa)	$E_z(NC)$ (MPa)	S_i (mm)	S (mm)
2.1	7.94	29.00	565.56	594.56	48.00	0.03	0.97	0.16	0.12	27.79	5.56	1.94	1.94
2.3	15.50	30.00	516.79	546.79	60.00	0.06	0.94	0.22	0.19	54.25	10.85	2.12	4.05
2.5	15.00	32.00	474.07	506.07	71.00	0.08	0.92	0.28	0.19	52.50	10.50	2.73	6.78
2.7	13.00	33.00	434.59	467.59	84.00	0.12	0.88	0.34	0.20	45.50	9.10	3.90	10.68
2.9	25.58	34.00	398.21	432.21	106.00	0.18	0.82	0.42	0.21	89.53	17.91	2.43	13.11
3.1	12.60	36.00	366.21	402.21	57.00	0.06	0.94	0.48	0.21	44.10	8.82	6.28	19.39
3.2	12.98	37.00	343.05	380.05	85.00	0.14	0.86	0.54	0.17	45.43	9.09	5.17	24.55
3.4	3.32	38.00	318.51	356.51	52.00	0.04	0.96	0.60	0.20	11.62	2.32	28.70	53.25
3.7	5.65	39.00	294.44	333.44	48.00	0.03	0.97	0.66	0.22	19.78	3.96	20.63	73.88
3.9	8.62	40.00	275.78	315.78	67.00	0.10	0.90	0.73	0.19	30.17	6.03	12.20	86.08
4.1	9.92	41.00	258.00	299.00	73.00	0.12	0.88	0.71	0.20	34.72	6.94	10.61	96.69
4.3	2.71	42.00	241.87	283.87	53.00	0.05	0.95	0.68	0.20	9.49	1.90	39.79	136.49
4.4	19.00	43.00	229.33	272.33	87.00	0.19	0.81	0.66	0.17	66.50	13.30	4.11	140.60
4.6	19.00	45.00	215.14	260.14	119.00	0.34	0.66	0.64	0.21	66.50	13.30	4.19	144.79
4.8	25.27	46.00	202.81	248.81	75.00	0.14	0.86	0.61	0.20	88.45	17.69	3.52	148.30
5.0	17.18	48.00	192.06	240.06	101.00	0.28	0.72	0.59	0.19	60.13	12.03	4.18	152.49
5.2	20.65	49.00	182.14	231.14	233.00	1.01	-0.01	0.56	0.19	72.28	14.46	0.81	153.30
5.4	18.90	51.00	172.97	223.97	116.00	0.38	0.62	0.54	0.19	66.15	13.23	3.12	***156.42***

Table 6.2b Settlement calculations for a square footing (4m by 4m) with a contact pressure of 0.60 MPa, (using standard dilatometer modulus, E_D; after Leonards and Frost, 1988 method).

Depth (m)	E_D *(MPa)*	σ_v' *(kPa)*	$\Delta\sigma_v'$ *(kPa)*	σ_f' *(kPa)*	p_c' *(kPa)*	$R_Z(OC)$	$R_Z(NC)$	I_Z	Δ_Z *(m)*	$E_Z(OC)$ *(MPa)*	$E_Z(NC)$ *(MPa)*	S_i *(mm)*	S *(mm)*
2.1	5.16	29.00	565.56	594.56	48.00	0.03	0.97	0.16	0.12	18.05	3.61	2.98	2.98
2.3	9.00	30.00	516.79	546.79	60.00	0.06	0.94	0.22	0.19	31.51	6.30	3.64	6.62
2.5	8.86	32.00	474.07	506.07	71.00	0.08	0.92	0.28	0.19	31.01	6.20	4.62	11.24
2.7	1.43	33.00	434.59	467.59	84.00	0.12	0.88	0.34	0.20	5.01	1.00	35.43	46.67
2.9	8.29	34.00	398.21	432.21	106.00	0.18	0.82	0.42	0.21	29.02	5.80	7.49	54.16
3.1	6.58	36.00	366.21	402.21	57.00	0.06	0.94	0.48	0.21	23.03	4.61	12.03	66.18
3.2	4.87	37.00	343.05	380.05	85.00	0.14	0.86	0.54	0.17	17.05	3.41	13.77	79.95
3.4	1.74	38.00	318.51	356.51	52.00	0.04	0.96	0.60	0.20	6.09	1.22	54.75	134.71
3.7	1.74	39.00	294.44	333.44	48.00	0.03	0.97	0.66	0.22	6.08	1.22	67.06	201.77
3.9	2.74	40.00	275.78	315.78	67.00	0.10	0.90	0.73	0.19	9.57	1.91	38.46	240.23
4.1	4.73	41.00	258.00	299.00	73.00	0.12	0.88	0.71	0.20	16.55	3.31	22.26	262.49
4.3	7.44	42.00	241.87	283.87	53.00	0.05	0.95	0.68	0.20	26.03	5.21	14.50	276.99
4.4	10.14	43.00	229.33	272.33	87.00	0.19	0.81	0.66	0.17	35.50	7.10	7.71	284.69
4.6	9.57	45.00	215.14	260.14	119.00	0.34	0.66	0.64	0.21	33.51	6.70	8.31	293.00
4.8	12.85	46.00	202.81	248.81	75.00	0.14	0.86	0.61	0.20	44.98	9.00	6.92	299.92
5.0	12.85	48.00	192.06	240.06	101.00	0.28	0.72	0.59	0.19	44.98	9.00	5.59	305.51
5.2	13.70	49.00	182.14	231.14	233.00	1.01	-0.01	0.56	0.19	47.96	9.59	1.23	306.74
5.4	12.99	51.00	172.97	223.97	116.00	0.38	0.62	0.54	0.19	45.47	9.09	4.54	***311.28***

The magnitudes of settlement calculated for different loading intensities using the standard dilatometer modulus, E_D, and modified dilatometer modulus, $E_{D(new)}$, are summarised in Table 6.3.

Table 6.3 Comparison of foundation settlement results predicted from the standard and modified dilatometer moduli

Contact Pressure (MPa)	Settlement from $E_{D(new)}$ (mm)	Settlement from E_D (mm)
0.70	187	370
0.60	156	311
0.20	41	82
0.13	20	42

It can be seen from the above results that due to conservatism in the standard dilatometer modulus, E_D, excessive settlements are predicted for all the loading intensities, which are reduced by about 50% when $E_{D(new)}$ is used in place of E_D.

6.4 Bearing capacity and settlement relation

Further, settlement calculations were undertaken for footings of different sizes and shapes, with the results being summarised in Table 6.1 alongside the allowable bearing capacity results. It can be seen from the results of Table 6.1 that in all the cases the allowable bearing capacities (calculated from Vesic bearing capacity equations) cause excessive settlements and have to be reduced considerably in order to limit the maximum settlements within the permissible limit of less than 20 mm.

The values of settlement are plotted against respective contact pressures for each of the square, rectangular and strip foundations in Figures 6.2a, 6.3a and 6.4a, respectively. The following observations are made from these figures.

- For all three types of foundations the settlement decreases linearly with decreasing contact pressures.

- For all three types of foundations the settlement decreases with decreasing size of foundation.

- The best results are obtained with a square foundation, 1.5m by 1.5m, where a contact pressure of 0.23 MPa causes settlement of only 20 mm (refer to Figure 6.2a and Table 6.1). The second best result is obtained with a rectangular foundation of size 1.5m by 3.0m, where a contact pressure of 0.18 MPa causes a settlement of nearly 20 mm. All the other foundations cause comparatively more settlement for the same values of contact pressures.

Figures 6.2a, 6.3a and 6.4a are further used to find out the exact bearing pressures which will cause 20, 50 and 100 mm settlements in each type of foundations. These values of bearing pressures are plotted against the respective foundation sizes in the form of design charts, as shown in Figures 6.2b, 6.3b and 6.4b. These design charts can be used as ready references for finding out the allowable bearing pressures for different types/sizes of foundations and for desired loading magnitudes. From these design charts it is evident that in order to minimise the settlement, the bearing pressures acting on the foundation as well as the foundation size have to be reduced to optimum values.

In summary, an allowable bearing capacity up to a maximum value of 0.23 MPa is acceptable for a square foundation of 1.5m by 1.5m size, from the settlement criteria. This value also agrees with the British standard for preliminary designs (Craig, 1987) which suggests a bearing capacity less than 0.20 MPa for loose sand and gravel. However, in the case of larger foundations, the contact pressure should not be allowed to exceed 0.13 MPa in order to limit settlement to less than 20 mm.

6.5 Summary

The use of modified dilatometer modulus, $E_{D(new)}$, in place of the standard dilatometer modulus, E_D, significantly reduces the magnitude of calculated settlement. As the modified dilatometer modulus is obtained from the data points corresponding to the elastic portion of the pressure-deflection curve, it is advisable to use $E_{D(new)}$ in place of E_D for the evaluation of the Young's modulus of soil, and subsequently use it for settlement calculations.

The allowable bearing capacity, calculated from the bearing capacity equations, causes excessive settlement of soil layers at the Port Adelaide test site. Therefore, the final assessment of the allowable bearing capacity is based on the settlement criteria rather than the shear failure, as the test site consists of loose and compressible soil layers.

The test site consists of sand and silt with varying degrees of cementation and thus their compressibilities vary significantly. Within a close space, layers of very high and very weak cementation are present which may cause differential settlement in case of isolated foundations. It is therefore worth considering a raft foundation as an alternative to the isolated foundations.

During the field testing, soundings were made up to a maximum depth of 6 metres below the ground level and a firm stratum was not found. So, in the case of piles, underreamed piles would be beneficial for providing extra end bearing. Alternatively, deeper soundings can be made with an aim to locate a firm substratum.

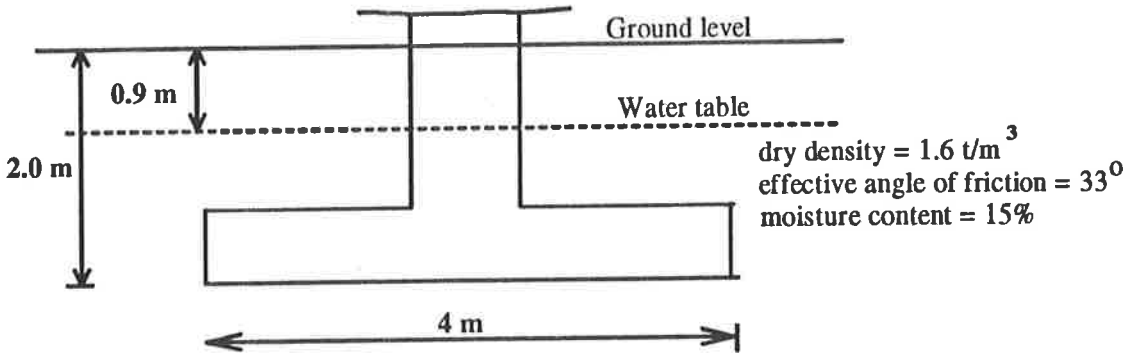

Figure 6.1 **Details of the isolated square footing considered for the illustration of bearing capacity and settlement calculations.**

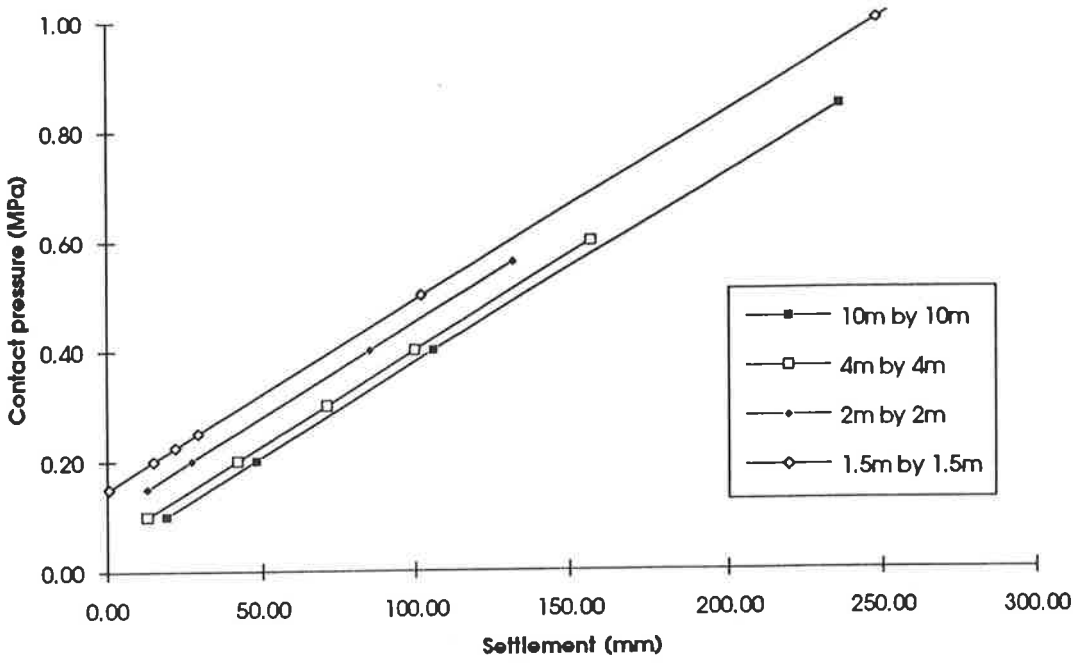

Figure 6.2a **Relation between contact pressure and settlement for square foundations of different sizes.**

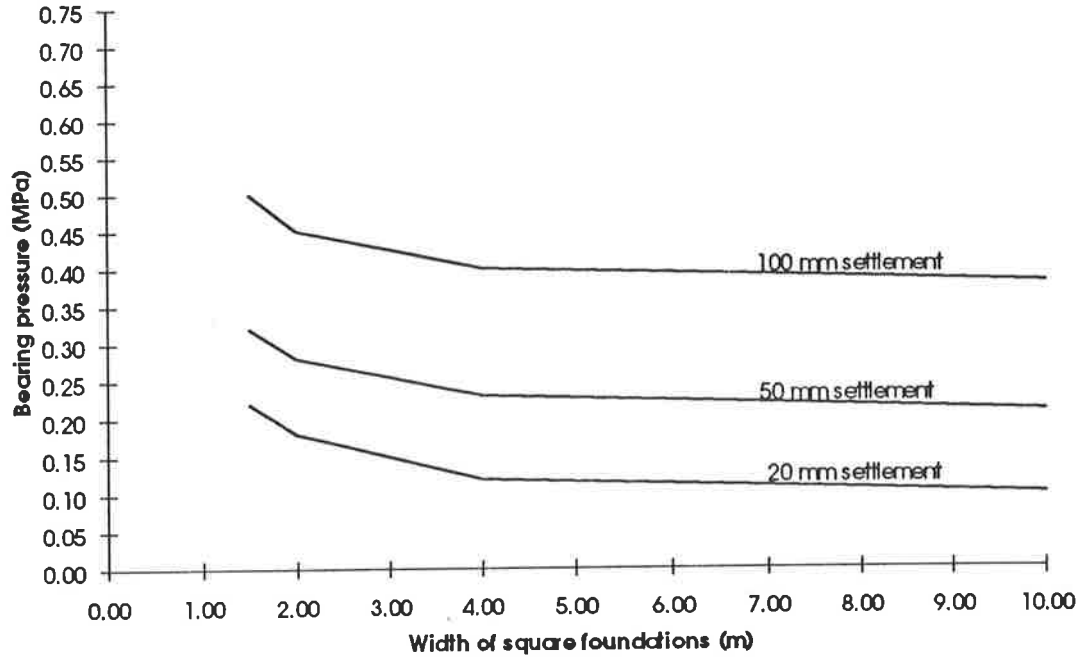

Figure 6.2b **Design chart for the selection of an appropriate size square foundation from the settlement criteria.**

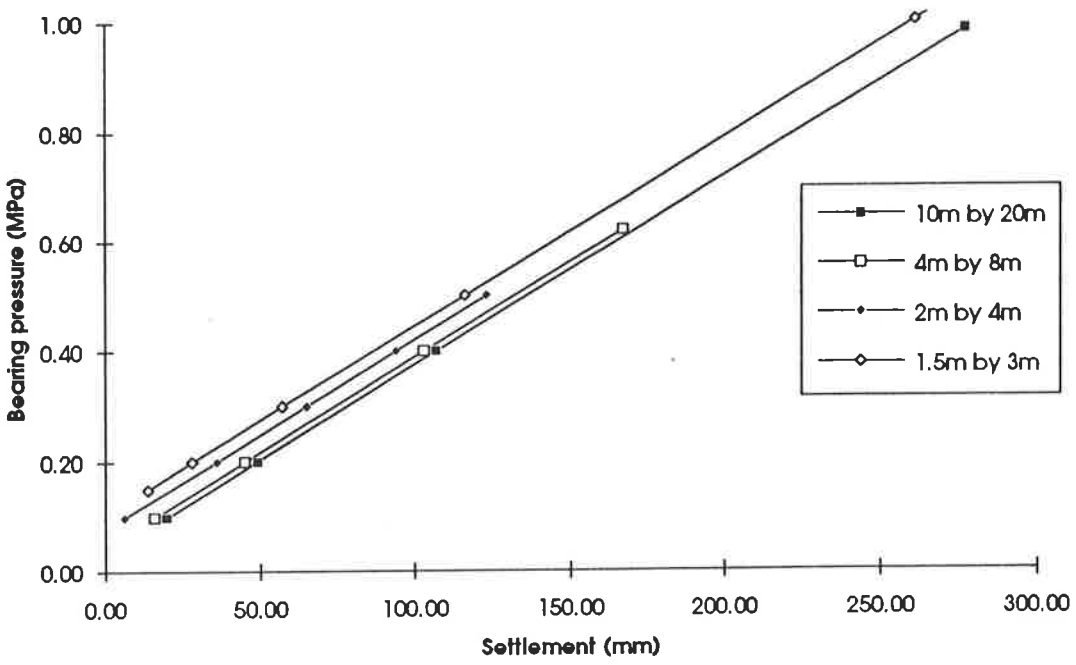

Figure 6.3a **Relation between contact pressure and settlement for rectangular foundations of different sizes.**

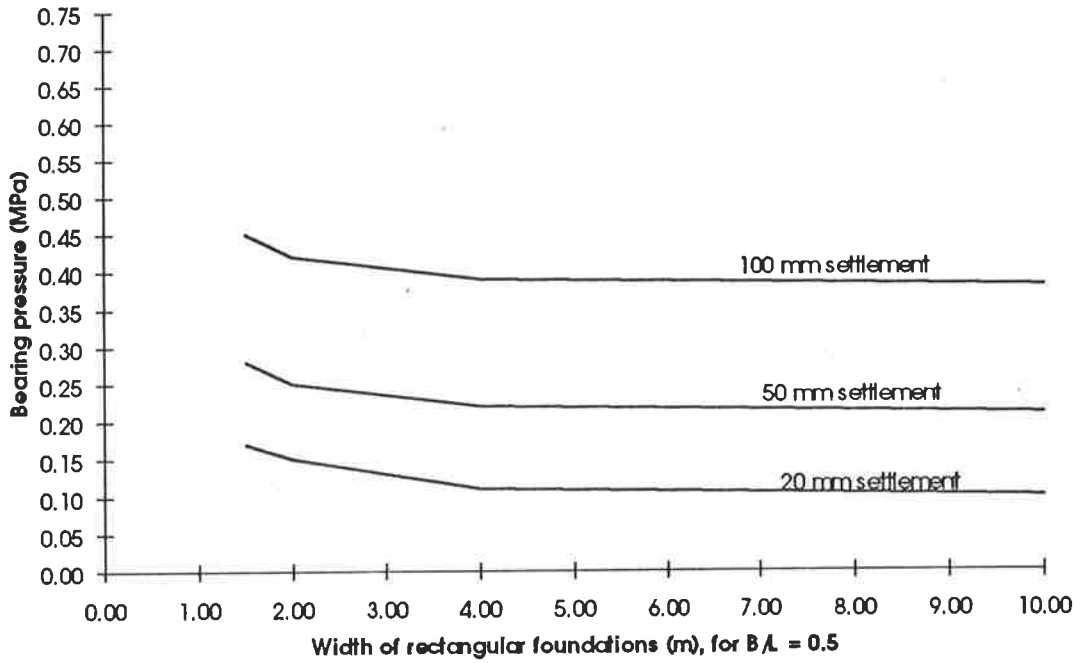

Figure 6.3b **Design chart for the selection of an appropriate size rectangular foundation from the settlement criteria.**

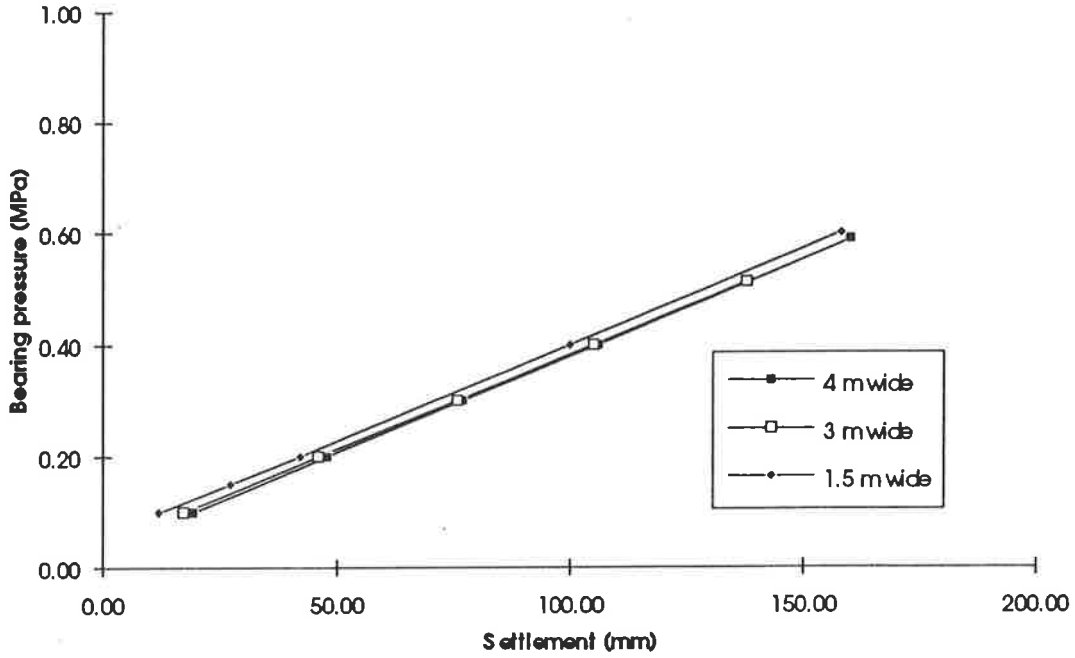

Figure 6.4a **Relation between contact pressure and settlement for strip foundations of different widths.**

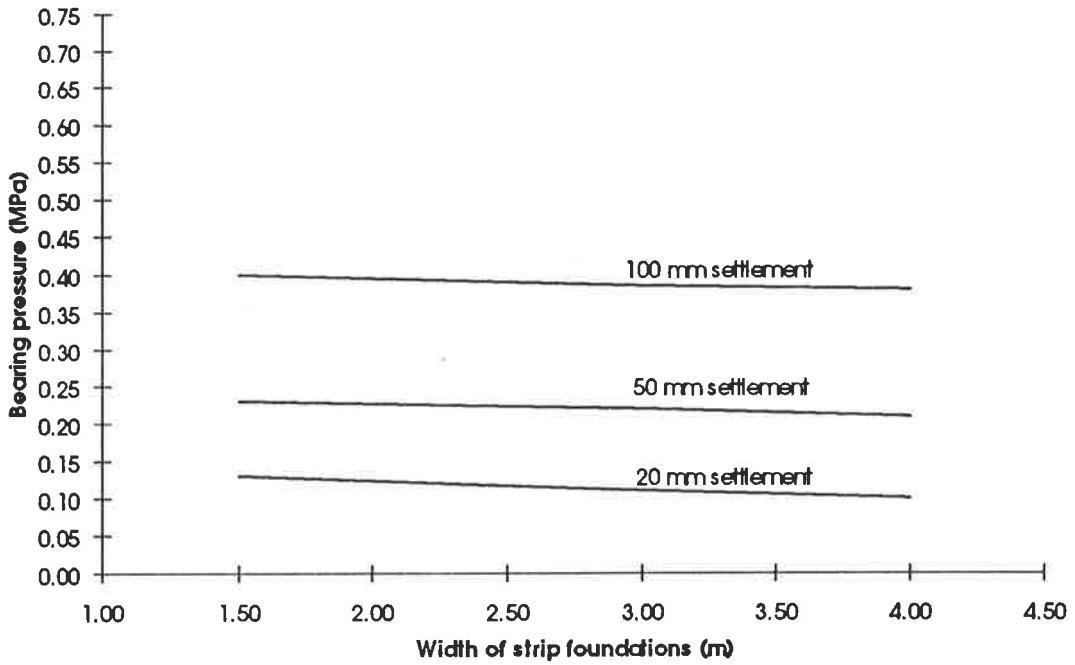

Figure 6.4b **Design chart for the selection of an appropriate width strip foundation from the settlement criteria.**

Chapter 7

SUMMARY

This Chapter contains a summary of the outcomes of the present research work and recommendations for future work.

7.1 Summary

Both the DMT and CPT in situ testing devices are capable of giving a fair idea of soil stratigraphy in the calcareous sands and are found helpful in detecting the layers of high and low cementation. These devices can also be utilised for reasonable estimates of the design parameters of calcareous sand, especially in weakly cemented layers, where the effect of cementation is less and the behaviour of calcareous sand resembles that of cohesionless sand.

However, the standard dilatometer suffers from a number of drawbacks. The main drawback is that the evaluation of soil parameters from standard dilatometer relies on pressure readings at two key membrane deflection positions, assuming a linear pressure-deflection relationship between the two points. Therefore it is susceptible to error if the relationship between pressure and deflection between these two positions is not linear. Secondly, there is no provision for measuring the dilatometer blade tip resistance in the standard dilatometer device and it is necessary to conduct adjacent CPT tests for recording the q_c values in order to evaluate K_o, ϕ , OCR and p_c'. Moreover, due to the manual operation of the standard DMT device there is the added possibility of operator error in data recording. In order to overcome these

limitations the standard dilatometer was modified to give continuous readings of membrane pressure and deflection. The nature of membrane expansion into the soil was studied from the pressure versus deflection curves. Such a study made possible better interpretation of soil parameters, particularly the Young's modulus of calcareous sediments, using continuous deflection versus pressure curves. Automation of the DMT was also accomplished to allow swift and automatic data recording using a microcomputer.

A comparative study of the Young's modulus evaluated from the standard dilatometer modulus, E_D, and modified dilatometer modulus, $E_{D(new)}$, shows that the standard dilatometer modulus, E_D, leads to conservative estimates of Young's modulus in cemented layers. This is due to the fact that most of the pressure versus deflection curves are non-linear, except in very loose sand and silt, where it is more or less linear. Hence for a more realistic evaluation of modulus of elasticity, the modified DMT can be used to obtain continuous pressure versus deflection curves for each layer. Young's modulus can then be evaluated from the modified dilatometer modulus, $E_{D(new)}$, based on the initial linear portion of the pressure-deflection curves. The values of Young's modulus evaluated from $E_{D(new)}$ are found to be up to 50% greater than those evaluated from E_D, especially in the layers of high cementation. However, in weakly cemented layers the values of modulus of elasticity evaluated from the two tests are in close agreement.

The modified dilatometer continuous pressure-deflection curves have the potential to show the variations in the in situ pore water pressure. Further tests with free draining sand are necessary for its full confirmation. The nature of these curves (shape and slope) are also helpful in giving an idea of different types of soil layers, such as, loose or tough, cemented or uncemented, sand or silt, etc.

A comparative study of q_d and q_c profiles indicate that the two differ from each other and the use of q_d rather than q_c in various correlations could lead to error, as the DMT-CPT correlations for $K_{o(oc)}$ and ϕ are developed mainly with q_c. A comparison of q_d and q_c profiles with corresponding P_0 and P_1 profiles indicate that the dilatometer blade tip resistance, q_d, is more sensitive to the horizontal stresses within the soil compared to q_c. Therefore, it can be used as an alternative horizontal stress index in the form of (q_d/σ_v'), similar to K_D, and correlations can be developed between $K_{o(oc)}$ - (q_d/σ_v') with the help of calibration chamber tests for the evaluation of $K_{o(oc)}$ in different types of soils.

The evaluation of other soil parameters, such as K_o, ϕ , OCR and p_c', from the DMT - CPT correlations, make use of only the contact membrane pressure, P_0, through the horizontal stress index, K_D. Hence, they are not affected by the non-linear relationship between membrane pressure and deflection and their evaluation from the standard dilatometer is acceptable. However, the in situ profiles of K_o, ϕ, D_r, OCR and p_c', should be taken as rough estimates rather than exact values, as the various DMT - CPT correlations used for their evaluation were established using silica sands which are devoid of any cementation.

All the in situ and laboratory test results indicate that the test site at Gillman, Port Adelaide, consists of moderately calcareous sand and silt with 25% carbonate content and varying degrees of cementation. There is a tough crust between 0.75 and 1.5 metres below ground level, below which there is a 1 metre deep highly compressible marshy layer consisting of silty sand, followed by sand deposit of medium rigidity and increased cementation.

The field test results show a great deal of variation which can be attributed to varying degree of cementation, and the interpreted results are not repeatable. However, the results from the weakly cemented layers are repeatable and as these values (summarised in Table 5.3), are in agreement with the laboratory results, their use is acceptable for design purposes. In general, the test site is a normally consolidated deposit of sand and silt ($K_o \simeq 0.45$), with average $\phi'_{ax} \simeq 33^o$ and average $E_{25} \simeq 20$ MPa below a depth of 3 metres.

The allowable bearing capacity calculated from the bearing capacity equations, causes excessive settlement of soil layers at Port Adelaide test site as it consists of loose and compressible soil layers. Therefore, the final assessment of the allowable bearing pressure should be based on the settlement criteria rather than shear failure. Bearing capacity and settlement calculations were carried out for different types of foundations and it was found that the best performance is that of a square foundation, 1.5m by 1.5m, where a contact pressure of 0.23 MPa causes settlement of only 20 mm. The second best performance is that of a rectangular foundation of size 1.5m by 3.0m, where a contact pressure of 0.18 MPa causes a settlement of nearly 20 mm. All the other foundations cause comparatively more settlement for the same loading magnitudes. Design charts were evaluated from the bearing capacity and settlement calculations of different types of foundations and are shown in Figures 6.2b, 6.3b and 6.4b of Chapter 6. These charts can be used as ready references for estimating the

allowable bearing pressures for foundations of different types, sizes and loading magnitudes so that the resulting settlements remain within tolerable limits.

7.2 Recommended future research

The present research work mainly concentrated on calcareous sands. However, the modified dilatometer will be of immense importance for automatic data recording in all types of soils. It will be interesting to conduct modified dilatometer tests in various types of soils, such as, different types of clays, sands and silts and compare the nature of their pressure - deflection curves. This will be helpful in the identification of soil stratigraphy and help in the evaluation of Young's modulus based on pressure - deflection curves. The difference in the Young's modulus evaluated from the modified dilatometer modulus, $E_{D(new)}$ and standard dilatometer modulus, E_D, and their laboratory verification will be helpful in proving the superiority of $E_{D(new)}$ over E_D for different types of soils.

Recent developments in the field of in situ testing indicate that piezometers are of great help in an accurate study of soil stratigraphy when installed inside penetrometer devices. It is therefore recommended to explore the possibility of incorporating a piezometer inside the dilatometer blade and also the cone penetrometer to enable the measurement of the in situ pore pressure during the tests.

At present it is necessary to use the CPT adjacent to DMT in order to evaluate ϕ, as the correlation is developed between $q_c/\sigma_v - K_D - \phi$. It is recommended that the measurement of q_d, in the case of dilatometer tests be made a regular feature and further calibration chamber tests be conducted with an aim to develop $q_d/\sigma_v - K_D - \phi$ correlation. By doing so, it would not be necessary to conduct CPT tests adjacent to DMT, and the DMT can be used independently.

7.3 Conclusions

In summary, the DMT and CPT in situ testing devices can be used for the evaluation of design parameters of moderately calcareous sand, utilising the existing correlations and local experience. High variations in the degree of cementation is a characteristic property of calcareous sands, which leads to a great deal of scatter in the profiles of the various evaluated soil parameters. However, the in situ parameters of weakly cemented layers are found to be in agreement with the laboratory evaluated results and their use in design practice should be towards the safer side.

The automation of the DMT is helpful in recording the test data swiftly and accurately during the field tests. The modifications of the internal membrane assembly enables a continuous data recording which indicates a non-linear relationship between membrane pressure and deflection and is helpful in a realistic evaluation of Young's modulus of soil.

The membrane depressurisation data recorded from the modified dilatometer can be used for the evaluation of in situ pore water pressure and the dilatometer tip resistance, q_d, can be correlated with K_o due to its sensitivity to the horizontal stress changes with the soil. However, further research is necessary to better estimate the pore pressures during the insertion of the blade and membrane expansion.

References

Auricht, D. J. and Sheffield, C. A. J. (1989). *"Evaluation of load deflection spade,"* Student Project Report, Dept. of Civil and Environmental Engineering, University of Adelaide.

Baguelin, F., Jezequel, J. F. and Le Mehaute, A. (1974). *"Self-boring placement method of soil characteristics measurement,"* Proc. ASCE speciality Conf. on subsurface exploration for underground excavation and heavy construction, Henniker, N. H., pp. 312-332.

Baldi, G., Bellotti, R., Ghionna, V., Jamiolkowski, M. and Pasqualini, E. (1981). *"Cone resistance in dry N.C. and O.C. sands,"* ASCE cone penetration testing and experience, Oct 1981, pp. 145-177.

Baldi, G., Bellotti, R., Ghionna, V., Jamiolkowski, M. and Pasqualini, E. (1982). *"Design parameters for sand from CPT,"* ESOPT II, Amsterdam.

Baldi, G., Bellotti, R., Ghionna, V., Jamiolkowski, M. and Pasqualini, E. (1985). *"Penetration Resistance and Liquefaction of sands,"* Proc. XI ICSMFE, San Francisco. pp. 1891-1897.

Baldi, G., Bellotti, R., Ghionna, V., Jamiolkowski, M., Marchetti, S. and Pasqualini, E. (1986). *"Flat dilatometer tests in calibration chambers,"* Proc. ASCE speciality Conf. on use of in situ tests in Geotechnical Engrg., Blacksburg, Va., pp 431-446.

Baligh, M. M. (1975). *"Theory of deep site static cone penetration resistance,"* Research report R 75-76, No. 517, Massachusetts Institute of Technology, Cambridge.

Barentsen, P. (1936). *"Short description of a field testing method with a cone shaped sounding apparatus,"* Proc. 1st Int. Con. on Soil Mechanics and Fond. Engrg., Harvard Univ., Boston (Mass), 1936, Vol. 2, 10.

Bellotti, R., Bizzi, G., Ghionna, V., Jamiolkowski, M., Marchetti, S. and Pasqualini, E. (1979). *"Preliminary calibration tests of electric cone and flat dilatometer in sand,"* Proc., 7th European Conference on Soil Mechanics and Foundation Engrg., Vol 2, Sept., 1979, Brighton, England, pp. 195-200.

Bellotti, R., Bizzi, G. and Ghionna, V. (1982). *"Design, construction and use of calibration chamber,"* Proc. ESOPT II, Amsterdam.

Bellotti, R. at. al. (1985). *"Laboratory validation of in situ tests,"* Geotechnical Engineering in Italy - an overview, Associazione Geotecnice Italiana, Rome, Italy, pp. 251-270.

Bellotti, R., Ghionna, V., Jamiolkowski, M., Lancelotta, R. and Manfredini, G. (1986). *"Deformation characteristics of cohesionless soils from In-Situ tests,"* ASCE Speciality Conf. In-Situ 86, Blacksburg, Va.

Berardi, R., Jamiolkowski, M. and Lancellotta, R. (1991). *"Settlement of shallow foundations on sands, selection of stiffness on the basis of penetration resistance,"* Geotechnical Engineering Congress, Vol I, pp. 185-200.

Beringen, F. L., Kolk, H. J. and Windle, D. (1982). *"Cone penetration testing and laboratory testing in marine calcareous sediments,"* Proc. Symp. on Geotechnical properties, behaviour and performance of calcareous soils (edited by K. R. Demars and R. C. Chenny), Florida, 1981, ASTM special technical publication STP 777, 1982, pp. 197-209.

Bogossian, F., Muxfeld, A. S., Dutra, A. M. B. (1989). *"Some results of flat dilatometer in Brazilian soils,"* Vol. I, XII Int. Conf. on Soil Mech. and Foundation Engrg., pp. 187-190.

Bowles, J. E. (1988). *"Foundation analysis and design," Mc. Graw-Hill International Editions,"* Civil Engineering services, 4th edition.

Brinch-Hansen, J. (1961). *"A general formula for bearing capacity,"* Bulletin No. 11, Danish Geotechnical Institute, Copenhagen, pp. 38-46.

Brinch-Hansen, J. (1966). *"Note concerning GI Bulletin No. 21,"* Danish Geotechnical Institute, Copenhagen, pp. 13.

Brooker, E. W. and Ireland, H. O. (1965). *"Earth pressure at rest related to stress history,"* Can. Geot. J., Vol . 2, No. 1, 1965, pp. 1-15.

Campanella, R. G. and Robertson, P. K (1983). *"Flat plate dilatometer testing: Research and development,"* Soil Mechanics Series No. 68, Dept. of C.E., University of British Coulombia, Vancouver.

Chia, C. E. P. and Dimas, S. F. (1987). *"The use of dilatometer to study the stiffness anisotropy and stress behaviour in Adelaide clay,"* Student Project Report, Deptt. of Civil and Environmental Engineering, University of Adelaide.

Clark, A. R. and Walker, B. F. (1977). *"A proposed scheme for the classification and nomenclature for use in the Engineering description of middle eastern sedimentary rocks,"* Geotechnique, Vol. 27, No. 1, pp. 93-99.

Coffey Partners International Pty. Ltd. (1991). *"Kinhill Delfin joint venture,"* MFP Adelaide site assessment study - preliminary Geotechnical groundwater and Agronomic investigation, Draft report no. A 2151/1-AS, December 1991.

Craig, R. F. (1987). *"Soil Mechanics,"* Van Nostrand Reinhold (UK), 4th edition.

Dahlberg, R. (1974). *"Penetration, pressuremeter and screw plate testing in a preloaded natural sand deposit,"* Proc. of the European Symp. on penetration testing, ESOPT I, Stockholm, Vol. 2.2.

D'Appolonia, D. J., D'Appolonia, E. and Brissette, R. F. (1970). closure to *"Settlement of spread footings on sand,"* Journal of the Soil Mechanics and Foundation Div., ASCE, Vol. 96, No. SM2, Proc. paper 5959, pp. 754-762.

Datta, M., Gulhati, S. K. and Rao, G. V. (1979). *"Crushing of calcareous sands during shear,"* Proc. 11th OTC Conf., Houston, paper PTC 3525, pp. 1459-1467.

De Beer, E.E., Golden, E., Heynen, W. J. and Joustra, K. (1988). *"Cone penetration test (CPT): International reference test procedure,"* ISOPT 1, De Ruiter(ed.), Orlando, Florida, AA, Balkema, Rotterdam, pp. 27-51.

De Ruiter, J. (1971). *"Electric Penetrometer for site investigation,"* J. Soil Mechanics and Foundations Div., ASCE, Vol. 97, SM 2, pp. 457-472.

De Ruiter, J. (1981). *"Current penetrometer practice,"* In cone penetration testing and experience, Geotech. Engrg. Div., ASCE, St. Louis, Missouri, pp. 1-48.

Douglas, B. J. and Olsen, R. S. (1981). *"Soil classification using electric cone penetrometer,"* (in cone penetration testing, edited by G. M. Norris and R. D. Holtz), Proc. Session sponsored by Geotechnical Div. at ASCE National Convention, St. Louis (Missouri), pp. 209-227.

Durgunoglu, H. T; and Mitchell, J. K. (1975). *"Static penetration resistance of soils,"* I- Analyses, II- Evaluation of theory and implications for practice, ASCE speciality Conf. on in situ measurement of soil properties, Raleigh N C. vol. I., pp. 151-189.

Ervin, M. C. (1985). *"Practical determination of in situ stress and deformation parameters,"* XI Int. Conf. on Soil Mech. and Foundation Engrg., San Francisco, Calif., pp. 2660-2662.

Fahey, M., and Randolph, M. F. (1985). Discussion of the *"Effects of Disturbance on Parameters Derived from Self-Boring Pressuremeter Tests in Sand,"* Geotechnique 35, no. 2, pp. 219-222.

Fahey, M. (1993). *"Selection of parameters for foundation design in calcareous soil,"* Research report No. G1077, Deptt. of Civil Engineering, Geomechanics group, University of Western Australia.

Fang, H. Y. (1991). *"Foundation Engineering Handbook,"* Van Nostrand Reinhold, New York, NY.

Fookes, P. G. and Higginbottom, I. E. (1975). *"The classification and description of near-shore carbonate sediments for Engineering purposes,"* Geotechnique, Vol. 25, No. 2, pp. 406-411.

Fugro (1979). *"Report K 1052 VIII,"* for Woodside petroleum Dev. Pty. Ltd.

Handy, R. L., Remubb, B., Lutenegger, A. J. and Trott, G. (1982). *"In situ stress determination by Iowa Stepped Blade,"* ASCE J. GED, GT11, pp. 1045-1422.

Hansen, J.B. (1970). *"A revised extended formulae for bearing capacity,"* Danish Geotechnical Institute Bulletin No. 28.

Head, K. H. (1990). *"Manual of Soil Laboratory Testing,"* Vol. I, II, III., ELE International Limited, Pentech press, London.

Hendron, A. J., Jr. (1963). *"The behaviour of sand in one dimensional compression,"* thesis presented to the University of Illinois, at Urbana, Champaign, in partial fulfilment of the requirement for the degree of Doctor of Philosophy.

Holden, J. C. (1976). *"The calibration of electrical penetrometers in sand,"* Final report N. G. I., Oslo.

Hryciw, R. D. and Dowdig, C. H. (1988). *"CPT and DMT in evaluation of blast densification of sand,"* Penetration testing, ISOPT-1, De Ruiter (ed.), 1988, Balkema, Rotterdam, ISBN, pp. 521-526.

Jaksa, M. B. (1990). *"A data acquisition system for the cone penetration test,"* Seminar on computing in Geomechanics, Aust. Geomech. Soc., SA Div., 1990, pp. 22-31.

Jaksa, M. B. and Kaggwa, W. S. (1994). *"A microcomputer based data acquisition system for the cone penetration test,"* Research report No. R116, Deptt. of Civil and Environmental Engineering, University of Adelaide.

Jaky, J. (1944). *"The coefficient of earth pressure at rest,"* Journal for society of Hungarian Architects and Engineers, Budapest, Hungary, pp. 355-358.

Jamiolkowski, M., Lancellotta, R., Marchetti, S., Nova, R., Pasqualini, E. (1979). *"Design parameters of soft clays,"* S.O.A. VII, ECSMFE, Brighton.

Jamiolkowski, M., Ladd, C. C., Germaine, J. T. and Lancellotta, R. (1985). *"New developments in the field and laboratory testing of soils,"* Theme Lecture No. 2, Proc. XI Int. Conference on Soil Mech. and foundation Engrg., San Francisco, Calif., Vol.1, pp. 57-153.

Jamiolkowski, M., Ghionna, V. N., Lancellotta, R., Pasqualini, E. (1988). *"New correlations of penetration tests for design practice,"* Proc. ISOPT I, Orlando, Fla.

Janbu, N. (1963). *"Soil compressibility as determined by oedometer and triaxial tests,"* Proceedings, 3rd European Conference, SM & FE, Wiesbaden, 1963, pp. 19-25.

Janbu, N. (1967). *"Settlement calculations based on the tangent modulus concept,"* three guest lectures at Moscow State University, Bulletin No. 2, Soil Mechanics, Norwegian Institute of Technology, 1967, pp. 1-57.

Janbu, N. (1985). *"Soil models in offshore Engineering,"* 25th Rankine lecture, Geotechnique, Vol. 35, No. 3, Sept. 1985, pp. 261.

Jewell, R. J. (1993). *"An introduction to calcareous sediments,"* Research report No. G1075, Deptt. of Civil Engineering, Geomechanics group, University of Western Australia.

Joustra, K. and Gijt, J. G. (1982). *"Results and interpretation of cone penetration tests in soils of different mineralogic composition,"* Proc. 2nd Europ. Symp. on Penetration testing, Amsterdam, 1982, pp. 615-626.

Kaggwa, W. S. and Poulos, H. G. (1990). *"Comparison of the behaviour of dense carbonate sediments and silica sand in cyclic triaxial tests,"* Research report No.R611, School of Civil and Mining Engineering, University of Sydney.

Kaggwa, W. S., Jaksa, M. B. and Jha, R. K. (1995). *"Development of automated dilatometer and comparison with cone penetration tests in the University of Adelaide, Australia,"* accepted for the Proceedings of International Conference on advance in site investigation practice, London., March 1995.

Lacasse, S. (1985). *"In situ determination of deformation parameters,"* XI Int. Conf. on Soil Mech. and Foundation Engrg., San Francisco, Calif., pp. 2663-2665.

Lacasse, S. and Lunne, T. (1986). *"Dilatometer tests in Sands,"* ASCE Speciality Conf. In-Situ 86, Blacksburg, Va., pp. 686-699.

Lacasse, S., and Lunne, T.(1988). *"Calibration of Dilatometer correlations,"* Proc. ISOPT I, Orlando, Florida. pp. 539-549.

Ladd, C. C., Foot, R., Ishihara, K., Schlosser, F. and Poulos, H. G. (1977). *"Stress deformation and strength characteristics,"* SOA report, Proc. of IX ICSMFE, Tokyo, Vol. II, pp. 421-424.

Lambrechts, J. R., and Leonards, G. A. (1978). *"Effects of stress history on deformation of sand,"* J. Geotech. Engrg. Div., 104 (GT 11), pp. 1371-1378.

Leonards, G. A. (1985). *"Discussion of new developments in field and laboratory testings of soils,"* by M. Jamiolkowski, et al., Proceedings XI Int. Conf. on Soil Mech. and Found. Engrg., San Francisco, Calif., Vol. 5.

Leonards, G. A., and Frost, J. D. (1988). *"Settlement of shallow foundations on Granular soils,"* J. Geotech. Engrg. Div., ASCE, 114 pp. 791-809.

Lunne, T. and Kleven, A. (1981). *"Role of CPT in North Sea Foundation Engineerings,"* Proc. ASCE National Convention at St. Louis cone penetration testing and experience.

Lutenegger, A. J. and Kabir, M. G. (1988). *"Current status of Marchetti dilatometer test,"* Penetration testing, ISOPT-1, De Ruiter (ed.), Balkema, Rotterdam, pp. 549-554.

Marchetti, S. (1979). *"Determination of design parameters of sands by means of quasi statically pushed probes,"* Proc. VII ECSMFE, Brighton, Vol 4, pp. 237-242.

Marchetti, S. (1979). *"In situ determination of an extended O.C.R. proceeding,"* VII th European Conf. on Soil Mech. and Foundation Engrg., Vol. 2, Sept, 1979, pp. 239-244.

Marchetti, S. (1980). *"In-situ tests by flat dilatometer,"* J. Geotechnical Engrg. Div., ASCE, 106 (GT3), pp. 299-321.

Marchetti, S. (1985). *"On the field determination of K_o in sand,"* Discussion Session No. 2A, XI Int. Conference on Soil Mech. and Foundation Engrg., San Francisco, Calif., pp. 2667-2672.

Mayne, P.W., and Kulhawy, F. H. (1982). *"K_o - OCR relationships in soil,"* J. Geotech. Engrg. Div., ASCE, 108 (GT6), pp. 851-872.

Meigh, A. C. (1987). *"Cone penetration testing: Methods and Interpretation,"* CIRIA/Butterworths, London.

Meyerhof, G. G. (1951). *"The ultimate bearing capacity of foundations,"* Geotechnique, Dec. 1951, 2 (No. 4), pp. 301-332.

Meyerhof, G. G. (1963). *"Some recent research on the bearing capacity of foundations,"* Canadian Geotechnical Journal, 1, No. 1, pp. 16-26.

Mitchell, J. K. and Durgunoglu, H. T. (1973). *"In Situ strength by static cone penetration test,"* Proc. XI Int. Conference on Soil Mech. and foundation Engrg., Moscow, U.S.S.R., Vol.1.2, pp. 279-286.

Mitchell, J. K. and Gardner, W. S. (1975). *"In situ measurement of volume change characteristics,"* Proceedings, Conference on in situ measurement of soil properties, ASCE speciality Conference, state-of-the-art paper, Raleigh, N.C., Vol. 2, pp. 279-345.

Mokkelbost, K. H., Baldi, G., Bellotti, R. and Jamiolkowski, M. (1989). *"Dilatometer tests in the ISMES calibration chamber,"* N.G.I., Oslo, International report.

Ortigo, J. A. R., Campello, S. L. F., Morrison, M. and Lamonica, L. De. (1986). *"In situ testing of Calcareous sand - Campos Basin,"* ASCE Speciality Conf., In Situ 86, Blacksburg, Va., pp. 887-899.

Parkin, A. K. and Lunne, T. (1982). *" Boundary effects in the laboratory calibration of a cone penetrometer for sand,"* Proc. ESOPT II, Amsterdam.

Poulos, H. G. (1980). *"A review of the behaviour and Engineering properties of carbonate soils,"* Research report No. R381, School of Civil Engineering, University of Sydney.

Powell, J. J. M., and Uglow, I. M. (1988). *"Marchetti dilatometer testing in U.K. soils,"* Proc. ISOPT, Florida, pp. 555-562.

Power, P. T. (1982). *"The use of electric cone penetrometer in the determination of the Engineering properties of chalk,"* Proc. 2nd Europ. Symp. on Penetration testing, Amsterdam, 1982, pp. 769-774.

PPK consultants, Hassel group and CSIRO (1992). *"Gillman / Dry Creek urban development proposals,"* MFP Australia, Draft Environment impact statement prepared for the Premier of South Australia.

Randolph, M. F., Finnie, I. M. and Jober, H. (1993). *"Performance of shallow and deep foundations on calcareous soil,"* Research report No. G1076, Deptt. of Civil Engineering, Geomechanics group, University of Western Australia.

Reyna, F. and Chameau, J. L. (1991). *"Statistical evaluation of CPT and DMT measurements at Heber Road site,"* Geotechnical Engineering Congress, ASCE, Geotech. Div., pp. 14-25.

Rezak, R. (1974). *"Deep-sea carbonates"* Deep-sea sediments, Ed. A. L. Inderbitzen, Plenum Press, pp. 453-461.

Robertson, P. K., and Capanella, R.G. (1984). *"Interpretation of cone penetration tests - Part 1 - Sand,"* Can. Geotech. J., 20 (4), pp. 718-733.

Robertson, P. K., Davies, M. P. and Campanella, R. G. (1988). *"Design of laterally loaded driven piles using the flat plate dilatometer,"* paper submitted to Geotechnical Testing Journal, ASTM.

Schmertmann, J. H. (1970). *"Static cone to compute settlement over sand,"* J. Soil Mech. and Found. Engrg., ASCE, 96 (SM3), pp. 1011-1043.

Schmertmann, J. H. (1976). *"An updated correlation between relative density, D_r, and Fugro-type electric cone bearing, q_c,"* unpublished report to WES, Vicksburg, Miss.

Schmertmann, J. H., Hartman, J. P., and Brown, P. R. (1978). *"Improved strain influence factor diagram,"* ASCE, J. GED, 104 no. GT8, pp. 1131-1135.

Schmertmann, J. H. (1979). *"Statics of SPT,"* ASCE J. GED, paper 14573, May, 1979, pp. 655-670.

Schmertmann, J. H. (1979). *"Discussion of Marchetti (1979) and closure by S. Marchetti,"* ASCE, J. GED, VOL. 107, No. GT 6, pp. 831-837.

Schmertmann, J. H. (1982). *"A method for determing the friction angle in sands from the Marchetti Dilatometer test,"* Proc. European Symposium on penetration Testing II, Amsterdam, Netherlands, 2, pp. 853-861.

Schmertmann, J. H. (1983). *"Revised procedure for calculating K_o and OCR from DMT's with I_D > 1.2 and which incorporate the penetration force measurement to permit calculating the plain strain friction angle,"* DMT workshop 16-18, Gainesville, Florida.

Schmertmann, J. H. (1986). *"Suggested method for performing the flat dilatometer test,"* Geotech. Testing J., ASTM, 9 (2), pp. 93-101.

Schmertmann, J. H. (1986a). *"Dilatometer to compute foundation settlement,"* Proc. ASCE Speciality Conf. on use of In Situ Tests in Geotecgnical Engrg., Blacksburg, Va., pp. 303-321.

Schmertmann, J., Baker, W., Gupta, R. and Kessler, K. (1986). *"CPT / DMT QC of ground modification at a power plant,"* ASCE Speciality Conf., In Situ 86, Blacksburg, Va., pp. 985-1001.

Schmidt, B. (1966). discussion of *"Earth pressures at rest related to stress history,"* Canadian Geotechnical Journal, National Research Council, Ottawa, Ontario, Canada, Vol. 3, No. 4, pp. 239-242.

Searle, I. W. (1979). *"The interpretation of Begemann friction jacket cone results to give soil types and design parameters,"* Proc. 7th Eur. Con. on soil Mechanics and foundation Engineering, Brighton, Vol. 2, pp. 265-270.

Senneset, K. and Janbu, N. (1985). *"Shear strength parameters obtained from static cone penetration tests,"* Paper A-84-1, Inst. of Geomechanics and Found. Engrg., Norwegian Inst. of Technology, Trondheim, (also published in ASTM Symp., San Deigo, California, 1984).

Sherif, M. A., Ishibashi, I. and Ryden, D. E. (1974). *"Coefficient of lateral earth pressure at rest in cohesionless soils,"* Soil Engineering research report No. 10, University of Washington, Seattle, Wash.

Skempton, A. W. and Mc. Donald, D. H. (1956). *"Allowable settlement of buildings,"* Proceedings ICE, 5, Part 3, pp. 727-768.

Standards Association of Australia (1977). *"Methods for testing soils for Engineering purposes,"* Sydney.

Terzaghi, K. (1943). *"Theoretical soil mechanics,"* John Wiley and Sons, New York.

Veismanis, A. (1974). *"Laboratory investigation of electrical friction cone penetrometers in sand,"* ESOPT, Stockholm, Vol. No. 2.2, pp. 407-419.

Vesic, A. S. (1970). *"Tests on instrumented piles, Ogeeechee River site,"* ASCE Journal of the Soil Mech. and Found. Div., 96(SM2), pp. 561-584.

Vesic, A. S. (1973). *"Analysis of ultimate loads of shallow foundations,"* Journal ASCE, 99, No. SM1, pp. 45-73.

Villet, W. C. and Mitchell, J. K. (1981). *"Cone resistance, relative density and friction angle,"* ASCE cone penetration testing and experience, Oct 1981, pp. 178-208.

Villet, W. C., Mitchell, J. K. and Tringale, P.T. (1981). *"Acoustic emissions generated during the quasi static cone penetration of soils,"* ASTM Symp. on acoustic emission in Geotech. Engrg., Detroit.

Wroth, C. P. and Hughes, J. M. O. (1973). *"An instrument for the in situ measurement of properties of soft clays,"* Proc. VIII Int. Conference on Soil Mech. and Found. Engrg., Moscow, USSR, Vol. 1.2, pp. 487-494.

Zamani, M. and Zahran, Z. (1986). *"The use of flat dilatometer for measurement of in situ properties in Adelaide soils,"* Student Project Report, Dept. of Civil and Environmental Engineering, University of Adelaide.